Satellite Perspective of Aerosol Intercontinental Transport: From Qualitative Tracking to Quantitative Characterization

Hongbin Yu [1,2], Lorraine A. Remer [3], Ralph A. Kahn [2], Mian Chin [2], Yan Zhang [4,2]

1. Earth System Science Interdisciplinary Center, University of Maryland, College Park, Maryland, 20740, USA
2. Earth Science Directorate, NASA Goddard Space Flight Center, Greenbelt, Maryland, 20771, USA
3. Joint Center for Earth Systems Technology, University of Maryland at Baltimore County, Baltimore, Maryland, 21228, USA
4. Universities Space Research Association, Columbia, Maryland, 21044, USA

Correspondence

Hongbin Yu

Climate and Radiation Laboratory

NASA GSFC Code 613

Greenbelt, MD 20771, USA

301-614-6209

301-614-6307

Hongbin.Yu@nasa.gov

Invited Review submitted to the *Atmospheric Research*

June 30, 2012

Abstract

Evidence of aerosol intercontinental transport (ICT) is both widespread and compelling. Model simulations suggest that ICT could significantly affect regional air quality and climate, but the broad inter-model spread of results underscores a need of constraining model simulations with measurements. Satellites have inherent advantages over in situ measurements to characterize aerosol ICT, because of their spatial and temporal coverage. Significant progress in satellite remote sensing of aerosol properties during the Earth Observing System (EOS) era offers opportunity to increase quantitative characterization and estimates of aerosol ICT, beyond the capability of pre-EOS era satellites that could only qualitatively track aerosol plumes. EOS satellites also observe emission strengths and injection heights of some aerosols, aerosol precursors, and aerosol-related gases, which can help characterize aerosol ICT. After an overview of these advances, we review how the current generation of satellite measurements have been used to (1) characterize the evolution of aerosol plumes (e.g., both horizontal and vertical transport, and properties) on an episodic basis, (2) understand the seasonal and inter-annual variations of aerosol ICT and their control factors, (3) estimate the export and import fluxes of aerosols, and (4) evaluate and constrain model simulations. Substantial effort is needed to further explore an integrated approach using measurements from on-orbit satellites (e.g., A-Train synergy) for observational characterization and model constraint of aerosol intercontinental transport and to develop advanced sensors for future missions.

Keywords: aerosols; satellite remote sensing; long-range transport

CONTENTS

1. Introduction 4

2. Recent advances in satellite aerosol measurements 9

2.1 Improved accuracy and coverage for AOD measurements 10

2.2 Emerging climatology of aerosol vertical distribution 13

2.3 Enhanced capabilities for characterizing aerosol properties 15

2.4 Feasibility of synergistic aerosol characterization 18

3. Application of Satellite Measurements to Characterizing and Estimating Aerosol Intercontinental Transport 22

3.1 Episode-based characterization of aerosol ICT from satellites 22

3.2 Climatological characterization of aerosol ICT from satellites 27

3.3 Estimates of aerosol export and import mass flux from satellites 35

3.4 Evaluation and constraint of model simulations by satellite measurements 42

4. Conclusions and Outlooks 51

Acknowledgements 56

Acronyms 57

References 58

Tables 83

Figures with captions 85

Supplementary Online Materials 98

A. Descriptions of Major EOS-era Aerosol Sensors 98

B. A movie: Aerosol intercontinental transport in 2001 as captured by MODIS and GOCART 106

1. Introduction

Atmospheric aerosols are solid or liquid particles suspended in the atmosphere, exhibiting great variability not only in concentration but also in size, composition, and shape. They are emitted directly into the atmosphere as primary aerosols, or are secondary aerosols, formed through chemical transformations from a variety of natural and man-made gaseous emissions. In high concentrations, aerosol, also known as particulate matter or PM, can be harmful to human health (Pope et al., 2002). Aerosols affect weather and climate by scattering and absorbing solar radiation (so-called "aerosol direct effects") (McCormick and Ludwig, 1967) and by modifying cloud properties, amount, and evolution (collectively referred to as "aerosol indirect effects") (Twomey, 1977; Gunn and Phillips, 1957; Albrecht, 1989). Absorption of solar radiation by particles changes the atmospheric stability and reduces the surface fluxes, which can change atmospheric circulations (Ramanathan et al., 2005; Lau and Kim, 2006; Lau et al., 2009; Zhang et al., 2009). Dust aerosol rich in iron also affects climate indirectly by changing biogeochemistry (Jickells et al., 2005). Aerosol also impairs visibility (White, 1976) and affects crop yields (Chameides et al., 1999).

Aerosols are removed from the atmosphere through gravitational settling, dry deposition, and wet scavenging, processes that typically produce lifetimes of hours to days in the atmospheric boundary layer and of weeks in the upper troposphere. Thus aerosols emitted from one continent are often transported long distances to another, in particular when aerosols are pumped out of the boundary layer. There is mounting evidence for

intercontinental and even hemispheric transport, provided by long-term surface monitoring networks, in-situ measurements from intensive field campaigns, and especially satellite observation, backed by model simulations. It was determined that the recurring phenomenon of "Arctic haze" in late winter and early spring is associated mainly with long-range transport of pollution and dust sources in Europe and Asia (Rahn et al., 1977; Shaw et al., 1983). Saharan dust routinely reaches the Amazon, the Caribbean Sea and southeastern U.S. after sweeping over the Atlantic Ocean (; Swap et al., 1992; Prospero, 1999; Prospero et al., 2005). Asian dust and pollution have long been observed in the western U.S. and beyond (Jaffe et al., 1999; Biscaye et al., 2000; VanCuren and Cahill, 2002; Grousset et al., 2003; Stohl et al., 2007). Because of the long-range transport, aerosols emitted or formed in one region could have important implications for climate, weather, and air quality in downwind regions/continents. As such, the long-range transport of air pollution has been an active topic of scientific research for several decades and has also been debated for formulating environmental policies and treaties (Holloway et al., 2003). One of the most recent coordinated efforts is the establishment of the Task Force on Hemispheric Transport of Air Pollutants (HTAP) by the United Nations Economic Commission for Europe, aiming to understand the growing body of scientific evidence of intercontinental transport and assess its impacts on air quality, climate, and ecosystems (HTAP, 2010).

Impacts of aerosol intercontinental transport (ICT) on regional air quality and climate change are potentially large, as estimated by chemical transport models (CTM) (HTAP, 2010); however, large uncertainties are associated with the ensemble CTMs employed in

the assessment. **Figure 1** shows the relative annual intercontinental response (RAIR) for surface aerosol concentration, a quantity related to air quality, and aerosol optical depth (AOD), a quantity related to aerosol climate forcing. RAIR is calculated from the source-receptor relationship experiments of multiple global aerosol models (HTAP, 2010; Yu et al., 2012a). By definition, RAIR in a receptor region represents the percentage contribution of the intercontinental transport of foreign emissions relative to the sum of foreign and domestic emissions (HTAP, 2010). Clearly, the aerosol import from ICT makes significant contribution to climate forcing and air quality. RAIR for surface concentration ranges from 5-20%, whereas RAIR for AOD is larger, having a range of 10-30%. Values of RAIR depend on both region and component. On the other hand, model simulations show a large spread, as reflected by the calculated standard deviations of RAIR and represented by the error bars in Figure 1. The large model diversity is likely associated with differences in the model treatment of numerous aerosol processes, as extensively documented in a number of inter-comparisons between models and observations (e.g., Kinne et al., 2006; Schulz et al., 2006; Textor et al., 2006; Textor et al., 2007; Shindell et al., 2008; Koch et al., 2009; Prospero et al., 2010).

There is a pressing need for reliable observations that constrain and improve model assessments of aerosol ICT and its regional impacts. Such observations need to meet some primary requirements. Measurements should have adequate spatial and temporal coverage to allow for tracking the evolution of aerosol transport over a global or hemispherical scale with a daily or hourly frequency. Measurements also should provide or can be used to derive highly accurate, quantitative information about aerosol

horizontal and vertical distributions, such as mass concentration, mass loading, aerosol optical depth (AOD), and vertical profiles of aerosol extinction. In the case of remote sensing observations, measurements should distinguish aerosol types, which is essential for the conversion between aerosol optical measurement (e.g., AOD and extinction or backscatter coefficient) and aerosol mass loading or concentration. Aerosol mass extinction efficiency and its dependence on relative humidity depend on aerosol type. Different types of aerosol also tend to follow different transport paths and exert different impacts on climate and human health.

Large-scale satellite measurements, complemented by regional and local aerosol characterizations from surface stations and field campaigns, can meet these fundamental requirements. Surface stations can offer detailed albeit local measurements of surface concentrations, AOD (Holben et al., 1998), and chemical (Malm et al., 2004), microphysical, and radiative (Dubovik et al., 2002) aerosol properties. Intensive field experiments can provide comprehensive snapshots of regional aerosols through implementing coordinated and multiplatform observation strategies (Russell et al., 1999; Huebert et al., 2003; Jacob et al., 2003; Reid et al., 2003; Tanré et al., 2003; Li et al., 2007; Singh et al., 2009; Jacob et al., 2010). For all of their advantages, field campaigns and surface stations are inherently limited by the relatively short duration and/or small spatial coverage, which alone are not adequate for assessing the temporal and spatial variations of cross-ocean aerosol transport. Even long-term surface networks, such as the Aerosol Robotic Network (AERONET) (Holben et al., 1998), are substantially limited in geographical coverage, particularly over oceans where intercontinental transport occurs.

This lack of oceanic coverage is being addressed in part by the Marine Aerosol Network (MAN) (Smirnov et al., 2009); but even so, marine aerosol coverage, both in space and time, remains exceedingly sparse. Satellite aerosol remote sensing can augment field campaigns and surface networks by expanding temporal and spatial scales because of the inherent advantage of daily or hourly measurements with global or continental coverage over decadal-scale durations. Indeed, ever since meteorological satellites were put into orbit, satellite imagers have been used to detect the aerial extent and motion of large-scale aerosol plumes, primarily in a qualitative or at most semi-quantitative way (e.g., Fraser, 1976; Lyons et al., 1978; Fraser et al., 1984; Chung et al., 1986; Ferrare et al., 1990; Dulac et al., 1992). In recent decades and particularly during the Earth Observing System (EOS) era, substantial progresses have been achieved in satellite remote sensing of aerosols (see summaries by Yu et al., 2009a; Kahn, 2011; and references therein). Satellites are currently providing global land and ocean measurements of AOD with much improved quality. Global measurements of aerosol vertical distributions in cloud-free atmosphere and above cloud are also emerging (Winker et al., 2010). Enhanced remote sensing capabilities for constraining aerosol shape, size, and absorption allow for the characterization of aerosol type (Tanré et al., 2001; Higurashi and Nakajima, 2002; Kaufman et al., 2005a; Kahn et al., 2007; Tanré et al., 2011). Several satellite sensors are also providing value-added observations for aerosol ICT by measuring trace gases such as SO_2 and CO, that are aerosol precursors or originate from the same sources as particles, and providing means for identifying major aerosol source regions and estimating emissions (e.g., Veefkind et al., 2011; Ichoku et al., 2012). These advances

have provided an unprecedented opportunity of going from qualitative tracking to increasingly quantitative characterization and estimates of aerosol ICT.

In this paper, we review: (a) the advances in satellite aerosol measurement over the last decade (section 2), (b) how the advanced satellite measurements have been used to improve the understanding of aerosol ICT variations on daily, seasonal, and decadal timescales and to estimate aerosol exports and imports (section 3.1-3.3), and (c) the progress of using satellite measurements to evaluate and constrain model simulations (section 3.4). Major conclusions and recommendations are summarized in section 4.

2. **Recent advances in satellite aerosol measurements**

Satellite imagers have been providing a wealth of qualitative or semi-quantitative information for intercontinental and hemispheric aerosol transport since the 1970s (e.g., Prospero and Carlson, 1972; Lyons et al., 1978; Chung, 1986; Herman J. et al., 1997). Some studies also attempted to estimate columnar atmospheric density and transport of desert dust (Fraser, 1976; Mekler et al., 1977; Sirocko and Sarnthein, 1989; Dulac et al., 1992), sulfate pollution (Fraser et al., 1984), and fire smoke (Ferrare et al., 1990) using early satellite measurements. However, such estimates were subject to large uncertainties because of poor data accuracy and the lack of constraints on aerosol microphysical properties and vertical distributions. Thus, quantitative assessments of aerosol intercontinental transport became possible only recently as a result of the much improved measurement accuracy and enhanced measurement capabilities achieved mainly in the EOS-era. **Table 1** lists major satellite observables currently available for studying aerosol ICT. In the following we provide an overview of major advances achieved primarily

over the last decade, including improved accuracy and coverage for AOD, the emerging climatology of aerosol vertical distribution, enhanced capabilities for characterizing aerosol properties, and the feasibility of synergistic aerosol characterization.

2.1. Improved accuracy and coverage for AOD measurements

AOD is the quantity most often provided by satellite remote sensing. It is a measure of the integrated aerosol extinction (scattering and absorption) through the atmosphere, which is related to aerosol mass loading, dependent upon aerosol composition and meteorological conditions. Early aerosol monitoring from space used data from sensors that were designed for other purposes, e.g., the Advanced Very High Resolution Radiometer (AVHRR), the Total Ozone Mapping Spectrometer and (TOMS), and the Geostationary Operational Environmental Satellite (GOES). They have provided a multi-decadal climatology of AOD that has significantly advanced the understanding of aerosol distributions (e.g., Herman J. et al., 1997; Husar et al., 1997; Mishchenko et al., 1999; 2003; Geogdzhayev et al., 2002; Torres et al., 2002; Zhao et al., 2008). However AOD accuracy from these early sensors is generally low. Major sources of AOD uncertainty are associated with instrument calibration, band characteristics, spatial resolution, cloud contamination, surface reflectance, and assumed aerosol optical models (Zhao et al., 2008).

In the past decade, significant progress has been made in reducing these uncertainties. On-orbit calibration has been implemented widely. Improvements in pixel resolution and spectral range make the cloud screening more robust than before (Martins et al., 2002),

though cloud contamination remains a major issue for aerosol remote sensing (Kaufman et al., 2005b; Zhang et al., 2005; Kahn et al., 2009). Several techniques based on enhanced sensor capabilities such as new channels (Kaufman et al., 1997; Hsu et al., 2004), multi-angle views (Diner et al., 1998; Martonchik et al., 1998; 2002; 2009) and polarization (Herman M. et al., 1997; Deuzé et al., 2001), have been developed to improve the separation of land surface from atmospheric reflectance and hence, the accuracy and coverage of AOD retrievals. The advanced datasets of land surface properties have also been used to better characterize and quantify surface contributions in the aerosol retrieval algorithms (Li et al., 2005; Lyapustin et al., 2011). The accumulation of detailed aerosol property measurements from dedicated field campaigns and long-term surface networks (Yu et al., 2006 and references therein) has provided strong constraints on aerosol optical properties used in satellite aerosol retrievals. Examples of passive sensors with the advanced capabilities include the Polarization and Directionality of the Earth's Reflectance (POLDER), MODerate resolution Imaging Spectroradiometer (MODIS), Multi-angle Imaging SpectroRadiometer (MISR), and Ozone Measurement Instrument (OMI). Major characteristics of these advanced sensors are described in *Supplementary Online Material (SOM)*. These sensors provide global measurements of AOD over both land and ocean with accuracy on order of 20% or ±0.05 (e.g., Chu et al., 2002; Remer et al., 2002, 2005; Levy et al., 2010; Hsu et al., 2004; Lyapustin et al., 2011; Kahn et al., 2005, 2010; Abdou et al., 2005; Fan et al., 2008; Ahn et al., 2007).

Remote sensing of AOD from the above daytime polar-orbiting sensors is complemented by measurements from infrared sensors such as the Atmospheric Infrared Sounder

(AIRS) and geosynchronous satellites. AIRS observations have also been used to detect large particles such as soil-derived dust in both day and night (Pierangelo et al., 2004; DeSouza-Machado et al., 2006; Peyridieu et al., 2010; DeSouza-Machado et al., 2010). AOD measurements from the polar-orbiting satellites do not sample frequently enough to characterize the wide range of daily AOD variability in different locations and seasons (Zhang et al., 2012). NOAA's GOES has been providing 30 min AOD measurements over the U.S. for many years (Knapp et al., 2002; Prados et al., 2007). The SEVIRI instrument on board Meteosat Second Generation (MSG) also offers new capabilities for monitoring aerosol transport over the Atlantic and Mediterranean at high temporal and spatial resolution (Thieuleux et al., 2005). Because these sensors generally have coarse spatial resolution and limited wavelength coverage, the AOD products from them have never reached the same level of accuracy and quality as aerosol products from the EOS-era polar orbiting missions. In the coming era of geostationary remote sensing, new instruments such as the Advanced Baseline Imager (ABI) onboard GOES-R (scheduled for launch in 2015) will provide AOD measurements with significantly improved accuracy (Laszlo et al., 2008).

Observing aerosols above low-level clouds from satellites has also been explored recently. CALIOP can measure backscatter and infer aerosol extinction profiles above low-level clouds (Winker et al., 2010) or above-cloud AOD and particle properties based on lidar observations of depolarization ratio or color ratio for underlying clouds (Hu et al., 2007; Chand et al., 2008), albeit with very limited coverage. Several passive sensors can also measure AOD above clouds, because the presence of aerosols can significantly

modify some attributes of radiances reflected by underlying clouds, such as the polarized light in certain scattering-angle ranges (Waquet et al., 2009) and the spectral contrast of radiation (Herman J. et al., 1997; Torres et al., 2007; Fromm et al., 2008). These constitute a basis for retrieving above-cloud AOD using multiangle polarization measurements from POLDER (Waquet et al., 2009) and the backscattered UV (BUV) measurements from OMI (Torres et al., 2012), respectively. A recent analysis shows that OMI absorbing aerosol index (AAI) in cloudy conditions (as determined from MODIS cloud measurements) correlates well with CALIOP above-cloud AOD, having a relationship that depends on cloud albedo (Yu et al., 2012b). The results may suggest the potential of combining OMI AAI and MODIS cloud masking to empirically derive above-cloud AOD with a spatial coverage much more extensive than CALIPSO (Yu et al., 2012b). These above-cloud aerosol measurement capabilities could provide new insights into aerosol intercontinental transport, because the transport often occurs above clouds (e.g., Dirksen et al., 2009). The above-cloud aerosol observations could reveal to some extent the role of cloud processes in pumping atmospheric boundary layer (ABL) aerosol up to the free troposphere (FT) for the subsequent cross-ocean transport. They are also essential to assessing aerosol direct radiative forcing (Abel et al., 2005; Chand et al., 2009) and influence on the formation and evolution of clouds (Johnson et al., 2004; Wilcox, 2010).

2.2. Emerging climatology of aerosol vertical distribution

A climatology of aerosol vertical distribution is emerging in recent years due to the deployment of space-based lidar technology, in particular the launch of CALIPSO in 2006 (Winker et al., 2009). Since then, CALIPSO has been collecting an almost

continuous record of high-resolution (333 m in the horizontal and as fine as 30 m in the vertical), day and night profiles of aerosols and clouds attenuated backscatter at 532 and 1064 nm wavelengths, along with polarized backscatter in the visible channel, covering the globe from 82°N to 82°S (Winker et al., 2009; 2010). Aerosol profiling from CALIOP is not limited to cloud-free conditions. Lasers can penetrate thin cirrus clouds and sense aerosol layers abvove low-level clouds. As such, a climatology of global aerosol and cloud vertical distributions over 5+ years is emerging.

Passive sensors also show some promise in sensing the height of aerosol layers. Radiances at the atmospheric windows (e.g., 8-12 um) are mostly sensitive to the altitude of dust layers, due to relatively large particle size and frequently high AOD, compared to other aerosol types (Pierangelo et al., 2004; DeSouza-Machado et al., 2006). Having nearly complete coverage of the 9-12 μm spectrum with high spectral resolution, AIRS has shown capability of detecting dust layer height both day and night (Peyridieu et al., 2010; DeSouza-Machado et al., 2010). The O_2-O_2 absorption feature at 477 nm from OMI also contains useful information on the altitude of cloud or aerosol layers (Acarreta et al., 2004). Scattering by clouds or aerosols reduces the probability of absorption by O_2-O_2 below these layers. The higher the cloud or aerosol layer, the larger the O_2-O_2 absorption reduction. From stereo imaging, the heights of clouds and aerosol plumes can also be derived geometrically (Moroney et al., 2002; Muller et al., 2002). This technique is not dependent on radiometric calibration accuracy, but is effective only near aerosol sources, where plumes exhibit sufficient spatial contrast to be matched in multiple angular views (Kahn et al., 2007; Scollo et al., 2010; Val Martin et al., 2010). It has been

shown that these passive techniques can be used to estimate the altitude of dust and smoke plumes under cloud-free conditions, providing essential information that is complementary to CALIPSO data (Kahn et al., 2008; Dirksen et al., 2009; Peyridieu et al., 2010).

2.3. Enhanced capabilities for characterizing aerosol properties

Satellite sensors, though not able to directly measure aerosol composition, can constrain particle size (i.e., fine versus coarse), shape (i.e., spherical versus non-spherical), and absorption (i.e., scattering versus absorbing), from multi-wavelength, multi-angle, and polarization measurements. The MODIS multi-wavelength measurements over wide spectral range make it feasible to retrieve quantitative aerosol size parameters (e.g., effective radius, fine-mode fraction or FMF of aerosol optical depth) over dark water (Kaufman et al., 2002; Remer et al., 2005; Levy et al., 2010). **Figure 2** shows spatial variations of aerosol type on April 11, 2001 as revealed by the composite of aerosol optical depth and fine-mode fraction from MODIS observations and the Goddard Chemistry Aerosol Radiative Transport (GOCART) simulations. Industrial pollution and biomass burning aerosols are predominately small particles and shown as red, whereas mineral dust and sea salt are primarily large particles and shown as green. Methods have been developed to estimate the optical depth of combustion aerosol (from industrial activities and biomass burning) and dust using the FMF and AOD (e.g., Kaufman et al., 2005a; Yu et al., 2009b). These methods are dependent on several important assumptions based on regional climatology and are not the same as using the information content of the observations directly to determine aerosol type. However, the methods have provided

several important estimates of dust and pollution aerosol transport across ocean basins. The use of MODIS deep blue channel also provides an approach of retrieving aerosol single-scattering albedo over land (Hsu et al., 2004).

The MISR multi-angle data sample scattering angles ranging from about 60˚ to 160˚ in mid-latitudes, yielding constraints on particle size, single-scattering albedo (SSA) (Kahn et al., 1998; 2001; 2005; 2010; Chen et al., 2008) and shape (Kalashnikova and Kahn, 2006). Having the ability to separate three-to-five bins in aerosol size (e.g., "small," "medium," and "large"), two-to-four bins in SSA, and spherical vs. non-spherical particles under favorable retrieval conditions, MISR can map aerosol-air-mass-types. These are derivations directly from the information content of MISR's observations, without the additional burden of the assumptions needed by MODIS to separate particle types. **Figure 3** shows such two examples that illustrate MISR's capability of characterizing the load and optical properties (size and shape) of smoke and dust plumes.

POLDER's unique capability of measuring spectral and angular polarization can yield additional insights into aerosol type. When the geometrical conditions are optimal (scattering angle ranging between 90°-160°), POLDER can derive the shape of coarse-mode particles over ocean (Herman et al., 2005). This allows for a discrimination of non-spherical, large dust particles from spherical, large sea-salt particles over ocean. Ongoing development of POLDER enhanced algorithms is expected to produce measurements of aerosol absorption and altitude (Tanré et al., 2011; Dubovik et al., 2011). OMI AAI can be used to distinguish UV-absorbing aerosols such as dust, smoke, and volcanic ash from

scattering aerosol like sulfate (Hsu et al., 1996; Herman J. et al., 1997). CALIOP allows for the measurements of particle depolarization ratio at 532 nm, a ratio of perpendicular component to parallel component of backscatter by aerosol particles, which can be used to distinguish non-spherical aerosol (e.g., dust, volcanic ash) from spherical aerosol (e.g., industrial pollution, biomass burning smoke, and marine aerosol) (Winker and Osborn, 1992; Cattrall et al., 2005). These quantities are of interest in–and-of themselves for identifying aerosol air mass types, and should also help further refine the accuracy of space-based AOD retrievals and particle property determinations.

The measurements of aerosol microphysical and optical properties can be used in conjunction with measurements of trace gases and identified source locations to improve aerosol characterization. SO_2 and NO_2 are important aerosol precursors that are now measured by OMI (Carn et al., 2007; Krotkov et al., 2008; Bucsela et al., 2006), the Global Ozone Monitoring Experiment (GOME) (Martin et al., 2002; Khokhar et al., 2005), and the Scanning Imaging Absorption Spectrometer for Atmospheric Chartography (SCIAMACHY) (Lee et al., 2008; Richter et al., 2005; Martin et al., 2006). The spatial and temporal correlations between concurrent measurements of AOD and tropospheric columns of NO_2 and SO_2 provide insights into regional pollution control of combustion processes (Veefkind et al., 2011). CO and fine particles have different atmospheric lifetimes, but have common sources from industrial pollution and biomass burning. Correlations between CO concentration and fine-mode AOD on different spatial and temporal scales can provide insights into aerosol emissions, transport, and chemical processes (Edwards et al., 2004; Bian et al., 2010). CO is now being derived from the

observations of the Measurements of Pollution in the Troposphere (MOPITT) (Deeter et al., 2003), AIRS (Warner et al., 2007), the Tropospheric Emission Spectrometer (TES) (Rinsland et al., 2006), and the Microwave Limb Sounding (MLS, for upper troposphere and low stratosphere (Livesey et al., 2008). In addition, satellite measurements offer the capability of identifying dust and smoke source locations. For example, AI has been used to identify major dust source regions (Prospero et al., 2002). Current satellites can detect active fires globally on a daily basis (see the review by Ichoku et al., 2012). These source identifications should provide additional constraints on microphysically based aerosol characterizations.

2.4. Feasibility of synergistic aerosol characterization

Rarely can a single sensor or variable provide unambiguous and complete aerosol characterization, because aerosol concentration and composition vary over a wide span of temporal and spatial scales. An approach that uses complementary information from multiple sensors can lead to improved aerosol characterization. Such synergy is feasible because of the recently formed A-Train, a constellation of satellites that overpass the equator within a few minutes of each other (Stephens et al., 2002). Radiance measurements from multiple A-Train sensors may be combined to retrieve new information of particle properties and/or improve retrieval accuracy (e.g., Jeong and Hsu, 2008; Satheesh et al., 2009). The process is challenging, and a great deal of effort is needed to explore the possibilities.

Currently the most often used multi-sensor synergy is to integrate retrieved products from several sensors to get more complete AOD coverage or constraints on aerosol properties

(e.g., Anderson et al., 2005; Christopher and Jones, 2007; Kalashnikova and Kahn, 2008; Satheesh et al., 2009; Yu et al., 2012b, 2012c). Such a synergy is particularly helpful in regions having complex mixtures of aerosol components. For example, the tropical Atlantic Ocean is often influenced in boreal winter by a complex mixture of dust and smoke transported from North Africa (e.g., Haywood et al., 2008; Tesche et al., 2009), which poses a big challenge to aerosol characterization and assessment of aerosol impacts (Yu et al., 2009b; Ben-Ami et al., 2012). **Figure 4a** shows a synergistic characterization of dust and smoke over the Gulf of Guinea on January 31, 2008 using a range of measurements from multiple A-Train sensors. OMI AI, a good indicator of elevated dust and smoke, shows two aerosol plumes, one in the northwestern part of the Gulf and another due south toward the coast. For convenience we refer to them as the "northwestern regime" and the "southern regime", respectively. The northwestern regime contains aerosol plumes with MODIS AOD of 0.7~0.9, AIRS CO of 2.9~3.1x10^{18} molecules cm^{-2}, and MODIS FMF of up to 0.8. The southern regime is characterized by higher AOD, up to 1.5, but relatively low CO (~2.8x10^{18} molecules cm^{-2}) and FMF (0.2~0.6). The FMF seems to anti-correlate with the incremental AOD/CO ratio (ΔAOD/ΔCO, which is calculated with background CO = 2.4 x10^{18} molecules cm^{-2} and AOD = 0.1). ΔAOD/ΔCO in the southern regime is 2~4x10^{-18} cm^2 $molecules^{-1}$, which is a factor of 2-4 larger than that in the northwestern regime. A higher ΔAOD/ΔCO indicates that not only biomass burning smoke contributes to the AOD enhancement (which would cause both AOD and CO to increase), but that dust aerosol also contributes (AOD increases but CO doesn't). These observations seem to consistently suggest that the northwestern regime is likely influenced more by fine-mode smoke than dust aerosol,

whereas the southern regime is influenced by dust and smoke mixed with a substantial dust contribution. The CALIPSO lidar measurements, albeit limited by their cross orbit coverage, provide layer structures of the plumes. The plume top in the northwestern regime is at about 1 km, much lower than 2-2.5 km in the southern regime. Also, the particulate depolarization ratio in the southern regime is somewhat higher than that in the northwestern regime, again indicating larger contribution of non-spherical dust in the southern regime. These observed distinct plumes over the Gulf can be further traced to their source regions through a HYSPLIT backward trajectory analysis (*Draxler and Rolph*, 2003), as shown in **Figure 4b** for two receptor locations, i.e., [9ºN, 15ºW] in the northwestern regime and [4ºN, 7.5ºW] in the southern regime. The air mass arriving at both locations on January 31, 2008 1400UTC had passed over the smoke-active Sahel region during the January 28-30 period (Tesche et al., 2009). During the January 26-27 period, the air mass arriving at [4ºN, 7.5ºW] passed over center of the Bodèlè Depression – the major source of Saharan dust in winter (Koren et al., 2006) and may have picked up a significant amount of dust, whereas that arriving at [9ºN, 15ºW] drifted north of the Bodèlè Depression. This case study demonstrates the advantage of multi-sensor synergy in characterizing aerosol type and long-range transport. Column-integrated aerosol properties observed by passive sensors are complemented by vertical layer structures observed by the active sensor. Aerosol type characterization based on particle size and shape is cross-examined with CO measurements and traced to source locations through the backward trajectory analysis.

The combination of polar-orbiting and geostationary satellite data could provide sub-daily information on the evolution of aerosol plumes during transport. Polar-orbiting satellites can sample a given location no more than twice a day, which is insufficient to capture diurnal or daytime variations adequately (Zhang et al., 2012). A use of geostationary satellite observations, such as half-hourly GOES AOD measurements, can characterize the daytime variations of intercontinental transport events (Kondragunta et al., 2008; Laszlo et al., 2008). Geostationary satellites can also capture diurnal variations of biomass burning smoke emissions with hourly or sub-hourly frequency (Zhang and Kondragunta, 2008; Reid et al., 2004), essential inputs to chemical transport models.

In summary, major advances have been achieved in both passive and active aerosol remote sensing from space in the last decade or so, providing better coverage, higher spatial resolution, improved retrieved AOD accuracy, and constraints on particle properties. Space-based lidars are for the first time providing global constraints on aerosol vertical distribution, and multi-angle imaging is supplementing this with maps of plume injection height in aerosol source regions. Satellite remote sensing of aerosols above clouds has also been demonstrated. Major advances have been made in distinguishing aerosol types from space, and the data are now useful for evaluating aerosol transport model simulations of aerosol air mass type distributions and transports, particularly over dark water. These advances provide unprecedented opportunities to develop a satellite-based approach, supplemented by in situ measurements and model simulations, to assess aerosol intercontinental transport. In the next section, we summarize major efforts and findings over the last decade and discuss future efforts at

maximizing the use of satellite observations to assess aerosol ICT and impacts on climate and air quality.

3. Application of Satellite Measurements to Characterizing and Estimating Aerosol Intercontinental Transport

The accumulation of satellite observations over the past decades has significantly advanced the understanding of aerosol intercontinental transport and its impacts on global and regional climate change and air quality. In this section we review how these observations have been employed to characterize the details of aerosol ICT episodes (3.1), study seasonal and inter-annual variations of aerosol ICT (3.2), and estimate the material fluxes of aerosols leaving a continent and arriving at another (3.3). In addition to these standalone observation-based applications, satellite measurements have also played an important role in evaluating and constraining model simulations of aerosol intercontinental transport (3.4). Both progress and challenges are discussed.

3.1 . Episode-based characterization of aerosol ICT from satellites

The daily or hourly observing frequency of satellites allows for tracking the evolution of significant aerosol ICT episodes, such as dust storm outbreaks, severe forest fire smoke, and abrupt volcanic eruption plumes. The extensive spatial coverage of satellite observations also helps establish linkages between in situ measurements in different locations that might be thousands of kilometers apart (Ansmann et al., 2009; Ben-Ami et al., 2010).

One of the first uses of satellites to characterize aerosol ICT episodes was simply to provide imagery of major aerosol events as those plumes crossed oceans. For example, Husar et al. (2001) used a combination of SeaWiFS, GOES 9, GOES 10 and TOMS UV aerosol index (UVAI) to analyze by hand the approximate location of a dust plume that developed over the Asian Gobi desert and then was transported across the Pacific Ocean over the course of 9 days. The arrival of the dust in the west shore as determined by satellite analysis, was consistent with elevated concentrations of dust particulate matter measured at in situ stations in California and Oregon. Although this satellite study and other similar ones provided little quantitative information about the aerosol transport, it was convincing illustration of aerosol transport across ocean basins.

Satellite analysis provided a more quantitative characterization of aerosol ICT in the 1980s and 1990s when applied to major volcanic eruptions that caused sulfate aerosol to form in the stratosphere. Solar occultation instruments such as the Stratospheric Aerosol and Gas Experiment I and II (SAGE and SAGE II), the Stratospheric Aerosol Measurements II (SAM II) or the Cryogenic Limb Array Etalon Spectrometer (CLAES) were able to track the spread of the El Chichon and Mount Pinatubo aerosol plumes as they spread from the point of injection above the volcano, eventually covering the entire tropical belt over the course of several years (Lambert et al., 1997; Bauman et al., 2003). These observations provided monthly and zonally averaged measures of aerosol extinction in the stratosphere, sometimes resolved into vertical profiles. Likewise the Advanced Very High Resolution Radiometer (AVHRR) followed the Mount Pinatubo

plume as long as it dominated the total column aerosol loading (Long and Stowe, 1994; Stowe et al., 1997; Stowe et al., 2002).

In contrast the EOS-era instruments offer a higher degree of quantitative characterization of episodic transport. For example, making use of the Terra-MODIS sensor's wide swath, validated AOD product and information that proportions AOD into fine and coarse modes, daily snap shots of the Earth's aerosol system became available (Remer et al., 2005). Applying temporal averaging to these daily global images and accumulating a year's set of images, animations were constructed that clearly showed intercontinental transport of fine and coarse particles [see Supplementary Online Material]. Saharan dust crossed the Atlantic not as a continuous stream, but in waves. Similarly, specific episodes of fine mode aerosol left the southeast U.S. for Europe and multi-modal aerosol crossed the Pacific as well-defined events.

However, the more significant EOS-era improvement was the ability to characterize particle properties, even beyond the simple designation of fine- or coarse-dominated AOD. Now satellites had opportunities for not only tracking the spatial extent of the influence of episodes, but also of characterizing particle property evolution during the cross-ocean transport. Kalashnikova and Kahn (2008) analyze the trans-Atlantic transport of four dust plumes during a peak dust season using MISR and MODIS aerosol products. They report the evolution of horizontal extent, AOD, particle size, and particle shape within the plumes. As dust is transported across the Atlantic, AOD and its non-spherical fraction systematically decrease, whereas Angstrom exponent increases. For the

thick part of the plume (AOD > 0.5), Angstrom exponent and spherical fraction of AOD increase by about 30% as the plumes travelled from the coast of North Africa to the Caribbean Sea. The study also demonstrates how a combination of complementary information from the two sensors can be used to gain better characterization of cross-ocean dust transport. MODIS provides more extensive coverage, whereas MISR's multi-angle retrievals include dust properties and fill in areas where glint precludes MODIS retrievals.

The most prevalent use of EOS-era satellite sensors to characterize aerosol ICT events or episodes makes use of the CALIPSO lidar that offers vertical profiling for identification of transport height, color ratio that provides qualitative particle size and depolarization that identifies non-spherical particles such as dust. With successive CALIPSO lidar profiles, Liu Z. et al. (2008) track the cross-Atlantic transport of a dust plume that originated in the Sahara desert on August 17, 2006 for a period of 10 days. They found that it took about a week for the dust plume to reach the Caribbean from North Africa, as the optical depth decreased significantly and the plume top descended by about 3.3 km. However, unlike the plumes studied with MISR observations (Kalashnikova and Kahn, 2008), the size and shape of the dust particles didn't show discernable changes during transport. After entering the Caribbean region, the transport slowed, and dust was mixed with other types of aerosol over the Gulf of Mexico, as indicated by changes in color ratio and lidar ratio.

Trans-Pacific transport of dust has also been characterized by using successive CALIOP curtains in conjunction with other satellite sensors or models, including Huang et al., (2008), Uno et al. (2008), Eguchi et al. (2009), Uno et al. (2009), Yumimoto et al. (2009), and Uno et al. (2011). **Figure 5** shows a three-dimensional view of the hemispherical journey of strong dust event originated from the Taklimakan desert during May 09-22, 2007 as provided by CALIOP for vertical distributions of depolarization ratio (a) and extinction coefficient (b), and a global aerosol transport model for horizontal distribution of dust extinction coefficient (c) (Uno et al., 2009). The HYSPLIT trajectory also illustrates the dust transport path in both horizontal and vertical directions. For this extreme dust storm, dust was lofted to 8-10 km and was transported to the mid-Pacific in 4 days, and in about 13 days, it traveled more than one full circuit around the Northern Hemisphere. On returning to the northwestern Pacific Ocean, the dust then descended within a large-scale high-pressure system.

Strong smoke and volcanic eruption events have also been characterized by satellite measurements. Dirksen et al. (2009) use OMI and CALIOP measurements to track a smoke aerosol plume released by intense forest fires in Australia that circumnavigated the world in 12 days. The study highlights the need to include the effect of pyro-convective lofting and the effect of smoke absorption on the atmospheric thermodynamics in global models. CALIPSO lidar data have also been used to characterize the transport of ash from the Eyjafjallajokull volcano in April 2010, including height and vertical extent of the layers and particle shape during both day and night (Winker et al., 2012). The

observed particle layers have strong lidar depolarization similar to mineral dust, suggesting the predominance of ash over sulfate in the plumes (Winker et al., 2012).

The transport of aerosols from mid-latitudes to the polar regions has great implications for climate change. Satellite measurements, in particular those from the active sensor CALIOP over day and night, are useful to some extent for characterizing transport events of eastern Asian aerosols to the Arctic (Di Pierro et al., 2011) and of Patagonian dust to Antarctica (Gasso and Stein, 2007; Li et al., 2010). However, the usually low aerosol loading in polar regions requires a space-borne lidar with a detection limit lower than CALIOP. In comparison to active sensors, passive sensors have much greater difficulties in detecting the poleward transport of aerosols at high latitudes, because of low solar signal and hence more uncertain aerosol retrieval, and the presence of abundant clouds in the roaring forties (Gassö and Stein, 2007; Li et al., 2010).

3.2 Climatological characterization of aerosol ICT from satellites

The long-term duration of satellite measurements makes it feasible to derive the seasonal and inter-annual variations of aerosol ICT. Satellite aerosol products are easily accumulated and averaged, and when these statistics are derived over oceans, we assume that the elevated aerosol loading is due to transport from continents. However, without additional information, either from tracking specific events, analysis of ancillary meteorological data, or model trajectories, the statistics of oceanic aerosol retrievals cannot be directly attributed to transport from a specific location. It helps if satellites provide additional information about the particle properties to identify certain mean

aerosol loading to be associated with an aerosol type originating from continents (e.g., dust or combustion particles.)

Seasonal variations of trans-Atlantic dust transport have been extensively studied using measurements from passive sensors, often supplemented with ancillary data, (e.g., Kaufman et al., 2005c; Schepanski et al., 2009; Huang et al., 2010; Ben-Ami et al., 2012; Ridley et al., 2012) and active sensors (Generoso et al., 2008; Ben-Ami et al., 2009; Huang et al., 2010; Yu et al., 2010; Ridley et al., 2012). An analysis of aerosol observations from TOMS, AVHRR, and MODIS looked for intra-seasonal variations in AOD over the tropical Pacific and Indian oceans, with inconclusive results due to difficulties in interpreting the satellite products on relatively short spatial and temporal scales in these regions (Tian et al., 2008). However, a follow-up study applied the same technique over the tropical Atlantic, and showed that about 25% of the total variance of MODIS AOD can be accounted for by the intra-seasonal variability related to the Madden-Julian Oscillation (MJO) (Tian et al. 2011). Given that dust and smoke are often mixed in winter and spring (Haywood et al., 2008), several studies have attempted to separate dust from other aerosols in their analysis (Kaufman et al., 2005c; Liu D. et al., 2008; Huang et al., 2010; Yu et al., 2010; Ben-Ami et al., 2012). This separation can be done by using depolarization from CALIOP (Liu D. et al., 2008), by retrieving detailed aerosol particle properties from multi-angle and/or polarization measurements (Kahn et al., 2007; Herman et al., 2005) or by combining size parameters derived from satellite sensor with assumptions gleaned from climatological analysis (Kaufman et al., 2005a, 2005c; Yu et al., 2009b).

The lidar depolarization method makes use of the fact that spherical particles such as pollution, smoke and sea salt do not create a depolarization signal, but irregularly shaped, large dust particles do (McNeil and Carswell, 1975). It has been observed that mineral dust has a high depolarization ratio of 0.2-0.4 (Barnaba and Gobbi, 2001; Murayama et al., 2001; Liu et al., 2002; Mattis et al., 2002; Liu Z. et al., 2008), whereas other types of aerosol have near zero depolarization ratios. Therefore this depolarization signal allows the lidar to determine dust layers in the vertical profile (Winker and Osborn, 1992).

Dust can also be separated from combustion particles such as smoke and pollution when a sensor characterizes the multi-dimensional reflectance field, including multiplewavelengths across a broad spectral range, multiple angle over a wide range of scattering angles and polarization states (Dubovik and King, 2000; Mishchenko et al., 2005). Different subsets of the full characterization offer different capabilities. MISR provides multi-wavelength, multi-angle measurements and provides retrievals of particle properties of which nonsphericity is the most important for identifying dust (Kalashnikova and Kahn, 2006; Kahn et al., 2007). PARASOL-POLDER is also multi-wavelength, multi-angle instrument and adds polarization, making it also capable of directly retrieving sufficient information on particle properties to discern dust (Herman et al., 2005).

On the other hand, MODIS with its single angle view of each scene and no polarization does not measure sufficient information to directly retrieve the particle properties that

unambiguously identify dust. Following Kaufman et al. (2005a), the MODIS studies assume:

$$\tau = \tau_{du} + \tau_{co} + \tau_{ma} \quad (1)$$

$$\tau_{fine} = f\,\tau = f_{du}\,\tau_{du} + f_{co}\,\tau_{co} + f_{ma}\,\tau_{ma} \quad (2)$$

where Eq. 1 assumes that the total AOD (τ) retrieved by MODIS is composed of a dust component (τ_{du}), a combustion aerosol component (τ_{co}) and a marine aerosol component (τ_{ma}). Eq. 2 assumes that the fine mode AOD ($\tau_{fine} = f\,\tau$, the fraction of the total AOD contributed by fine particles) is composed of a sum of the fine mode AODs of each component in Eq. 1. Note that the fine mode fraction (f) is the ratio of fine mode AOD and the total AOD,

$$f = \frac{\tau_{fine}}{\tau} \quad (3)$$

MODIS derives two pieces of information, the total AOD (τ) and the fine-mode fraction (f). This means that all but two of the parameters on the right hand side of Eqs. (1) and (2) must be assumed. The assumed quantities are f_{du}, f_{co}, f_{ma} and τ_{ma}. The values for these assumptions are taken from MODIS retrievals of f and τ in regions that are expected to be pure dust, pure combustion aerosol etc. f_{ma} was found to vary spatially and seasonally (Yu et al., 2009b) and is therefore a function of location and time. Given these assumptions and the MODIS direct retrievals of f and τ, τ_{du} and τ_{co} can be inferred.

Note that at no point in this method is it assumed that dust is pure coarse mode ($f_{du} \neq 0$) or combustion aerosol is pure fine mode ($f_{co} \neq 1$), but the actual values are fixed for a given season and region, and are obtained as described above.

Because each sensor, to differing degrees of quantification accuracy, can discern dust from the total aerosol signal observed, all have been used to characterize seasonal and inter-annual variations of dust transport. As an illustration, **Figure 6** shows a multi-sensor (including MODIS, MISR, and PARASOL) view of seasonal variations of trans-Atlantic dust transport and its comparison with the Goddard Chemistry Aerosol Radiation Transport (GOCART) model. In general, these satellite observations and the model show consistent seasonal variations of trans-Atlantic dust transport, i.e., stronger in summer and spring than in winter and fall. On the other hand, notable differences exist in the magnitude of dust AOD. For example, although PARASOL only senses the coarse-mode non-spherical particles in this plot (Tanré et al., 2011), its AOD value is comparable to the sum of fine-mode and coarse-mode dust AOD as seen by MODIS and MISR. Note that fine-mode dust makes significant (e.g., 37%) contributions to the total dust AOD for MODIS observations (Yu et al., 2009b). In the Gulf of Guinea, MODIS and PARASOL show much higher dust AOD than MISR and GOCART do in winter. The complexity of dust and smoke mixture in the region creates a challenging environment for distinguishing dust from smoke using satellites (Kahn et al., 2009; Yu et al., 2009b). In such a situation, MISR would be the sensor of choice, though the known issues with that product (e.g., Kahn et al., 2010) should also be taken into account. As PARASOL algorithms are further developed to make better use of the full complement of its

measurements and information content (Dubovik et al., 2011), we anticipate that its retrievals will draw closer to MISR's.

In comparison to the satellite observations, GOCART modeled cross-ocean transport generally drifts southward in summer and decays more rapidly (i.e., weak transport efficiency). Such differences are apparently not limited to the GOCART model, as several other models show similar deviations from satellite observations (e.g., Generoso et al., 2008; Huneeus et al., 2012; Ridley et al., 2012). Reasons for such observation-model discrepancies are not yet fully understood. It has been argued that model treatment of aerosol removal processes needs to be improved (Generoso et al. 2008; Prospero et al., 2010; Huneeus et al., 2012; Ridley et al., 2012). Dust can influence the cross-ocean transport, through its feedbacks on atmospheric circulations and the water cycle, that are not accounted for in most CTMs. For example, Lau et al. (2009) found that dust absorption can enhance rainfall and cloudiness over the West Africa and Eastern Atlantic Intercontinental Convergence Zone (ITCZ), but suppresses rainfall and cloudiness and rainfall over the West Atlantic and Caribbean region. Wilcox et al. (2010) found that Saharan dust outbreaks coincide with a northward shift of the North Atlantic Ocean ITCZ in summer. If these feedbacks and coincidences are supported by independent observations and can be reproduced by aerosol models, the modeled summertime cross-ocean transport would have shifted northward and the transport efficiency or the gradient of dust AOD between the East and West Atlantic would increase.

The seasonal variations of columnar AOD observed by passive sensors are complemented by lidar measurements of aerosol vertical distributions. Recently available

CALIPSO data confirm the previously observed seasonal differences of trans-Atlantic dust transport heights, namely higher in summer than in winter (Generoso et al., 2008; Ben-Ami et al., 2009; Huang et al., 2010; Yu et al., 2010; Ridley et al., 2012). These same analyses also show that a significant part of the dust is transported near and within the marine boundary layer, suggesting significant dust deposition to the ocean and hence important implications for ocean biogeochemistry. Vertical structures of dust and pollution transport on global and hemispherical scales have also been analyzed using CALIOP measurements (Liu D. et al., 2008; Yu et al., 2010; Ford and Heald, 2012; Koffi et al., 2012).

Decadal-scale satellite measurements of aerosols, many relying on pre-EOS-era satellites to obtain longer time series, have been used to study inter-annual variations of aerosol ICT and their controlling factors. Such studies are not necessarily trend studies, which are particularly sensitive to calibration drift in the sensors (Levy et al., 2010; Zhang and Reid, 2010). If focused on a particular region with high aerosol loading and strong interannual amplitudes, the aerosol variability can be distinguished above sensor artifacts (Zhang and Reid, 2010). Several studies have investigated interannual variation in the export of Saharan dust using satellite data. Moulin et al. (1997) used daily Meteosat observations of dust from 1984-1994 and found that inter-annual variability of dust export to the North Atlantic Ocean and the Mediterranean Sea are well correlated with the North Atlantic Oscillation (NAO). By using multi-decadal TOMS AI and ground-based dust measurements, Chiapello et al. (2005) found that the Sahel drought has a large-scale impact on dust emissions and trans-Atlantic transport in both the subsequent

winter and summer, and that the NAO controls the northern branch of wintertime transport. Doherty et al. (2008), also using the multi-decadal TOMS AI data, found that African dust is transported into the Caribbean via two routes associated with distinct source regions and controlled by different meteorology. In the northern mode, dust mobilized from the Sahara is transported westward, controlled primarily by the longitudinal displacement of the Azores High. In contrast, in the southern mode, dust originating from the Sahel region is transported to the Caribbean via the Gulf of Guinea, controlled primarily by longitudinal displacement and surface pressure fluctuations of the Hawaiian High. Note that the pre-EOS era sensors of Meteosat and TOMS sensors alone cannot distinguish dust from smoke in the above studies, whereas it is necessary to assess how inter-annual variations of smoke aerosol may have contributed to the analyzed inter-annual variations of dust.

Climatology of aerosol parameters has been constructed from the EOS-era satellites (Remer et al, 2008; Dey and Di Girolamo, 2010 ; Tanré et al., 2011). These do show interannual variability of the aerosol system, including interannual variability of aerosol distribution across ocean basins. Nevertheless the question of the variability of ICT specifically is not adequately addressed in these relatively short time series. Undoubtedly, an aerosol data record longer than the 10 years of EOS-era satellite observations is essential for a better understanding of the climate impacts of aerosol ICT and controlling processes. There have been a few attempts at extending the relatively short EOS era datasets by using pre-EOS sensors as proxies. Evan and Mukhopadhyay (2010) attempted to extend the MODIS-estimated dust AOD (Kaufman et al., 2005c)

over the northern tropical Atlantic back to 1955 by simply scaling AVHRR total AOD with the MODIS dust AOD fraction and using a proxy record of atmospheric dust (namely crustal helium-4 flux from a coral 5 m under the water near Sal Island). However, such an extension would be more credible if build upon understanding and reconciliation of AOD differences between the EOS-era and historic sensors (Jeong et al., 2005). For this a closer examination of relevant issues associated with individual sensors is urgently needed, including instrument calibration, algorithm assumptions, cloud screening, data sampling and aggregation, among others (Zhao et al., 2008). Substantial efforts have been dedicated toward addressing these issues across the EOS-era sensors (Zhang et al., 2005; Kahn et al., 2009; Levy et al., 2009; Zhang and Reid., 2010). However, the cross examination of EOS-era sensors and historical sensors remains basically unexplored. A reliable long-term data record will only be accessible after these issues have been adequately addressed.

3.3. Estimates of aerosol export and import mass flux from satellites

The vast majority of studies that address aerosol ICT using satellite data alone have fallen under the subject of the previous two sections: characterizing specific events and episodes, or providing insight into seasonal and interannual variation. These studies progressed from qualitatively following an aerosol plume across ocean basins, to gradually adding quantitative information about the evolution of particle properties and height. The aerosol climatology across ocean basins could be interpreted as aerosol transport, with the relative changes from season-to-season or year-to-year identified, even if the quantitative total transport was not addressed. In recent years, a few studies have

taken advantage of the advances in aerosol remote sensing to quantitatively estimate the trans-Atlantic transport of dust mass (Kaufman et al., 2005c; Koren et al., 2006), trans-Pacific transport of combustion aerosol mass (including industrial pollution and biomass burning smoke) (Yu et al., 2008) and dust mass (Yu et al., 2012c), and cross-Mediterranean Sea transport of European pollution mass (Rudich et al., 2008).

Such estimates of material fluxes in continental outflows and inflows generally follow a three-step approach. First, satellite measurements of AOD and aerosol microphysical properties (e.g., size, shape) are used to distinguish mineral dust from combustion-related aerosol (Kaufman et al., 2005a; Yu et al., 2009b; and Section 3.2). Second, AOD for dust or combustion aerosol is converted to aerosol (dry) mass concentration profile using in-situ measurements of aerosol hygroscopic property (depending on relative humidity and aerosol type) and lidar measurements of aerosol vertical distributions (Yu et al., 2008, 2012). Third, the aerosol mass concentration in combination with zonal wind speed is used estimate the zonal export and import of aerosol.

There has been a progression in these studies as new information became available. The first study of this type (Kaufman et al., 2005c) determined aerosol height from a few field experiments, confirmed by applying a technique that used paired Terra and Aqua MODIS images to determine transport displacement over a few hours and correlated this with wind speed at various heights using reanalysis data (Koren and Kaufman, 2004). They also assumed single value for $f_{ma,}$ f_{du}, and f_{co}. In contrast, the most recent study of this type (Yu et al., 2012c) uses CALIPSO lidar-derived climatology to determine transport

height, and accepts that f_{ma} varies as a function of latitude and season (Yu et al. 2009b). Furthermore, the backbone of these studies is the MODIS aerosol AOD, which has undergone considerable refinement over the 7-year span of these studies, including the option of selecting a severely cloud-cleared and uncontaminated product (Shi et al., 2011) that was used by Yu et al. (2012c) to correct cloud contamination in AOD.

The satellite-based estimates of aerosol import and export in the zonal direction have offered important insights into aerosol intercontinental transport and its impacts on regional air quality, climate change, and biogeochemical cycle. Kaufman et al. (2005c) estimated that out of the 240±80 Tg of dust transported annually from Africa to the Atlantic ocean, 140±40 Tg is deposited in the Atlantic ocean and 50± 15 Tg reaches and fertilizes the Amazon basin. This estimated dust input to the Amazon basin is four times the previous estimate by Swap et el. (1992), which might explain a paradox regarding the source of nutrients for the Amazon forest. Koren et al. (2006) further estimated that about half the annual dust supply to the Amazon basin is emitted from a single, small-area spot, namely the Bodèlè depression, located northeast of Lake Chad. Recently, model sensitivity studies have argued that these estimates may represent the upper bound (Schepanski et al., 2009; Ridley et al., 2012), because of uncertainties associated with the assumed aerosol vertical distributions (Schepanski et al., 2009). On the other hand, model simulations tend to give a lower bound, due to excessive wet removal in models (Ridley et al., 2012; Huneeus et al., 2012).

Trans-Pacific aerosol transport and its contribution to North America have been assessed based on satellite measurements by Yu et al. (2008) and Yu et al. (2012c). **Figure 7** shows the satellite-based estimate of meridional variations of annual trans-Pacific dust and combustion aerosol import to North America (at the west shore) and its comparisons with GOCART and the Global Modeling Initiative (GMI) model simulations. The satellite-based estimate of trans-Pacific import is 60 Tg yr^{-1} with an estimated uncertainty of 55-100%, which is predominated by dust (about 90%) entering the west shore between 30°-50°N. The GOCART and GMI model is respectively lower than satellite-based estimate by 15% and 42%. The much lower import by GMI presumably results from very efficient dust scavenging by convection in the model. Also the satellite-based estimate is generally higher than model simulations in regions south of 50°N, but are lower north of 50°N. By taking into account the trans-Atlantic dust import (north of 20°N) of 4 Tg yr^{-1} (Kaufman et al., 2005c), the total aerosol import to North America is estimated at 64 Tg yr^{-1}, which is comparable to the estimated total (69 Tg yr^{-1}) of domestic emissions and production of aerosols (Yu et al., 2012c). The air quality impact of imported aerosols may be minor, because the transport occurs predominantly above the boundary layer, as indicated by CALIPSO lidar measurements (Yu et al., 2012c). However, the imported dust and combustion aerosol can have significant impacts on weather and climate. Yu et al. (2012c) estimated that dust and combustion aerosols from intercontinental transport collectively introduce a reduction of cloud-free net solar radiation of -1.7 and -3.0 Wm^{-2} at top-of-atmosphere (TOA) and surface, respectively, which represents 31% and 37% of the total direct aerosol radiative effect over North America. For comparison, a recent model simulation estimates that the decrease of US anthropogenic aerosols over 1990-

2010 yields a decrease of 0.8 Wm^{-2} for all-sky direct radiative forcing at TOA (Leibensperger et al., 2012). Besides the aerosol direct radiative effects, the imported aerosols could have other significant impacts, such as changing atmospheric stability by absorbing solar radiation (Yu et al., 2002; Ramanathan and Carmichael, 2008), altering cloud and precipitation processes through acting as ice nuclei (Sassen et al., 2002; Ault et al., 2011), and accelerating the melting of snow in the Sierra Nevada by deposition on snow (Hadley et al., 2010). It is possible that a change in meteorological conditions resulting from these processes could further influence surface PM concentrations and air quality. These potential impacts need to be investigated with the state-of-the-science modeling.

The dust deposition into oceans has important implications for ocean biogeochemistry and climate (Jickells et al., 2005; Mahowald et al., 2005). Considering that aerosol meridional transport is generally much weaker than zonal transport, a difference between zonal export and import could be considered as a proxy for aerosol depositional flux into the ocean during the cross-ocean transport. The ratio of import to export flux is generally referred to as "transport efficiency". For the same export in continental outflow, higher transport efficiency generally corresponds to lower aerosol deposition over ocean. **Table 2** compares satellite-based estimates of the trans-Pacific dust transport efficiency and dust deposition to the North Pacific (Yu et al., 2012c), with results based on model simulations and in situ observations in the literature. The annual trans-Pacific dust transport efficiency is estimated at about 40% from MODIS and CALIOP measurements (Yu et al., 2012c), which is at the upper bound of the model simulations listed in Table 2

(15-43%). Note that the highest model value of 43% is estimated for an extreme event, where dust was transported rapidly at 8-10 km elevation (Uno et al., 2009), whereas the lowest model value of 15% was estimated for dust transport in summer, when dust removal from atmosphere is faster and dust transport is slower than in other seasons. The trans-Pacific dust transport efficiency is also reasonably higher than the 26% for trans-Pacific pollution aerosol estimated from satellite (Yu et al., 2008), because dust is transported at generally higher altitudes than the pollution aerosol (Yu et al., 2012c). Satellite-estimated dust deposition to the North Pacific of 84 Tg a^{-1} is compared to the estimated range of 31-96 Tg a^{-1} in the modeling literature. (These values exclude the highest and lowest estimates from two early studies, as well as two estimates made only over the East China Sea.)

The satellite-estimated mass fluxes are subject to large uncertainties, on an order of 55-100% (Yu et al., 2008; 2012c). Major sources of uncertainty include satellite-derived component AOD, mass extinction efficiency, hygroscopic properties, transport height, and satellite sampling (Yu et al., 2008; Kaufman et al., 2005c). To accurately assess the potentially large impacts of aerosol ICT, the uncertainties represented by the above studies must be significantly reduced. The component AOD derived from MODIS measurements entails significantly larger uncertainties than the total AOD. As discussed in section 2 and demonstrated by Kalashnakova and Kahn (2008), by combining the MODIS observations with aerosol type retrievals from other sensors such as CAILPSO, AIRS, or MISR, component AOD can be derived with better accuracy.

Determining seasonally and geographically dependent aerosol vertical profiles or transport heights is another major source of uncertainty in estimating the aerosol mass fluxes (Yu et al., 2008; Schepanski et al., 2009). To calculate mass fluxes, vertical profiles are needed for selecting representative wind speed, and representative RH to account for particle growth by humidification. The sensitivity of aerosol mass flux to transport height varies with region and season, depending on wind shear patterns and atmospheric humidity profiles. The CALIPSO lidar measurements have recently been used to determine the climatology of aerosol vertical distributions over broad areas with seasonal distinctions (e.g., Liu D. et al., 2008; Huang et al., 2010; Yu et al., 2010, 2012c), which provide tighter constraints on the estimated material fluxes. Because of the near-zero swath of CALIPSO lidar, however, it is difficult to examine daily variations of aerosol fluxes. Because of CALIPSO's low sensitivity to vertically resolved extinction, some aerosol plumes having moderate AOD but large vertical extent may be missed by the lidar. This drawback can be mediated by suborbital measurements at key locations to calibrate the satellite data sets.

Several satellite-sampling issues also contribute to the uncertainties in the flux estimates. The above studies have only used polar-orbiting satellite measurements, having sampling frequency of no greater than twice per day. An integration of polar orbiting and geostationary satellites could be pursued to characterize the diurnal variations of aerosol export and import. Current studies have also assumed that dry aerosol mass derived from satellite retrievals in cloud-free conditions are representative of all-sky conditions, even over frontal cloud systems. Unlike in broken cloud fields where satellite retrievals of

aerosols are sometimes possible in the gaps between clouds, frontal cloud systems usually extend over wide areas and completely eliminate aerosol retrievals in those areas using current approaches. For example, because the trans-Pacific transport is associated with the warm conveyor belt (WCB), and the WCB is associated with rising air in warm fronts that also produce widespread cloudiness, passive sensors such as MODIS can miss important transport events. If dry aerosol mass in these events is significantly different from that observed under cloud-free conditions, the estimated aerosol flux could have large uncertainties or biases. It has been suggested that a variety of compensating processes in and nearby clouds control the formation and removal of aerosols and hence determine their loading. While clouds can effectively remove aerosols through scavenging and rainout, they can also generate aerosol (e.g., in-cloud aqueous production of sulfate). Some studies suggest that significant biases may exist in some regions, when satellite measurements only for cloud-free conditions are assimilated into a model (Reid et al., 2004; Zhang and Reid, 2009). Recent developments in satellite retrievals as discussed in section 2.2, could provide partial constraints on the aerosol load above clouds.

3.4. **Evaluation and constraint of model simulations by satellite measurements**

The previous sections addressed the contribution that satellites make towards characterizing aerosol ICT when satellite data is used exclusively. Satellites also make a contribution when they work in support of model simulations. The satellite role in support of modeling efforts of intercontinental aerosol transport takes generally three paths: (1) characterization of the aerosol sources including location, timing, injection

height, and magnitude of emissions, (2) evaluation of aerosol transport simulations, and (3) assimilation of aerosol products into the model for improving model forecasts.

3.4.1 Source characterization

For a model to properly simulate aerosol distribution and transport, it must first incorporate accurate location, timing, and magnitude of particles and gaseous precursor emissions. In comparison to industrial emissions, episodic emissions such as biomass burning smoke from fires and mineral dust from dust storms are more difficult to accurately represent in a model. Correct transport modeling of smoke aerosol is almost entirely dependent on satellite-derived products that either identify and count fire hotspots or more quantitatively measure fire radiative power and relate that to aerosol emissions (Ichoku et al., 2008; Pereia et al., 2009; Reid et al., 2009; Giglio et al., 2010; van der Werf et al., 2010; Ichoku et al., 2012 and references therein; Petrenko et al., 2012). The diurnal pattern of smoke emissions can be determined by applying overpasses at multiple times per day by the twin MODIS sensors on the polar orbiting Terra and Aqua satellites (Vermote et al., 2009; Ichoku et al., 2008), or using geostationary satellite observations (Zhang and Kondragunta, 2008). For mineral dust, most models rely on satellite data of land surface classification to identify the location of deserts, and a few models use satellite vegetation index data to impose the seasonal variation of the surface bareness for better temporal variation of dust emission (e.g., Zender et al., 2003; Kim et al., 2012). More direct use of satellite AOD for dust emission has merged, such as the AOD distributions from MISR (Koven and Fung, 2008), Meteosat SEVIRI (Schepanski, et al., 2007) or more recently MODIS Deep Blue (Ginoux et al., 2012). Satellite

observations have also been used to cap the total emissions of carbonaceous aerosol (Heald et al., 2010).

Satellites also contribute directly to aerosol source characterization through inverse modeling techniques. In these techniques an observed satellite field such as satellite-derived AOD or measured radiances are used in conjunction with a transport model to identify the sources and estimate the emissions that produced the observed field. Examples of this technique include Dubovik et al., (2008), who combined MODIS AOD observations with the GOCART transport model to characterize global aerosol sources of fine particles, Yumimoto et al. (2010) who combined lidar data and model, and Wang et al., (2012) who combined MODIS-observed radiances with the GEOS-Chem model, focusing on Asian dust sources.

Because heat from fires can propel particles quickly out of the boundary layer to higher layers of the atmosphere, these particles are sometimes injected into faster-flowing air streams. The resulting transport will be different from a model simulation that fails to consider such fast convective processes and instead leaves the particles in the slower moving boundary layer, where more efficient removal occurs. The importance of injection height has been discussed in context of boreal fire smoke in Canada being transported over the U.S. eastern seaboard (Colarco et al., 2004) and Amazon biomass burning smoke (Freitas et al., 2006). Satellites have made a major contribution here, especially the multi-angle MISR that uses stereo views and parallax to determine the heights of well defined smoke plumes (Kahn et al., 2007), and CALIOP that provides

vertical aerosol profiles (Amiridis et al., 2010). These products offer models information on injection heights for specific cases. The two products are complementary, as MISR provides greater coverage than the curtain-wide CALIOP, whereas CALIOP offers greater details in the vertical and provides the height of smoke after it becomes diffuse (Kahn et al., 2008). Val Martin et al. (2010) pushed one step beyond the individual case studies by establishing a climatology of injection heights using five years of MISR data over North America, as shown in **Figure 8**. This climatology linked the 4-12% of the plumes that permeated the boundary layer, based on MISR data, with specific meteorological conditions and with higher fire radiative power measured by the MODIS sensor. Guan et al. (2010) found the linear relationship between coincident OMI AAI and CALIOP plume height for young biomass burning plumes, allowing the identification of high-altitude plumes in the multi-decadal TOMS and OMI AAI data, and hence making it possible to construct a data set for validating global fire plume heights in chemistry transport models. These associations from satellite products, begin to give the modeling community the information they need to develop and refine plume rises models, so smoke from fires can be placed at the correct altitude within the model, thus improving aerosol transport modeling (Sessions et al., 2011). Injection heights have been characterized by satellite also for dust plumes (Kahn et al., 2007; Yumimoto et al., 2009) and volcanic plumes (Haywood et al., 2010; Scollo et al., 2010).

3.4.2 Model evaluation

Satellite observations of AOD and vertical distributions have been used extensively to evaluate model simulations, which in many cases is the best way to bound model

estimates of aerosol transport. One of the earliest uses of satellites to evaluate model simulations of aerosol transport was Tegen et al., (1997) who showed both the advantages and challenges of matching model results with satellite products, in their case AOD from AVHRR. Their comparisons revealed both model inaccuracies and retrieval problems. Other studies followed, to the point that model comparison against satellite AOD has become almost a standard requirement. In the 1990s and 2000s, the comparisons relied on the TOMS and AVHRR products (e.g., Chin et al., 2002) or simple imagery (Colarco et al., 2003). When EOS-era aerosol satellite products became available, studies made use of the new, more quantitative products, mostly MODIS AOD, but also MISR AOD over land and ocean (Chin et al., 2004; Heald et al., 2006; Colarco et al., 2010; Ford and Heald, 2012; Ridley et al., 2012). Evaluation can also include comparison of Angstrom Exponent or size parameter (Colarco et al., 2010) and anthropogenic component of AOD (Yu et al., 2009b; Yu et al., 2012a). A composite of multiple satellite products, pre- and post-EOS era, became the standard to which the AEROCOM ensemble of models were held (Kinne et al., 2006). Then with the addition of CALIOP, the ability to evaluate the vertical distribution of aerosol became possible (Generoso et al., 2008; Yu et al., 2010; Koffi et al., 2012; Ridley et al., 2012).

An evaluation of GOCART three-dimensional distributions of aerosols with MODIS and CALIOP measurements on a global scale is shown in **Figure 9** and **10** (Yu et al., 2010). Figure 9 shows a comparison of GOCART AOD with collocated CALIOP and MODIS AOD, and Figure 10 compares the aerosol scale height between GOCART simulations and CALIOP measurements. The aerosol scale height is defined as a characteristic

altitude below which 63% of total columnar AOD is present. As shown in Figure 9, CALIOP, MODIS, and GOCART give generally consistent spatial patterns of AOD and its seasonal variations, with major continental source regions and the trans-Atlantic transport of Saharan dust being readily identified. Several major differences are evident on regional and continental scales. One of other most pronounced differences is associated with the intercontinental transport of aerosols. Both MODIS and GOCART show that the trans-Pacific transport of aerosol from East Asia to North America is fairly strong in MAM, with AOD greater than 0.15 over the nearly entire mid-latitude North Pacific. However, the CALIOP observations show a much weaker trans-Pacific transport. Similar differences also exist for the trans-mid-Atlantic transport of aerosol from North America to West Europe. On the contrary, the westward transport of aerosol, mainly Saharan dust, by trade winds over tropical Atlantic is stronger and more extended from MODIS and CALIOP observations than the GOCART model.

As shown in Figure 10, the GOCART aerosol scale heights are consistently higher than the CALIOP observations. The differences are particularly large at the polar regions and northern hemispheric mid-latitudes away from the source regions where aerosols are generally transported from outside. The long-range transport of aerosol in these regions is usually associated with mid-latitude cyclones that can effectively lift pollution from the atmospheric boundary layer (ABL) to the upper troposphere. Note that the general high bias of modeled aerosol scale height is not limited to GOCART model, as indicated by a recent AeroCom comparison that involves a dozen models (Koffi et al., 2012). As discussed in Yu et al. (2010), the much lower CALIOP scale height than model

simulations in these regions may result from the CALIOP sampling of cloud-free observations that may bias the scale height to low altitudes. CALIOP may miss to detect some optically thin layers in the FT because of the detection limit of lidar, resulting in lower scale heights. It is also possible that models overestimate the vertical transport of aerosols and gives higher scale heights.

Comparisons of model simulations against satellite observations provide valuable hints for improving model representations of crucial processes such as aerosol scavenging removal (Bourgeois and Bey, 2011; Ridley et al., 2012) and the rise of smoke plumes (Sessions et al., 2011; Dirksen et al., 2009). Most recently, Ridley et al., (2012) demonstrate the extent to which a suite of satellite products can be used to evaluate a model's ability to simulate aerosol transport, in this case multi-year Saharan dust transport over the Atlantic. The model is shown to capture the variability of these dust plumes by correlation with MODIS and MISR and to match the vertical distribution of the plumes as they exit the African continent by quantitative comparison with CALIOP. They also find that the lifetime of the simulated dust is a few days shorter than that observed from satellite. Comparison of model rain rates with TRMM satellite-derived rain rates shows that wet deposition in the model is too strong.

3.4.3 Integrated approach

Integrating satellite measurements and aerosol transport models is necessary for a comprehensive characterization of aerosol intercontinental transport. On one hand, satellite measurements provide observational evidence of aerosol intercontinental

transport that can be quantitative (Section 3.3). However, these observations are restricted by limited satellite capabilities such as observing only once or twice daily, and for most sensors, only under cloud-free conditions. Space-borne lidars add an essential third dimension to the characterization, but lidars are limited by extremely narrow swaths and poor spatial sampling. On the other hand, model simulations offer a much more comprehensive picture of aerosol intercontinental transport by providing multi-dimensional characteristics of aerosol in a continuous manner, including clearly distinguishing by aerosol species. But they are limited by their imperfect ability to simulate physical and chemical processes in the atmosphere. A number of studies have used this satellite-model integrated analysis approach to characterize the intercontinental transport of dust and pollution aerosol (Eguchi et al., 2009; Hara et al., 2009; Itahashi et al., 2010; Uno et al., 2008, 2009, 2011; Yumimoto et al., 2009, 2010).

Satellite aerosol products can be assimilated into run-time models to actively nudge models towards real-world conditions, often producing better representation of the aerosol field and aerosol transport. This is especially useful for real-time aerosol forecasting. One of the earliest examples of aerosol assimilation involved the Model of Atmospheric Transport and Chemistry (MATCH) and how it was applied to the INDOEX experiment in 1999 (Collins et al., 2001). The model was run to produce an aerosol field, then that field was adjusted to better resemble the AOD as derived from AVHRR satellite observations. The results, both model-alone and model-with-satellite assimilation, were compared to shipboard sunphotometers; the assimilated results show much closer agreement to the sunphotometer measurements. The assimilation provided aerosol

information when satellite retrievals were impossible: at night and in cloudy situations (Rasch et al., 2001). In recent years, other modeling groups have assimilated EOS-era satellite aerosol information for real-time aerosol forecasting. MODIS aerosol optical depth, over land and ocean, is automatically ingested and assimilated into the European Centre for Medium Range Forecasting (ECMWF) for aerosol predictions (Benedetti et al., 2009). **Figure 11** shows comparisons between AODs from the free-running ECMWF model and the ECMWF-MODIS analysis compared to MODIS observations for 5–6 March 2004 Saharan dust outbreak. **Figure 12** shows a corresponding comparison between AOD at 670 nm from the analysis and the free-running forecast and AERONET AODs at 675 nm for Agoufou (Mali), Dakar (Senegal) and Cape Verde. Although the satellite observed shape of the dust outflow is well represented in the free-running model, the magnitude of the AODs is much lower than both MODIS and AERONET measurements. The analysis shows much better agreement with AERONET measurements. The peaks shown in the AERONET data were well captured by the analysis, with the exception of the 8–9 March AOD maximum over Agoufou.

MODIS aerosol optical depth is also assimilated into the Naval Research Laboratory (NRL) Atmospheric Variational Data Assimilation System (NAVDAS) over ocean (Zhang et al., 2008) and is being prepared for assimilation over land (Hyer et al., 2011). Likewise, CALIOP vertical profiles (Campbell et al., 2010) and MISR-derived aerosol properties have also been assimilated into the same system. By adding these satellite data products, model forecasts and aerosol transport results were quantitatively improved (Zhang et al., 2011). Other assimilation studies include Yumimoto and Takemura (2011)

who assimilated one month of Terra and Aqua MODIS AOD. Studies have also used satellite products to constrain model simulations through diagnostic analysis (Yu et al., 2003; Matsui et al., 2004; Liu et al., 2005). However data assimilation and analysis currently provide more total AOD than component AOD constraints, due to the lack of accurate, global aerosol type observations from satellites.

Satellite measurements can also be integrated with model systems to assess the influences of aerosol intercontinental transport on atmospheric composition, air quality, weather, and climate. Over ocean, the intercontinental transport of continental aerosols can often be distinguished from relatively clean marine aerosols and the interactions of aerosols with cloud and precipitation may be inferred from a correlative analysis of satellite measured aerosols, clouds, and precipitation (e.g., Kaufman et al., 2005d; Koren et al., 2005; Zhang et al., 2007), though significant uncertainty still apply. Over land, however, distinguishing ICT aerosols from local sources remains a great challenge for satellite remote sensing. Aerosols from different continents usually have similar characteristics; and current satellites are not capable of discerning the usually marginal differences between continents. Thus assessing the impacts of aerosol ICT on air quality, weather, and climate in downwind continents has to rely on model systems that link important atmospheric processes at local, regional, and hemispheric scales. Global models are needed to provide regional models with appropriate boundary and initial conditions, whereas regional models with higher resolution are needed to adequately represent major chemical and meteorological processes important for air quality, weather, and climate. Considering large uncertainties associated with global aerosol models, measurements

from satellites should be used to provide chemical boundary conditions of aerosol ICT for regional models.

4. Conclusions and Outlooks

Satellites provide ideal platforms for studying aerosol intercontinental transport, because of the frequent sampling over global and multi-year scales. In the last decade or two, major advances have been achieved in both passive and active aerosol remote sensing from space, providing better coverage, higher spatial resolution, improved AOD accuracy, emerging climatology of vertical distributions, and enhanced capabilities to characterize aerosol type, as provided by observational constraints on particle properties. Satellites also provide correlative measurements of trace gases, as well as the strengths and properties of aerosol source. These advances offer unprecedented opportunities to develop a measurement-based assessment of aerosol intercontinental transport.

The accumulation of advanced satellite observations over the past decade has significantly improved the understanding of aerosol intercontinental transport and its impacts on climate and air quality, from largely qualitative characterization to increasingly quantitative assessment. The observations have been used to characterize the three-dimensional evolution of aerosol loading and particle properties (size, and shape) during intercontinental transport on an episodic basis. Long-term measurements with daily frequency have been used to characterize seasonal and inter-annual variations of aerosol ICT and associated controlling factors. Most recently, estimates of aerosol export and import have been performed using the satellite measurements of aerosol optical

depth, vertical distribution, and microphysical properties over ocean. The findings have important implications for air pollution control and climate mitigation.

Measurement-based quantitative assessment of aerosol ICT requires a synthesis of multiple data sets. No sensor, known or expected in the foreseeable future, has sufficient capability to fully characterize aerosol ICT without additional information. For example, MODIS offers among the most complete coverage, which is essential to capturing specific transport events, but cannot directly identify transport height or aerosol type. MISR provides much better characterization of aerosol particle properties and how those evolve along the transport path, but has a more limited sampling. CALIOP is the ideal instrument to identify transport height and can distinguish dust from combustion aerosol, but is extremely limited in its sampling. The other satellite sensors also each make their own specific contributions. Combining information from different sensors is shown to provide quantitative estimates of the material flux imported and exported at continental boundaries, albeit still with large error bars. Narrowing these error bars requires continued characterization of the aerosol using additional data sets and new validated products from the current suite of satellite sensors (i.e., more accurate particle properties, AOD above clouds). In turn, validation of the satellite data sets requires a concerted effort from suborbital observations.

In addition to the satellite-alone observation-based applications, satellite measurements have also provided several critical inputs for constraining chemical transport models, and valuable datasets for evaluating and improving model simulations of aerosol

intercontinental transport. The ultimate means to quantify aerosol ICT will necessarily involve a combination of multiple satellite observations and models. This may take the form of directly assimilating satellite aerosol products into models, or constraining models with observational results. These constraints amount to more than just requiring the model to match the satellite-derived AOD, or even the satellite-derived particle properties. The models also need to simulate the satellite-derived material fluxes into and out of continents at the continental boundaries. It is recommended that AeroCom and HTAP model experiments consider including the export/import flux requirement into their data protocols, so that models can be evaluated with satellite observations.

Despite this significant progress, substantial effort is needed in the future to fully explore the potential offered by existing satellites, and to develop new and enhanced satellite missions:

(a) *Geostationary satellite measurements have been underused.* Although such measurements usually do not have adequate spatial coverage to track the evolution of aerosol plumes along the entire intercontinental transport path, in combination with polar orbiting satellite measurements they can provide the hour-to-hour evolution of the plumes in many regions of interest.

(b) *Satellite-based studies should extend to all major ICT paths.* The trans-Atlantic transport of Saharan dust has been well studied, and there are studies addressing the trans-Pacific transport of dust and pollution. However, except for a few efforts, the Indian Ocean, the Southern Hemisphere, pollution transport from North America has not been addressed by observationally based work.

(c) *More information can be extracted from existing sensors*. The integrated use of multiple satellite measurements can potentially improve the characterization of aerosol temporal and spatial distribution, distinguish aerosol types and overcome uncertainties introduced by sampling issues. In particular, integration of non-aerosol products such as carbon monoxide and SO_2 gas can add valuable information, but are mostly missing from current studies. Novel analysis techniques that include combining absorption Angstrom exponent and extinction Angstrom exponent for better aerosol type characterization (Russell et al., 2010) or retrieving AOD from above clouds using passive sensors (Waquet et al., 2009; Torres et al., 2012; Yu et al., 2012b) could also aid in improving assessment of aerosol ICT from satellite measurements alone.

(d) *Satellite products require suborbital validation*. As more information is extracted from existing sensors, these new products require validation that only suborbital measurements can supply. Validation has to go beyond comparing AOD with AERONET, to make use of the detailed particle property measurements being made from airborne and ground-based instruments.

(e) *Continuity and enhancement of satellite capabilities.* Now that we are fully exploiting the information content and synergy of the EOS-era satellites, we note that these sensors are aging and are operating almost a decade beyond their initial mission lifetimes. New and future satellites (ie. Suomi-NPP VIIRS, GOES-R ABI, the Earthcare suite of sensors) can continue some, but far from all EOS-era capability. Key to future abilities is the Earthcare ATLID, a lidar to succeed CALIOP, although its different spectral configuration raises questions of

continuity. We are missing a next-generation multi-angle, polarimeter imager that can provide the detailed particle properties we have come to expect from MISR and POLDER.

(f) *Consequences of aerosol ICT should be explored.* What is the radiative effect of this transport over oceans and over continents? What is the effect on air quality? How are these consequences partitioned between dust and combustion aerosols? How much is anthropogenic and how much is natural? The answers to these questions will require a synthesized combination of multiple observation systems and multi-scale models. However, satellite-based observations can take a leading role, and make significant quantitative contribution to finding the answer to these important questions.

(g) *Satellite-based assessments alone are insufficient to answer all the questions*. Modeling studies will be necessary, but models must use the information gained by satellite studies to constrain emissions, evaluate AOD distributions and compare with import/export assessments at continental boundaries. Assimilation provides one way forward, but sacrifices the ability of the model studies to understand aerosol processes in the atmosphere through the exercise of modeling/evaluation/model improvement.

Acknowledgements: HY, LAR, MC, and YZ acknowledge the NASA support of this work via NNXAH66G (The Science of Terra and Aqua program) and NNX11AJ91G (Atmospheric Composition Modeling and Analysis – ACMAP program), both managed by Richard Eckman. MC was also supported in part by NASA Modeling, Analysis, and

Projection program managed by David Considine. The work of RK was supported in part by NASA's Climate and Radiation Research and Analysis Program under Hal Maring, ACMAP program under Richard Eckman, and the EOS-MISR instrument project.

Acronyms

AAI:	Absorbing Aerosol Index (sometimes as AI)
AATSR:	Advanced Along-Track Scanning Radiometer
ABI:	Advanced Baseline Imager
ABL:	Atmospheric Boundary Layer
ACA:	Above Cloud Aerosol
ACE:	Aerosol-Cloud-Ecosystem (NASA mission in planning)
ADEOS:	Advanced Earth Observing Satellite
AE:	Angstrom Exponent
AEROCOM:	Aerosol Comparisons between Observations and Models
AERONET:	AErosol RObotic NETwork
AIRS:	Atmospheric Infrared Sounder
AOD:	Aerosol Optical Depth
ATLID:	Atmospheric Lidar
ATSR:	Along Track Scanning Radiometer
AVHRR:	Advanced Very High Resolution Radiometer
BUV:	Backscatter UV
CALIOP:	Cloud-Aerosol Lidar with Orthogonal Polarisation
CALIPSO:	Cloud-Aerosol Lidar with Orthogonal Polarisation
CLAES:	Cryogenic Limb Array Etalon Spectrometer
CTM:	Chemical Transport Model
ECMWF:	European Centre for Medium Range Forecasting
EOS:	Earth Observing System
EP:	Earth Probe
ERS:	European Remote Sensing
FMF:	Fine Mode Fraction (aerosol)
FT:	Free Troposphere
GEOS-Chem:	Goddard Earth Observing System (GEOS) - Chemistry model
GLAS:	Geoscience Laser Altimeter System
GMI:	Global Modeling Initiative
GOCART:	Goddard Chemistry Aerosol Radiation and Transport model
GOES:	Geostationary Operational Environmental Satellites
GOME:	Global Ozone Monitoring Experiment
HSRL:	High Spectral Resolution Lidar.
HTAP:	Hemispheric Transport of Air Pollutants
HYSPLIT:	Hybrid Single Particle Lagrangian Integrated Trajectory Model
IASI:	Infrared Atmospheric Sounding Interferometer
ICT:	InterContinental Transport
INDOEX:	Indian Ocean Experiment
ITCZ:	Inter-Tropical Convergence Zone
LH:	Layer Height (aerosol)
LITE;	Lidar In-Space Technology Experiment

MAIAC:	MultiAngle Implementation of Atmospheric Correction
MAN:	Marine Aerosol Network
MATCH:	Model of Atmospheric Transport and Chemistry
MERIS:	MEdium Resolution Imaging Spectrometer
MISR:	Multi-angle Imaging SpectroRadiometer
MJO:	Madden–Julian Oscillation
MLS:	Microwave Limb Sounder
MODIS:	Moderate Resolution Imaging Spectroradiometer
MOPIIT:	Measurements Of Pollution In The Troposphere
MSG:	Meteosat Second Generation
NAO:	North Atlantic Oscillation
NAVDAS:	NRL Atmospheric Variational Data Assimilation System
NPP:	NPOESS Preparatory Project
NRC:	National Research Council
NRL:	Naval Research Laboratory
NSF:	Non-Spherical Fraction (aerosol)
OMI:	Ozone Monitoring Instrument
PARASOL:	Polarization and Anisotropy of Reflectances for Atmospheric Sciences Coupled with Observations from a Lidar
PM:	Particulate Matter
POLDER:	Polarization and Directionality of the Earth's Reflectance
RAIR:	Relative Annual Intercontinental Response
RH:	Relative Humidity
SAGE:	Stratospheric Aerosol and Gas Experiment
SAM:	Sample Analysis at Mars
SCIAMACHY:	Scanning Imaging Absorption Spectrometer for Atmospheric Chartography/Chemistry
SeaWiFS:	Sea-viewing Wide Field-of-view Sensor
SEVIRI:	Spinning Enhanced Visible Infra-Red Imager
SSA:	Single-Scattering Albedo (aerosol)
TES:	Thermal Emission Spectrometer
TOA:	Top-Of-Atmosphere
TOMS:	Total Ozone Mapping Spectrometer
TRMM:	Tropical Rainfall Measuring Mission
UV:	Ultra-violet (radiation)
VIIRS:	Visible Infrared Imaging Radiometer Suite
VP:	Vertical Profile (aerosol)
WCB:	Warm Convey Belt

References

Abdou, W. A., Diner, D. J., Martonchik, J. V., Bruegge, C. J., Kahn, R. A., Gaitley, B. J., Crean, K. A., 2005. Comparison of coincident MISR and MODIS aerosol optical depths over land and ocean scenes containing AERONET sites. J. Geophys. Res., 110, D10S07, doi:10.1029/2004JD004693.

Abel, S. J., Highwood, H. J., Haywood, J. M., Stringer, M. A., 2005. The direct radiative effect of biomass burning aerosols over southern Africa. Atmos. Chem. Phys., 5, 1999–2018.

Acarreta, J. R., De Haan, J. F., Stammes, P., 2004. Cloud pressure retrieval using the O_2-O_2 absorption band at 477 nm. J. Geophys. Res., 109, D05204, doi:10.1029/2003JD003915.

Ahn, C., Torres, O., Bhartia, P. K., 2008. Comparison of Ozone Monitoring Instrument UV aerosol products with Aqua/Moderate Resolution Imaging Spectroradiometer and Multiangle Imaging Spectroradiometer observations in 2006. J. Geophys. Res., 113, D16S27, doi:10.1029/2007JD008832.

Albrecht, B., 1989. Aerosols, cloud microphysics, and fractional cloudiness. Science, 245, 1227-1230.

Amiridis, V., Giannakaki, E., Balis, D. S., Gerasopoulos, E., Pytharoulis, I., Zanis, P., Kazadzis, S., Melas, D., Zerefos, C., 2010. Smoke injection heights from agricultural burning in Eastern Europe as seen by CALIPSO. Atmos. Chem. Phys., 10, 11567-11576, doi:10.5194/acp-10-11567-2010.

Anderson, T. L., Charlson, R. J., Bellouin, N., Boucher, O., Chin, M., Christopher, S. A., Haywood, J., Kaufman, Y. J., Kinne, S., Ogren, J. A., Remer, L. A., Takemura, T., Tanré, D., Torres, O., Trepte, C. R., Wielicki, B. A., Winker, D. M., Yu, H., 2005. An "A-Train" strategy for quantifying direct aerosol forcing of climate. Bull. Am. Met. Soc., 86(12), 1795-1809.

Ansmann, A., Baars, H., Tesche, M., Müller, D., Althausen, D., Engelmann, R., Pauliquevis, T., Artaxo, P., 2009. Dust and smoke transport from Africa to South America: Lidar profiling over Cape Verde and the Amazon rainforest. Geophys. Res. Lett., 36, L11802, doi:10.1029/2009GL037923.

Ault, A. P., Williams, C. R., White, A. B., Neiman, P. J., Creamean, J. M., Gaston, C. J., Ralph, F. M., Prather, K. A., 2011. Detection of Asian dust in California orographic precipitation. J. Geophys. Res., 116, D16205, doi:10.1029/2010JD015351.

Barnaba, F., Gobbi, G. P., 2001. Lidar estimation of tropospheric aerosol extinction, surface area and volume: Maritime and desert-dust cases, J. Geophys. Res., 106(D3), 3005–3018, doi:10.1029/2000JD900492.

Bauman, J. J., Russell, P. B., Geller, M. A., Hamill, P., 2003. A stratospheric aerosol climatology from SAGE II and CLAES measurements: 2. Results and comparisons, 1984–1999. J. Geophys. Res., 108, 4383, doi:10.1029/2002JD002993.

Ben-Ami, Y., Koren, I., Altaratz, O., 2009. Patterns of North African dust transport over the Atlantic: winter vs. summer, based on CALIPSO first year data, Atmos. Chem. Phys., 9, 7867–7875, doi:10.5194/acp-9-7867-2009.

Ben-Ami, Y., Koren, I., Rudich, Y., Artaxo, P., Martin, S. T., Andreae, M. O., 2010. Transport of North African dust from the Bod´el´e depression to the Amazon Basin: a case study. Atmos. Chem. Phys., 10, 7533–7544, doi:10.5194/acp-10-7533-2010.

Ben-Ami, Y., Koren, I., Altaratz, O., Kostinski, A., Lehahn, Y., 2012. Discernible rhythm in the spatio/temporal distributions of transatlantic dust. Atmos. Chem. Phys., 12, 2253-2262.

Benedetti, A., Morcrette, J.-J., Boucher, O., Dethof, A., Engelen, R. J., Fisher, M., Flentje, H., Huneeus, N., Jones, L., Kaiser, J. W., 2009. Aerosol analysis and forecast in the European Centre for Medium-Range Weather Forecasts Integrated Forecast System: 2. Data assimilation. J. Geophys. Res., 114, D13205, doi:10.1029/2008JD011115.

Bian, H., Chin, M., Kawa, R., Yu, H., Diehl, T., Kucsera, T., 2010. Multi-scale carbon monoxide and aerosol correlations from satellite measurements and GOCART model: implication for emissions and atmospheric evolution. J. Geophys. Res., 115, D07302, doi:10.1029/2009JD012781.

Biscaye, P., Grousset, F. E., Svensson, A. M., Bory, A., 2000. Eurasian air pollution reaches eastern North America, Science, 290, 2258-2259, doi:10.1126/science.290.5500.2258.

Bourgeois, Q., and I. Bey, 2011. Pollution transport efficiency toward the Arctic: Sensitivity to aerosol scavenging and source regions. J. Geophys. Res., 116, D08213, doi:10.1029/2010JD015096.

Bucsela, E. J., Celarier, E. A., Wenig, M. O., Gleason, J. F., Veefkind, J. P., Booersma, K. F., Brinksma, E. J., 2006. Algorithm for NO2 vertical column retrieval from the Ozone Monitoring Instrument. IEEE Trans. Geosci. Rem. Sens., 44(5), doi:10.1109/TGRS.2005.863715, 1245--1258.

Campbell, J. R., Reid, J. S., Westphal, D. L., Zhang, J., Hyer, E. J., Welton, E. J., 2010. CALIOP aerosol subset processing for global aerosol transport model data assimilation. IEEE Journal of Selected Topics in Applied Earth Observations and Remote Sensing, 3, doi:10.1109/JSTARS.2010.2044868.

Carn, S. A., Krueger, A. J., Krotkov, N. A., Yang, K., Levelt, P. F., 2007. Sulfur dioxide emissions from Peruvian copper smelters detected by the Ozone Monitoring Instrument. Geophys. Res. Lett., 34, L09801, doi:10.1029/2006GL029020.

Cattrall, C., Reagan, J., Thome, K., Dubovik, O., 2005. Variability of aerosol and spectral lidar and backscatter and extinction ratios of key aerosol types derived from selected Aerosol Robotic Network locations. J. Geophys. Res., 110:D10S11. doi:10.1029/2004JD005124.

Chameides, W. L., Yu, H., Liu, S. C. et al. 1999. A case study of the effects of atmospheric aerosols and regional haze on agriculture: An opportunity to enhance crop yields in China through emission controls? Proc. Natl. Acad. Sci. 96, 13626-13633.

Chand, D., Anderson, T. L., Wood, R., Charlson, R. J., Hu, Y., Liu, Z., Vaughan, M., 2008. Quantifying above-cloud aerosol using spaceborne lidar for improved understanding of cloudy-sky direct climate forcing. J. Geophys. Res., 113, D13206, doi:10.1029/2007JD009433.

Chand, D., Wood, R., Anderson, T. L., Satheesh, S. K., Charlson, R. J., 2009. Satellite-derived direct radiative effect of aerosols dependent on cloud cover. Nat. Geosci., 2, 181–184, doi:10.1038/ngeo437.

Chen, W-T, Kahn, R., Nelson, D., Yau, K., Seinfeld, J., 2008. Sensitivity of multi-angle imaging to optical and microphysical properties of biomass burning aerosols. J. Geophys. Res. 113, D10203, doi:10.1029/2007JD009414.

Chiapello, I., Moulin, C., Prospero, J. M., 2005. Understanding the long-term variability of African dust transport across the Atlantic as recorded in both Barbados surface concentrations and large-scale Total Ozone Mapping Spectromenter (TOMS) optical thickness. J. Geophys. Res., 110, D18S10, doi:10.1029/2004JD005132.

Chin, M., Ginoux, P., Kinne, S., Torres, O., Holben, B. N., Duncan, B. N., Martin, R. V., Logan, J. A., Higurashi, A., Nakajima, T., 2002. Tropospheric aerosol optical thickness from the GOCART model and comparisons with satellite and sunphotometer measurements. J. Atmos. Sci., 59, 461–483.

Chin, M., Chu, A., Levy, R., Remer, L. A., Kaufman, Y. J., Holben, B. N., Eck, T., Ginoux, P., Gao, Q., 2004. Aerosol distribution in the Northern Hemisphere during ACE-Asia: Results from global model, satellite observations, and Sun photometer measurements. J. Geophys. Res., 109, D23S90, doi:10.1029/2004JD004829.

Chin, M., Diehl, T., Ginoux, P., Malm, W., 2007. Intercontinental transport of pollution and dust aerosols: implications for regional air quality. Atmos. Chem. Phys., 7, 5501-5517, doi:10.5194/acp-7-5501-2007.

Christopher, S. A., Jones, T., 2007. Satellite-based assessment of cloud-free net radiative effect of dust aerosols over the Atlantic Ocean. Geophys. Res. Lett., 34, L02810, doi:10.1029/2006GL027783.

Chu, D. A., Kaufman, Y. J., Ichoku, C., Remer, L. A., Tanre, D., Holben, B. N., 2002. Validation of MODIS aerosol optical depth retrieval over land. Geophys. Res. Lett., 29, 10.1029/2001GLO13205.

Chung, Y. S., 1986. Air pollution detected by satellites: The transport and deposition of air pollutants over oceans. Atmos. Environ., 20, 617-630.

Colarco, P. R., et al., 2003. Saharan dust transport to the Caribbean during PRIDE: 2. Transport, vertical profiles, and deposition in simulations of in situ and remote sensing observations. J. Geophys. Res., 108, 8590, doi:10.1029/2002JD002659.

Colarco, P. R., Schoeberl, M. R., Doddridge, B. G., Marufu, L. T., Torres, O., Welton, E. J., 2004. Transport of smoke from Canadian forest fires to the surface near Washington, D.C.: Injection height, entrainment, and optical properties. J. Geophys. Res., 109, D06203, doi:10.1029/2003JD004248.

Colarco, P., da Silva, A., Chin, M., Diehl, T., 2010. Online simulations of global aerosol distributions in the NASA GEOS-4 model and comparisons to satellite and ground-based aerosol optical depth. J Geophys Res, 115, D14207, doi:10.1029/2009JD012820.

Collins, W. D., Rasch, P. J., Eaton, B. E., Khattatov, B. V., Lamarque, J.-F., Zender, C. S., 2001. Simulating aerosols using a chemical transport model with assimilation of satellite aerosol retrievals: Methodology for INDOEX. J. Geophys. Res., 106(D7), 7313–7336, doi:10.1029/2000JD900507.

Deeter, M. N., et al., 2003. Operational carbon monoxide retrieval algorithm and selected results for the MOPITT instrument. J. Geophys. Res., 108(D14), 4399, doi:10.1029/2002JD003186.

DeSouza-Machado, S., Strow, L. L., Motteler, H., and Hannon, S., 2006. Infrared dust spectral signatures from AIRS. Geophys. Res. Lett., 33, L03801, doi:10.1029/2005GL024364.

DeSouza-Machado, S. G., Strow, L. L., Imbiriba, B., McCann, K., Hoff, R. M., Hannon, S. E., Martins, J. V., et al., 2010. Infrared retrievals of dust using AIRS: Comparisons of optical depths and heights derived for a North African dust storm to other collocated EOS A-Train and surface observations. J. Geophys. Res., 115, D15201, doi:10.1029/2009JD012842.

Deuzé, J. L., Herman, M., Goloub, P., Tanré, D., Marchand, A., 1999. Characterization of aerosols over ocean from POLDER/ADEOS-1. Geophys. Res. Lett., 26(10), 1421–1424, doi:10.1029/1999GL900168.

Deuzé, J. L., et al., 2001. Remote sensing of aerosols over land surfaces from POLDER-ADEOS-1 polarized measurements. J. Geophys. Res., 106(D5), 4913–4926, doi:10.1029/2000JD900364.

Dey, S., Di Girolamo, L., 2010. A climatology of aerosol optical and microphysical properties over the Indian subcontinent from 9 years (2000–2008) of Multiangle Imaging Spectroradiometer (MISR) data. J. Geophys. Res., 115, D15204, doi:10.1029/2009JD013395.

Diner, D. J., Beckert, J. C., Reilly, T. H., Bruegge, C. J., Conel, J. E., Kahn, R., Martonchik, J. V., Ackerman, T. P., Davies, R., Gerstl, S.A.W., Gordon, H. R., Muller, J.-P., Myneni, R., Sellers, J., Pinty, B., Verstraete, M. M., 1998. Multiangle Imaging Spectroadiometer (MISR) description and experiment overview. IEEE Trans. Geosci. Remt. Sensing 36, 1072-1087.

Diner, D. J., Beckert, J. C., Bothwell, G. W., Rodriguez, J. I., 2002. Performance of the MISR Instrument During Its First 20 Months in Earth Orbit. IEEE Trans. Geosci. Remote Sensing., 40, 1449-1466.

Diner, D. J., et al., 2005. The value of multiangle measurements for retrieving structurally and radiatively consistent properties of clouds, aerosols, and surfaces. Remote Sens. Environ., 97, 495-518.

Di Pierro, M., Jaeglé, L., Anderson, T. L., 2011. Satellite observations of aerosol transport from East Asia to the Arctic: three case studies, Atmos. Chem. Phys., 11, 2225-2243, doi:10.5194/acp-11-2225-2011,.

Dirksen, R. J., Boersma, K. F., de Laat, J., Stamnes, P., van der Werf, G. R., Val Martin, M., Kelder, H. M., 2009. An aerosol boomerang: Rapid around-the-world transport of smoke from the December 2006 Australian forest fires observed from space, J. Geophys. Res., 114, D21201, doi:10.1029/2009JD012360.

Draxler, R. R., Rolph, G. D., 2003. HYSPLIT (HYbrid Single-Particle Lagrangian Integrated Trajectory) Model access via the NOAA ARL READY Website, NOAA Air Resour. Lab., Silver Spring, Md. (Available at http://www.arl.noaa.gov/ready/hysplit4.html).

Doherty, O. M., Riemer, N., Hameed, S., 2008. Saharan mineral dust transport into the Caribbean: Observed atmospheric controls and trends, *J. Geophys. Res.*, 113, D07211, doi:10.1029/2007JD009171.

Dubovik, O., M. D. King, 2000. A flexible inversion algorithm for retrieval of aerosol optical properties from Sun and sky radiance measurements. J. Geophys. Res., 105(D16), 20,673–20,696, doi:10.1029/2000JD900282.

Dubovik, O., Holben, B. N., Eck, T. F., Smirnov, A., Kaufman, Y. J, King, M. D., Tanre, D., Slutsker, I., 2002: Variability of absorption and optical properties of key aerosol types observed in worldwide locations, J. Atmos. Sci., **59**, 590-608 .

Dubovik, O., Lapyonok, T., Kaufman, Y. J., Chin, M., Ginoux, P., Kahn, R., Sinyuk, A., 2008. Retrieving global aerosol sources from satellites using inverse modeling. Atmos. Chem. Phys., 8(2), 209-250, doi:10.5194/acp-8-209-2008.

Dubovik, O., Herman, M., Holdak, A. Lapyonok, T., Tanré, D., Deuzé, J. L., Ducos, F., Sinyuk, A., Lopatin, A., 2011. Statistically optimized inversion algorithm for enhanced retrieval of aerosol properties from spectral multi-angle polarimetric satellite observations. Atmos. Meas. Tech., 4, 975-1018.

Duce, R. A., Unni, C. K., Ray, B. J. 1980. Long-range atmospheric transport of soil dust from Asia to the tropical North Pacific: Temporal variability. Science 209, 1522-1524.

Duce, R. A., et al., 1991. The atmospheric input of trace species to the world ocean, Global Biogeochem. Cycles, 5(3), 193–259.

Dulac, F., Tanre, D., Bergametti, G., Buat-Menard, P., Desbois, M., Sutton, D., 1992. Assessment of the African airborne dust mass over the western Mediterranean Sea using Meteosat data. J. Geophys. Res., 97, 2489-2506.

Edwards, D. P., et al., 2004. Observations of carbon monoxide and aerosols from the Terra satellite: Northern Hemisphere variability. J. Geophys. Res., 109, D24202, doi:10.1029/2004JD004727.

Eguchi, K., Uno, I., Yumimoto, K., Takemura, T., Shimizu, A., Sugimoto, N., Liu, Z., 2009. Trans-Pacific dust transport: Integrated analysis of NASA/CALIPSO and a global aerosol transport model, Atmos. Chem. Phys., 9, 3137–3145, doi:10.5194/acp-9-3137-2009

Amato T. E., Mukhopadhyay, S., 2010. African dust over the northern tropical Atlantic: 1955–2008. J. Appl. Meteor. Climatol., 49, 2213-2229, doi: 10.1175/2010JAMC2485.1.

Fan, X., Goloub, P., Deuzé, J. L., Chen, H., Zhnag, W., Tanré, D., Li, Z., 2008. Evaluation of PARASOL aerosol retrieval over North East Asia. Remote Sens. Environ., 112, 697-707.

Ferrare, R. A., Fraser, R. S., Kaufman, Y. J.. 1990. Satellite measurements of large-scale air pollution: Measurements of forest fire smoke. J. Geophys. Res., 95, 9911-9925.

Ford, B., and Heald, C. L., An A-train and model perspective on the vertical distribution of aerosols and CO in the Northern Hemisphere, J. Geophys. Res., 117, D06211, doi:10.1029/2011JD016977, 2012.

Fraser, R. S., 1976. Satellite measurement of mass of Sahara dust in the atmosphere. Appl. Opt., 15, 2471-2479.

Fraser, R. S., Kaufman, Y. J., Mahoney, R. L., 1984. Satellite measurement of aerosol mass and transport. Atmos. Environ., 18, 2577-2584.

Freitas, S. R., Longo, K. M., Andreae, M. O., 2006. Impact of including the plume rise of vegetation fires in numerical simulations of associated atmospheric pollutants. Geophys. Res. Lett., 33, L17808, doi:10.1029/2006GL026608.

Fromm, M., Torres, O., Diner, D., Lindsey, D., Vant Hull, B., Servranckx, R., Shettle, E. P., Li, Z., 2008. Stratospheric impact of the Chisholm pyrocumulonimbus eruption: 1. Earth viewing satellite perspective. J. Geophys. Res., 113, D08202, doi:10.1029/2007JD009153.

Gao, Y., Arimoto, R., Duce, R. A., Zhou, M. Y., Chen, C. A., Zhang, X. Y., Zhang, G. Y., An, Z. S., 1997. Temporal and spatial distribution of dust and its total deposition to the China Sea, Tellus, 49B, 172-189.

Gasso, S., Stein, A. F., 2007. Does dust from Patagonia reach the sub-Antarctic Atlantic Ocean?, Geophys. Res. Let., 34, L01801, doi: 10.1029/2006GL027693.

Generoso, S., Bey, I., Labonne, M., Bréon, M., 2008. Aerosol vertical distribution in dust outflow over the Atlantic: Comparisons between GEOS-Chem and Cloud-Aerosol Lidar and Infrared Pathfinder Satellite Observation (CALIPSO), J. Geophys. Res., 113, D24209, doi:10.1029/2008JD010154.

Geogdzhayev, I. V., Mishchenko, M. I., Rossow, W. B., Cairns, B., Lacis, A. A., 2002. Global two-channel AVHRR retrievals of aerosol properties over the ocean for the period of NOAA-9 observations and preliminary retrievals using NOAA-7 and NOAA-11 data. J. Atmos. Sci., 59, 262-278.

Giglio, L., Randerson, J. T., van der Werf, G. R., Kasibhatla, P. S., Collatz, G. J., Morton, D. C., DeFries, R. S., 2010. Assessing variability and long-term trends in burned area by merging multiple satellite fire products, Biogeosciences, 7, 1171-1186, doi:10.5194/bg-7-1171-2010.

Ginoux, P., Chin, M., Tegen, I.,. Prospero, J. M., Holben, B., Dubovik,O., Lin, S. J., 2001. Sources and distributions of dust aerosols simulated with the GOCART model, J. Geophys. Res., 106(D17), 20,255–20,273.

Ginoux, P., Prospero, J. M., Gill, T. E., Hsu, C., M. Zhao, 2012. Global scale attribution of anthropogenic and natural dust sources and their emission rates based on MOIDS Deep Blue aerosol products. Rev. Geophys., 2012, in press.

Goloub, P., Tanré, D., Deuzé, J. L., Herman, M., Marchand, A., Bréon, F. M., 1999. ValidationofthefirstalgorithmappliedforderivingtheaerosolpropertiesovertheoceanusingthePOLDER/ADEOSmeasurements. IEEET.Geosci.Remote, 37, 1586–1596.

Grousset, F., Ginoux, P., Bory, A., Biscaye, P. E., 2003. Case study of a Chinese dust plume reaching the French Alps. Geophys. Res. Lett., 30(6), 1277, doi:10.1029/2002GL016833.

Gunn, R., Philips, B. B., 1957. An experimental investigation of the effect of air pollution on the initiation of rain. J. Meteorol., 14, 272-280.

Guan, H., Esswein, R., Lopez, J., Bergstrom, R., Warnock, A., Follette-Cook, M., Fromm, M., Iraci, L. T., 2010. A multi-decadal history of biomass burning plume heights identified using aerosol index measurements, Atmos. Chem. Phys., 10, 6461-6469, doi:10.5194/acp-10-6461-2010.

Hadley, O. L., Corrigan, C. E., Kirchstetter, T. W., Cliff, S., Ramanathan, V., 2010. Measured black carbon deposition on the Sierra Nevada snow pack and implication for snow pack retreat. Atmos. Chem. Phys. **10**, 7505-7513.

Hara, Y., Yumimoto, K., Uno, I., Shimizu, A., Sugimoto, N., Liu, Z., Winker, D. M., 2009. Asian dust outflow in the PBL and free atmosphere retrieved by NASA CALIPSO and an assimilated dust transport model, Atmos. Chem. Phys., 9, 1227-1239, doi:10.5194/acp-9-1227-2009.

Haywood, J. M., et al., 2008. Overview of the Dust and Biomass-burning Experiment and African Monsoon Multidisciplinary Analysis Special Observing Period-0, J. Geophys. Res., 113, D00C17, doi:10.1029/2008JD010077.

Haywood, J. M., et al., 2010. Observations of the eruption of the Sarychev volcano and simulations using the HadGEM2 climate model. J. Geophys. Res., 115, D21212, doi:10.1029/2010JD014447.

Heald, C.L., et al., 2006. Transpacific transport of Asian anthropogenic aerosols and its impact on surface air quality in the United States, J. Geophys. Res., 111, D14310, doi:10.1029/2005JD006847.

Heald, C. L., Ridley, D. A., Kreidenweis, S. M., Drury, E. E., 2010. Satellite observations cap the atmospheric organic aerosol budget. Geophys. Res. Lett., 37, L24808, doi:10.1029/2010GL045095.

Herman, J., Bhartia, P., Torres, O., Hsu, C., Seftor, C., Celarier, E., 1997. Global distribution of UV-absorbing aerosols from Nimbus-7/TOMS data. J. Geophys. Res. 102, 16911-16922.

Herman, M., Deuze, J. L., Marchand, A., Roger, B., Lallart, P., 1997. Aerosol remote sensing over land surfaces including polarization measurements: applications to POLDER measurements. J. geophys. Res., 102, 17039-17050.

Herman, M., Deuzé, J. L., Marchand, A., Roger, B., Lallart, P., 2005. Aerosol remote sensing from POLDER/ADEOS over the ocean: Improved retrieval using a nonspherical particle model, J. Geophy. Res., 110, D10S02.

Higurashi, A., Nakajima, T. 2002. Detection of aerosol types over the East China sea near Japan from four-channel satellite data. Geophys. Res. Lett., 29, 1836, doi:10.1029/2002GL015357.

Holben, B. N., et al., 1998. AERONET-A federated instrument network and data archive for aerosol characterization. Remote Sens. Environ., 66(1), 1–16.

Holloway, T., Fiore, A., Hastings, M. G., 2003. Intercontinental Transport of Air Pollution: Will Emerging Science Lead to a New Hemispheric Treaty? Environ. Sci. Technol., 37, 4535-4542.

Hsu, N.C., Herman, J. R., Bhartia, P. K., Seftor, C. J., Torres, O., Thompson, A. M., Gleason, J. F., Eck, T. F., Holben, B. N., 1996. Detection of biomass burning smoke from TOMS measurements. Geophys. Res. Lett.,, 23, 745-748.

Hsu, N. C., Tsay, S.-C., King, M. D., Herman, J. R., 2004. Aerosol properties over bright-reflecting source regions. IEEE Trans. Geosci. Remote Sens., 42, 557-569.

Hsu, N.C., Tsay, S.-C., King, M. D., Herman, J. R., 2006. Deep blue retrievals of Asian aerosol properties during ACE-Asia. IEEE Trans. Geosci. Remote Sens., 44, 3180-3195, 10.1029/2005JD006549.

Hsu, N. C., Li, C., Krotkov, N. A., Liang, Q., Yang, K., Tsay, S.-C., 2012. Rapid transpacific transport in autumn observed by the A-Train satellites. J. Goephys. Res., 117, D06312, doi:10.1029/2011JD016626.

HTAP (2010), Hemispheric Transport of Air Pollution 2010 - Part A: Ozone and Particulate Matter, Air Pollution Studies No. 17, edited by Frank Dentener, terry Keating, and Hajime Akimoto, United Nations, New York and Geneva, 2010.

Hu, Y., Vaughan, M, Liu, Z., Powell, K., Rodier, S., 2007. Retrieving optical depths and lidar ratios for transparent layers above opaque water clouds from CALIPSO lidar measurements. IEEE Geoscience & Remote Sens. Lett., 4 (4), 523-526.

Huang, J., Minnis, P., Chen, B., Huang, Z., Liu, Z., Zhao, Q., Yi, Y., Ayers, J. K., 2008. Long-range transport and vertical structure of Asian dust from CALIPSO and surface measurements during PACDEX. J. Geophys. Res., 113, D23212, doi:10.1029/2008JD010620.

Huang, J., Zhang, C., Prospero, J. M., 2010, African dust outbreaks: A satellite perspective of temporal and spatial variability over the tropical Atlantic Ocean. J. Geophys. Res., 115, D05202, doi:10.1029/2009JD012516.

Huebert, B. J., Bates, T., Russell, P. B., Shi, G., Kim, Y. J., Kawamura, K., Carmichael, G., Nakajima, 2003. An overview of ACE-Asia: Strategies for quantifying the relationships between Asian aerosols and their climatic impacts. J. Geophys. Res., 108, 8633, doi:10.1029/2003JD003550.

Huneeus, N., Chevallier, F., Boucher, O., 2012. Estimating aerosol emissions by assimilating observed aerosol optical depth in a global aerosol model. Atmos. Chem. Phys., 12, 4585-606.

Husar, R. B., Prospero, J. M., Stowe, L. L., 1997. Characterization of tropospheric aerosols over the oceans with the NOAA advanced very high-resolution radiometer optical thickness operational product. J. Geophys. Res., 102(D14), 16,889–16,909.

Husar, R. B., et al., 2001. The Asian dust events of April, 1998. J. Geophys. Res. 106, 18317-18330.

Hyer, E. J., Reid, J. S., Zhang, J., 2011. An over-land aerosol optical depth data set for data assimilation by filtering, correction, and aggregation of MODIS Collection 5 optical depth retrievals. Atmos. Meas. Tech., 4, 379–408, doi:10.5194/amt-4-379-2011.

Ichoku, C., Giglio, L., Wooster, M. J., Remer, L. A., 2008. Global characterization of biomass-burning patterns using satellite measurements of Fire Radiative Energy. Remote Sens. Environ., 112, 2008., 2950-2962, doi:10.1016/j.rse.2008.02.009

Ichoku, C., Kahn, R., Chin, M., 2012. Satellite contributions to the quantitative characterization of biomass burning for climate modeling. Atmos. Res, 111, 1-28, doi:10.1016/j.atmosres.2012.03.007.

Itahashi, S., Yumimoto, K., Uno, I., Eguchi, K.,Takemura, T., Hara, Y., Shimizu, A., Sugimoto, N., Liu, Z., 2010. Structure of dust and air pollutant outflow over East Asia in the spring. Geophys. Res. Lett., 37, L20806, doi:10.1029/2010GL044776..

Jacob, D. J., Crawford, J. H., Kleb, M. M., Connors, V. S., Bendura,R. J., Raper, J. R., Sachse, G. M., Gille, J. C., Emmons, L. C. L. Heald, 2003. Transport and Chemical Evolution over the Pacific (TRACE-P) aircraft mission: Design, execution, and first results. J. Geophys. Res., 108, 9000, doi:10.1029/2002JD003276.

Jacob, D. J., et al., 2010. The Arctic Research of the Composition of the Troposphere from Aircraft and Satellites (ARCTAS) mission: design, execution, and first results. Atmos. Chem. Phys., 10, 5191-5212.

Jaffe, D., et al. 1999. Transport of Asian air pollution to North America, Geophys. Res. Lett., 26, 711-714.

Jeong, M.-J., Li, Z., Chu, D. A., Tsay, S.-C., 2005. Quality and compatibility analyses of global aerosol products derived from the advanced very high resolution radiometer and Moderate Resolution Imaging Spectroradiometer. J. Geophys. Res., 110, D10S09, doi:10.1029/2004JD004648.

Jeong, M.-J., Hsu, N. C., 2008. Retrievals of aerosol single-scattering albedo and effective aerosol layer height for biomass-burning smoke: Synergy derived from Geophys. Res. Lett., L24801, 35, 10.1029/2008GL036279

Jickells, T. D., et al., 2005. Global Iron Connections Between Desert Dust, Ocean Biogeochemistry and Climate, Science, 308, 67-71.

Johnson, B. T., Shine, K. P., Forster, P. M., 2004. The semi-direct aerosol effect: Impact of absorbing aerosols on marine stratocumulus. Q. J. R. Meteorol. Soc., 130, 1407-1422.

Kahn, R. A., Banerjee, P., McDonald, D., Diner, D., 1998. Sensitivity of multiangle imaging to aerosol optical depth, and to pure-particle size distribution and composition over ocean. J. Geophys. Res., 195-32,213, 103, 32.

Kahn, R., Banerjee, P., McDonald, D., 2001. The sensitivity of multiangle imaging to natural mixtures of aerosols over ocean, J. Geophys. Res., 106, 18219-18238, 2001.

Kahn, R. A., Gaitley, B., Martonchik, J., Diner, D., Crean, K., Holben, B. N., 2005. MISR global aerosol optical depth validation based on two years of coincident AERONET observations. J. Geophys. Res., 110, doi: 10: 1029/2004JD004706.

Kahn, R. A., Li, W.-H. ,Moroney, C., Diner, D. J., Martonchik, J. V., Fishbein, E., 2007. Aerosol source plume physical characteristics from space-based multiangle imaging. J. Geophys. Res., 112, D11205, doi: 10.1029/2006JD007647.

Kahn, R. A., Chen, Y., Nelson, D., Leung, F.-Y., Li, Q., Diner, D., Logan, J., 2008. Wildfire Smoke Injection Heights - Two perspectives from Space. Geophys. Res. Lett., 35, 4, doi:10.1029/2007GL032165.

Kahn R. A., Nelson, D. L., Garay, M., Levy, R. C., Bull, M. C., Martonchik, J. V., Diner, D. J., Paradise, S. R., Wu, D., Hansen, E. G., Remer, L. A., 2009. MISR Aerosol product attributes, and statistical comparisons with MODIS. IEEE Trans. Geosci. Rem. Sens., 47(12), 4095-4114, doi:10.1109/TGRS.2009.2023115.

Kahn, R. A., Gaitley, B. J., Garay, M. J., Diner, D. J., Eck, T., Smirnov, A., Holben, B. N., 2010. Multiangle Imaging SpectroRadiometer global aerosol product assessment by comparison with the Aerosol Robotic Network. J. Geophys. Res. 115, D23209, doi: 10.1029/2010JD014601.

Kahn, R. A., 2011. Reducing the Uncertainties in Direct Aerosol Radiative Forcing. Surveys in Geophysics, doi:10.1007/s10712-011-9153-z

Kalashnikova O. V., Kahn, R. A., 2006. Ability of multiangle remote sensing observations to identify and distinguish mineral dust types: Part 2. Sensitivity over dark water. J. Geophys. Res., 111, D11207, doi:10.1029/2005JD006756.

Kalashnikova, O. V, Kahn, R. A., 2008. Mineral dust plume evolution over the Atlantic from combined MISR/MODIS aerosol retrievals. J. Geophys. Res. 113, D24204, doi:10.1029/2008JD010083.

Kaufman, Y. J., Boucher, O., Tanré, D., Chin, M., Remer, L. A., Takemura, T., 2005a. Aerosol anthropogenic component estimated from satellite data. Geophys. Res. Lett. 32, L17804, doi:10/1029/2005GL023125.

Kaufman, Y. J., Remer, L. A., Tanré, D. et al., 2005b. A critical examination of the residual cloud contamination and diurnal sampling effects on MODIS estimates of aerosol over ocean. IEEE TGRS 43 (12), 2886-2897.

Kaufman, Y. J., Koren, I., Remer, L. A., Tanré, D., Ginoux, P., Fan, S., 2005c. Dust transport and deposition observed from the Terra-Moderate Resolution Imaging Spectroradiometer (MODIS) spacecraft over the Atlantic Ocean. J. Geophys. Res., 110, D10S12, doi:10.1029/2003JD004436.

Kaufman, Y. J., Koren, I., Remer, L. A., Rosenfeld, D., Rudich, Y., 2005d. The effect of smoke, dust and pollution aerosol on shallow cloud development over the Atlantic Ocean. Proc. Natl. Acad. Sci., 102 (32), 11207-11212.

Kaufman, Y. J., Tanré, D., and Boucher, O., 2002. A satellite view of aerosols in the climate system. Review. Nature, 419**,** 215-223.

Kaufman, Y. J., Tanré, D., Remer, L. A., Vermote, E., Chu, A., Holben, B. N., 1997. Operational remote sensing of tropospheric aerosol over land from EOS Moderate Resolution Imaging Spectroradiometer. J. Geophys. Res., 102**,** 17051-17067.

Khokhar M. F., Frankenberg, C., Beirle, S., Kühl, S., Van Roozendael, M., Richter, A., Platt, U., Wagner, T., 2005. Satellite observations of atmospheric SO2 from volcanic eruptions during the time period of 1996 to 2002. J. Adv. Space Res., 36, 879-887, 10.1016/j.asr.2005.04.114.

Kim, D., Chin, M., Bian, H., Tan, Q., Brown, M. E., Zheng, T., You, R., Diehl, T., Ginoux, P., Kucsera, T., 2012. The effect of the dynamic surface bareness to dust source function, emission, and distribution. submitted to J. Geophys. Res., 2012.

Kinne, S., et al., 2006. An AeroCom initial assessment optical properties in aerosol component modules of global models. Atmos. Chem. Phys. 6, 1815-1834.

Knapp, K. R., Vonder Haar, T. H., Kaufman, Y. J., 2002. Aerosol optical depth retrieval from GOES-8: Uncertainty study and retrieval validation over South America. J. Geophys. Res., 107(D7), 4055, doi:10.1029/2001JD000505.

Koch, D., Schulz, M., Kinne, S., McNaughton, C., Spackman, J. R., Bond, T. C., Balkanski, Y., et al., 2009. Evaluation of black carbon estimations in global aerosol models. Atmos. Chem. Phys., 9, 9001-9026.

Koffi, B., et al., 2012. Application of the CALIOP layer product to evaluate the vertical distribution of aerosols estimated by global models: AeroCom phase I results. J. Geophys. Res., 117, D10201, doi:10.1029/2011JD016858.

Kokhanovsky, A. A., et al., 2010. The inter-comparison of major satellite aerosol retrieval algorithms using simulated intensity and polarization characteristics of reflected light. Atmos. Meas. Tech., 3, 909-932, doi: 10.5194/amt-3-909-2010.

Kondragunta. S., et al., 2008. Air quality forecast verification using satellite data, J. of Applied Meteorology and Climatology, doi:10.1175/2007JAMC1392.1.

Koren I., Kaufman, Y. J., 2004. Direct wind measurements of Saharan dust events from Terra and Aqua satellites. Geophys. Res. Lett., 31, L06122, doi:10.1029/2003GL019338.

Koren I., Kaufman, Y. J., Rosenfeld, D., Remer, L. A., Rudich, Y., 2005. Aerosol invigoration and restructuring of Atlantic convective clouds. Geophys. Res. Lett., 32, LI4828, 10.1029/2005GL0231872005.

Koren, I., Kaufman, Y. J., Washington, R., Todd, M. C., Rudich, Y., Martins, J. V., Rosenfeld, D., 2006. The Bodélé depression: A single spot in the Sahara that provides most of the mineral dust to the Amazon forest. Environ. Res. Lett., 1, 014005, doi:10.1088/1748-9326/1/1/014005.

Koven, C. D., Fung, I., 2008. Identifying global dust source areas using high-resolution land surface form. J. Geophys. Res., 113, D22204, doi:10.1029/2008JD010195.

Krotkov, N. A., et al., 2008. Validation of SO_2 retrievals from the Ozone Monitoring Instrument over NE China. J. Geophys. Res., 113, D16S40, doi:10.1029/2007JD008818.

Lambert, A., Grainger, R. G., Rodgers, C. D., Taylor, F. W., Mergenthaler, J. L., Kumer, J. B., Massie, S. T., 1997. Global evolution of the Mt. Pinatubo volcanic aerosols observed by the infrared limb-sounding instruments CLAES and ISAMS on the Upper Atmosphere Research Satellite. J. Geophys. Res., 102(D1), 1495–1512, doi:10.1029/96JD00096.

Laszlo I., Ciren, P., Liu, H., Kondragunta, S., Tarpley, T. D., Goldberg, M. D., 2008. Remote sensing of aerosol and radiation from geostationary satellites. Adv. Space Res., 41, 11, 1882-1893, doi: 10.1016/j.asr.2007.06.047

Lau, K.-M., Kim, K.-M., 2006. Observational relationships between aerosol and Asian monsoon rainfall, and circulation. Geophys. Res. Let., 33, L21810, doi:10.1029/2006GL027546.

Lau, K. M., Kim, K. M. Kim, Sud, Y. C., Walker, G. K., 2009. A GCM study of the response of the atmospheric water cycle of West Africa and the Atlantic to Saharan dust radiative forcing. Ann. Geophys., 27, 4023–4037.

Lee, T. F., Miller, S. D., Turk, F. J., Schueler, C., Julian, R., Deyo, S., Dills, P., Wang, S., 2006. The NPOESS VIIRS day/night visible sensor. Bull. Amer. Meteor. Soc., 87, 191-199.

Lee, C., Richter, A., Weber, M., Burrows, J. P., 2008. SO_2 Retrieval from SCIAMACHY using the Weighting Function DOAS (WFDOAS) technique: comparison with Standard DOAS retrieval. Atmos. Chem. Phys., 8, 6137-6145, doi:10.5194/acp-8-6137-2008.

Leibensperger, E. M., Mickley, L. J., Jacob, D. J., Chen, W.-T., Seinfeld, J. H., Nenes, A., Adams, P. J., Streets, D. G., Kumar, N., Rind, D., 2012. Climatic effects of 1950–2050 changes in US anthropogenic aerosols – Part 1: Aerosol trends and radiative forcing, Atmos. Chem. Phys., 12, 3333-3348, doi:10.5194/acp-12-3333-2012.

Levy, R., Remer, L. A., Mattoo, S., Vermote, E., Kaufman, Y. J., 2007. Second-generation algorithm for retrieving aerosol properties over land from MODIS spectral reflectance. J. Geophys. Res., 112, D13211, doi:10.1029/2006JD007811.

Levy R., Leptoukh, G., Kahn, R., Zubko, V., Gopalan, A., Remer, L., 2009. A critical look at deriving monthly aerosol optical depth from satellite data IEEE Trans. Geosci. Remote Sens., No. 9,, 47(8), 2942-2956.

Levy, R., Remer, L. A., Kleidman, R. G., Mattoo, S., Ichoku, C., Kahn, R., Eck, T. F., 2010. Global evaluation of the Collection 5 MODIS dark-target aerosol products over land. Atmos. Chem. Phys., 10, 10399-10420, doi:10.5194/acp-10-10399-2010.

Li, F., Ginoux, P., Ramaswamy, V., 2010. Transport of Patagonian Dust to Antarctica. J. Geophys. Res., **115**, D18217, doi:10.1029/2009JD012356.

Li, R. -R., Remer, L. A., Kaufman, Y. J., Mattoo, S., Gao, B.-C., Vermote, E., 2005. Snow and Ice Mask for the MODIS Aerosol Products. IEEE Geo. and Rem. Sens. Lett., 3, 2, 306-310

Li, Z., et al., 2007. Preface to special section on East Asian Studies of Tropospheric Aerosols: An International Regional Experiment (EAST-AIRE). J. Geophys. Res., 112, D22S00, doi:10.1029/2007JD008853.

Liu, D., Wang, Z., Liu, Z., Winker, D., Trepte, C., 2008. A height resolved global view of dust aerosols from the first year CALIPSO lidar measurements. J. Geophys. Res., 113, D16214, doi:10.1029/2007JD009776.

Liu, H., Pinker, R. T., Holben, B. N., 2005. A global view of aerosols from merged transport models, satellite, and ground observations. J. Geophys. Res., 110, D10S15, doi:10.1029/2004JD004695.

Liu, Z., Sugimoto, N., and Murayama, T., 2002. Extinction-to-backscatter ratio of Asian dust observed with high-spectral-resolution lidar and Raman lidar. Appl. Opt., 41, 2760-2767, doi:10.1364/AO.41.002760.

Liu, Z., et al., 2008. CALIPSO lidar observations of the optical properties of Saharan dust: A case study of long-range transport. J. Geophys. Res., 113, D07207, doi:10.1029/2007JD008878, 2008.

Liu, Z., et al., 2009. The CALIPSO lidar cloud and aerosol discrimination: Version 2 algorithm and initial assessment of performance. J. Atmos. Oceanic Technol., 26, 1198-1213, doi:10.1175/2009JTECHA1229.1

Livesey, N. J., et al., 2008.Validation of Aura Microwave Limb Sounder O3 and CO observations in the upper troposphere and lower stratosphere. J. Geophys. Res., 113, D15S02, doi:10.1029/2007JD008805.

Long, C. S., Stowe, L. L., 1994. Using the NOAA/AVHRR to study stratospheric aerosol optical thicknesses following the Mt. Pinatubo Eruption. Geophys. Res. Lett., 21(20), 2215–2218, doi:10.1029/94GL01322.

Luo, C., Mahowald, N., del Corral, J., 2003. Sensitivity study of meteorological parameters on mineral aerosol mobilization, transport and distribution. J. Geophys. Res., 108(D15), 4447, doi:10.1029/2003JD003483.

Lyons, W. A., Dooley Jr., J. C., Whitby, K. T., 1978. Satellite detection of long-range pollution transport and sulfate aerosol hazes. Atmos. Environ., 12, 621-631.

Lyapustin, A., Wang, Y., Laszlo, I., Kahn, R., Korkin, S., Remer, L., Levy, R., Reid, J., 2011. Multi-Angle implementation of atmospheric correction (MAIAC): Part 2. Aerosol algorithm J. Geophys. Res., 116(D03211), doi:10.1029/2010JD014986

Mahowald, N. M., Baker, A. R., Bergametti, G., Brooks, N., Duce, R. A., Jickells, T. D., Kubilay, N., Prospero, J. M., Tegen, I., 2005. Atmospheric global dust cycle and iron inputs to the ocean. Global Biogeochem. Cycles, 19, GB4025, doi:10.1029/2004GB002402.

Malm, W. C., Schichtel, B. A., Pitchford, M. L., Ashbaugh, A. A., Eldred, R. A., 2004. Spatial and monthly trends in speciated fine particle concentration in the United States. J. Geophys. Res., 109, D03306, doi:10.1029/2003JD003739.

Martin, R. V., et al., 2002. An improved retrieval of tropospheric nitrogen dioxide from GOME. J. Geophys. Res., 107, 4437, doi:10.1029/2001JD001027.

Martin, R. V., Sioris, C. E., Chance, K., Ryerson, T. B., Bertram, T. H., Wooldridge, P. J., Cohen, R. C., Neuman, J. A., Swanson, A., Flocke, F. M., 2006. Evaluation of space-based constraints on global nitrogen oxide emissions with regional aircraft measurements over and downwind of eastern North America, J. Geophys. Res., 111, D15308, doi:10.1029/2005JD006680.

Martins, J. V., Tanre, D., Remer, L. A., Kaufman, Y. J., Mattoo, S., Levy, R., 2002. MODIS cloud screening for remote sensing of aerosol over oceans using spatial variability. Geophys. Res. Lett., 29, 10.1029/2001GL01352.

Martonchik, J. V., Diner, D. J., Kahn, R., Verstraete, M. M., Pinty, B., Gordon, H. R., Ackerman, T. P., 1998. Techniques for the Retrieval of aerosol properties over land and ocean using multiangle data, IEEE Trans. Geosci. Remt. Sensing 36, 1212-1227.

Martonchik, J. V., Diner, D. J., Crean, K., Bull, M., 2002. Regional aerosol retrieval results from MISR. IEEE Trans. Geosci. Remt. Sensing 40, 1520-1531.

Martonchik, J. V., Kahn, R. A., Diner, D. J., 2009. Retrieval of Aerosol Properties over Land Using MISR Observations. In: Kokhanovsky, A.A. and G. de Leeuw, ed., Satellite Aerosol Remote Sensing Over Land. Springer, Berlin, pp.267-293.

Matsui, T., Kreidenweis, S., Pielke Sr., R. A., Schichtel, B., Yu, H., Chin, M., Chu, A., Niyogi, D., 2004. Regional comparison and assimilation of GOCART and MODIS aerosol optical depth across the eastern U.S., Geophys. Res. Lett., 31, L21101, doi:10.1029/2004GL021017.

Mattis, I., A. Ansmann, D. Muller, U. Wandinger, and D. Althausen, Dual-wavelength Raman lidar observations of the extinction-to-backscatter ratio of Saharan dust, Geophys. Res. Lett., 29, 1306, doi:10.1029/2002GL014721, 2002.

McCormick, R. A., Ludwig, J. H., 1967. Climate modification by atmospheric aerosols. Science, 156, 1358-1359.

McNeil, W., and A. Carswell, Lidar polarization studies of the troposphere. Appl. Opt., 14, 2158-2168, 1975.

Mekler, Y., Quenzel, H., Ohring, G., Marcus, I., 1977. Relatiove atmospheric aerosol content from ERTS observations. J. Geophys. Res., 82, 967-970.

Mishchenko, M. I., Geogdzhayev, I. V., Cairns, B., Rossow, W. B., Lacis, A. A., 1999. Aerosol retrievals over the ocean using channel 1 and 2 AVHRR data: A sensitivity analysis and preliminary results. Appl. Opt., 38, 7325-7341, doi:10.1364/AO.38.007325.

Mishchenko, M. I., Geogdzhayev, I. V., Liu, L., Ogren, J. A., Lacis, A. A., Rossow, W. B., Hovenier, J. W., Volten, H., Muñoz, O., 2003. Aerosol retrievals from AVHRR radiances: Effects of particle nonsphericity and absorption and an updated long-term global climatology of aerosol properties. J. Quant. Spectrosc. Radiat. Transfer, 79-80, 953-972.

Mishchenko, M. I., Cairns, B., Chowdhary, J., Geogdzhayev, I. V., Liu, L., Travis, L. D., 2005. Remote sensing of terrestrial tropospheric aerosols from aircraft and satellites. J. Phys. Conf. Series, **6**, 73-89, doi:10.1088/1742-6596/6/1/005.

Moroney, C., Davies, R., Muller, J.-P., 2002. Operational retrieval of cloud-top heights using MISR data. IEEE Trans. Geosci. Rem. Sens. 40, 1532–1540.

Muller, J.-P., Mandanayake, A., Moroney, C., Davies, R., Diner, D. J., Paradise, S., 2002. Operational retrieval of cloud-top heights using MISR data. IEEE Trans. Geosci. Remote Sens. 40, 1532– 1546.

Moulin, C., Lambert, C., Dulac, F., Dayan, U., 1997. Control of atmospheric export of dust from North Africa by the North Atlantic Oscillation. Nature, 387, 691– 694.

Murayama, T., et al., Ground-based network observation of Asian dust events of April 1998 in east Asia, J. Geophys. Res., 106, 18345-18360, 2001.

Omar, A., et al., 2009. The CALIPSO automated aerosol classification and lidar ratio selection algorithm. J. Atmos. Oceanic Technol., 26, 1994-2014, doi:10.1175/2009JTECHA1231.1.

Pereira, G., Freitas, S. R., Moraes, E. C., Ferreira, N. J., Shimabukuro, Y. E., Rao, V. B., Longo, K. M., 2009. Estimating trace gas and aerosol emissions over South America: Relationship between fire radiative energy released and aerosol optical depth observations. Atmos. Environ., 43, 6388-6397.

Petrenko, M., Kahn, R. A., Chin, M., Soja, A., Kucsera, T., Harshvardhan, 2012. The use of satellite-measured aerosol optical depth to constrain biomass burning emissions source strength in a global aerosol model (GOCART). J. Geophy., Res, (Submitted)

Peyridieu, S., Chedin, A., Tanre, D., Capelle, V., Pierangelo, C., Lamquin, N., Armante, R., 2010. Saharan dust infrared optical depth and altitude retrieved from AIRS: a focus over North Atlantic – comparisons to MODIS and CALIPSO. Atmos. Chem. Phys., 10, 1953-1967.

Pierangelo, C., Chédin, A., Heilliette, S., Jacquinet-Husson, N., Armante, R., 2004. Dust altitude and infrared optical depth from AIRS. Atmos. Chem. Phys., 4, 1813-1822.

Pope, C. A. III, Burnett, R. T., Thun, M. J., Calle, E. E., Krewski, D., Ito, K., et al. 2002. Lung cancer, cardiopulmonary mortality, and long-term exposure to fine particulate air pollution. J. Amer. Med. Assoc., 287, 1132–1141.

Prados, A. I., Kondragunta, S., Ciren, P., Knapp, K. R., 2007. GOES Aerosol/Smoke Product (GASP) over North America: Comparisons to AERONET and MODIS observations. J. Geophys. Res., 112, D15201, doi:10.1029/2006JD007968.

Prospero, J. M., Carlson, T. N., 1972. Vertical and areal distribution of Saharan dust over the western equatorial North Atlantic Ocean. J. Geophys. Res., 77(27), 5255–5265, doi:10.1029/JC077i027p05255.

Prospero, J. M., 1996. The atmospheric transport of particles to the ocean, in Particle Flux in the Ocean. edited by V. Ittekkot et. al., pp. 19–52, John Wiley, Hoboken, N. J.

Prospero, J. M., 1999. Long-range transport of mineral dust in the global atmosphere: Impact of African dust on the environment of the southeastern United States. Proc. Natl. Acad. Sci. USA, 96, 3396-3403.

Prospero, J. M., Ginoux, P., Torres, O., Nicholson, S. E., Gill, T. E., 2002. Environmental characterization of global sources of atmospheric soil dust identified with the NIMBUS 7 Total Ozone Mapping Spectrometer (TOMS) absorbing aerosol product. Rev. Geophys., 40(1), 1002, doi:10.1029/2000RG000095.

Prospero, J. M., Blades, E., Mathison, G., Naidu, R., 2005. Interhemispheric transport of viable fungi and bacteria from Africa to the Caribbean with soil dust. Aerobiologia, 21(1), 119, doi:10.1007/s10453-004-5872-7.

Prospero, J. M., Landing, W. M., Schulz, M., 2010. African dust deposition to Florida: Temporal and spatial variability and comparisons to models. J. Geophys. Res., 115, D13304, 10.1029/2009JD012773.

Rahn, K. A., Borys, R., Shaw, G. E., 1977. The Asian source of Arctic haze bands. Nature 268, 713-715.

Ramanathan, V., Chung, C., Kim, D., Bettge, D., Buja, L., Kiehl, J. T., Washington, W. M., Fu, Q., Sikka, D. R., Wild, M., 2005. Atmospheric brown clouds: Impacts on South Asian climate and hydrological cycle. Proc. Natl. Acad. Sci., 102, 5326-5333.

Ramanathan, V., Carmichael, G., 2008. Global and regional climate changes due to black carbon. Nature Geoscience **1,** 221-227.

Rasch, P. J., Collins, W. D., Eaton, B. E., 2001. Understanding the Indian Ocean Experiment (INDOEX) aerosol distributions with an aerosol assimilation, J. Geophys. Res., 106(D7), 7337–7355, doi:10.1029/2000JD900508.

Reid, J. S., et al., 2003. Analysis of measurements of Saharan dust by airborne and ground-based remote sensing methods during the Puerto Rico Dust Experiment (PRIDE). J. Geophys. Res., 108, 8586, doi:10.1029/2002JD002493.

Reid, J. S., Prins, E. M.,Westphal, D. L., Schmidt, C. C., Richardson, K. A., Christopher, S. A., Eck, T. F., Reid, E. A., Curtis, C. A., Hoffman, J. P., 2004. Real-time monitoring of South American smoke particle emissions and transport using a coupled remote sensing/box-model approach. Geophys. Res. Lett., 31, L06107, doi:10.1029/2003GL018845.

Reid, J. S., Hyer, E. J., Prins, E. M., Westphal, D. L., Zhang, J., Wang, J., Christopher, S. A., Curtis, C. A., Schmidt, C. C., Eleuterio, D. P., Richardson, K. A., Hoffman, J. P., 2009. Global Monitoring and Forecasting of Biomass-Burning Smoke: Description of and Lessons from the Fire Locating and Modeling of Burning Emissions (FLAMBE) Program. IEEE Journal of Selected Topics in Applied Earth Observations and Remote Sensing, JSTARS-2009-00034.

Remer, L. A., Tanré, D., Kaufman, Y. J., et al., 2002. Validation of MODIS aerosol retrieval over ocean. Geophys Res. Lett., 29, doi: 10.1029/2001GL013204.

Remer, L.A., Kaufman, Y. J., Tanré, D., et al., 2005. The MODIS aerosol algorithm, products, and validation. J. Atmos. Sci., 62, 947-973.

Remer, L. A., Kleidman, R. G., Levy, R. C., Kaufman, Y. J., Tanre, D., Mattoo, S., Martins, J. V., Ichoku, C., Koren, I., Yu, H. B., Holben, B. N., 2008. Global aerosol climatology from the MODIS satellite sensors. J. Geophys. Res., 113, D14S07, doi:10.1029/2007JD009661.

Richter, A., Burrows, J. P., Nüß, H., Granier, C., Niemeier, U., 2005. Increase in tropospheric nitrogen dioxide over China observed from space, Nature, 437, 129-132.

Ridley, D. A., Heald, C. L., Ford, B., 2012. North African dust export and deposition: A satellite and model perspective. J. Geophys. Res., 117, D02202, doi:10.1029/2011JD016794.

Rinsland, C. P., et al., 2006. Nadir measurements of carbon monoxide distributions by the Tropospheric Emission Spectrometer instrument onboard the Aura Spacecraft: Overview of analysis approach and examples of initial results. Geophys. Res. Lett., 33, L22806, doi:10.1029/2006GL027000.

Rudich, Y., Kaufman, Y. J., Dayan, U., Yu, H., Kleidman, R. G., 2008. Estimation of transboundary transport of pollution aerosols by remote sensing in the eastern Mediterranean, J. Geophys. Res., 113, D14S13, doi:10.1029/2007JD009601.

Russell, P. B., Hobbs, P. V., Stowe, L. L., 1999. Aerosol properties and radiative effects in the United States East Coast haze plume: An overview of the Tropospheric Aerosol Radiative Forcing Observational Experiment (TARFOX). J. Geophys. Res., 104(D2), 2213–2222, doi:10.1029/1998JD200028.

Russell, P. B., Bergstrom, R. W., Shinozuka, Y., Clarke, A. D., DeCarlo, P. F., Jimenez, J. L., Livingston, J. M., Redemann, J., Dubovik, O., Strawa, A., 2010. Absorption Angstrom Exponent in AERONET and related data as an indicator of aerosol composition, Atmos. Chem. Phys., 10, 1155-1169, doi:10.5194/acp-10-1155-2010.

Sassen, K., 2002. Indirect climate forcing over the western US from Asian dust storms. Geophys. Res. Lett. **29,** 1465.

Satheesh, S. K., Torres, O., Remer, L. A., Babu, S. S., Vinoj, V., Eck, T. F., Kleidman, R. G., Holben, B. N., 2009. Improved assessment of aerosol absorption using OMI-MODIS joint retrieval. J. Geophys. Res., 114, D05209, doi:10.1029/2008JD011024.

Schepanski, K., Tegen, I., Laurent, B., Heinold, B., Macke, A., 2007. A new Saharan dust source activation frequency map derived from MSG-SEVIRI IR-channels. Geophys. Res. Lett., 34, L18803, doi:10.1029/2007GL030168.

Schepanski, K., Tegen, I., Macke, A., 2009. Saharan dust transport and deposition towards the tropical northern Atlantic. Atmos. Chem. Phys., 9, 1173–1189, doi:10.5194/acp-9-1173-2009.

Schulz, B. E., 2001. Spaceborne laser altimetry: 2001 and beyond, in Plag, H.P. (ed.), Book of Extended Abstracts, WEGENER-98, Norwegian Mapping Authority, Honefoss, Norway, 1998.

Schulz, M., Textor, C., Kinne, S., Balkanski, Y., Bauer, S., Berntsen, T., Berglen, T., et al., 2006. Radiative forcing by aerosols as derived from the AeroCom present-day and pre-industrial simulations. Atmos. Chem. Phys., 6, 5225-5246.

Scollo, S., Folch, A., Coltelli, M., Realmuto, V. J., 2010. Three-dimensional volcanic aerosol dispersal: A comparison between Multiangle Imaging Spectroradiometer (MISR) data and numerical simulations. J. Geophys. Res. 115, D24210. doi:10.1029/2009JD013162.

Sessions, W. R., Fuelberg, H. E., Kahn, R. A., Winker, D. M., 2011. An investigation of methods for injecting emissions from boreal wildfires using WRF-Chem during ARCTAS, Atmos. Chem. Phys., 11, 5719-5744, doi:10.5194/acp-11-5719-2011.

Shaw, G. E. 1983. Evidence for a central Eurasian source area of Arctic haze in Alaska. Nature 299, 815-818.

Shi, Y., Zhang, J., Reid, J. S., Holben, B., Hyer, E. J., Curtis, C., 2011. An analysis of the collection 5 MODIS over-ocean aerosol optical depth product for its implication in aerosol assimilation, Atmos. Chem. Phys., 11, 557-565, doi:10.5194/acp-11-557-2011.

Shindell, D., Chin, M., Dentener, F., Doherty, R. M., Faluvegi, G., Fiore, A. M., Hess, P., et al., 2008. A multi-model assessment of pollution transport to the Arctic. Atmos. Chem. Phys., 8, 5353-5372.

Singh, H. B., Brune, W. H., Crawford, J. H., Flocke, F., Jacob, D. J., 2009. Chemistry and transport of pollution over the Gulf of Mexico and the Pacific: Spring 2006 INTEX-B campaign overview and first results. Atmos. Chem. Phys., 9, 2301-2318.

Sirocko, F., Sarnthein, M., 1989. Wind-borne deposits in the Northwestern Indian Ocean: record of Holocene sediments versus modern satellite data. In M. Leinen & M. Sarnthein (Eds.), Paleoclimatology and Paleometeorology, NATO ASI Series, C, Math. and Phys. Sciences (Vol. 282, pp. 401-433). Dordrecht, Boston, London: Kluwer Academic Publishers.

Smirnov, A., et al., 2009. Maritime Aerosol Network as a component of Aerosol Robotic Network. J. Geophys. Res., 114, D06204, doi:10.1029/2008JD011257.

Spinhirne, J. D., Palm, S. P., Hart, W. D., Hlavka, D. L., Welton, E. J., 2005. Cloud and aerosol measurements from the GLAS space borne lidar: initial results. Geophys. Res. Lett., 32, L22S03, doi:10.1029/2005GL023507.

Stephens, G. L., Vane, D. G., Boain, R. J., Mace, G. G., Sassen, K., Wang, Z., Illingworth, A. J., 2002. The CloudSat mission and the A-Train: A new dimension o space-based observation of clouds and precipitation. Bull. Am. Meteorol. Soc., 83, 1771–1790.

Stohl, A., Forster, C., Huntrieser, H., et al., 2007. Aircraft measurements over Europe of an air pollution plume from Southeast Asia – aerosol and chemical characterization, Atmos. Chem. Phys., 7, 913-937.

Stowe, L. L., Ignatov, A. M., Singh, R. R., 1997. Development, validation, and potential enhancements to the second-generation operational aerosol product at the National Environmental Satellite, Data, and Information Service of the National Oceanic and Atmospheric Administration. J. Geophys. Res., 102(D14), 16,923–16,934, doi:10.1029/96JD02132.

Stowe, L. L., Jacobowitz, H., Ohring, G., Knapp, K. R., Nalli, N. R., 2002. The Advanced Very High Resolution Radiometer (AVHRR) Pathfinder Atmosphere (PATMOS) Climate Dataset: Initial Analyses and Evaluations. J Clim, 15(11), 1243.

Su, L., Toon, O. B., 2011. Saharan and Asian dust: similarities and differences determined by CALIPSO, AERONET, and a coupled climate-aerosol microphysical model, Atmos. Chem. Phys., 11, 3263-3280, doi:10.5194/acp-11-3263-2011.

Swap, R., Garstang, M., Greco, S., Talbot, R., Kallberg, P., 1992. Saharan dust in the Amazon Basin. Tellus, 44B, 133-149.

Tanré, D., Kaufman, Y. J., Herman, M., Mattoo, S., 1997. Remote sensing of aerosol properties over oceans using the MODIS/EOS spectral radiances. J. Geophys. Res., 102**,** 16971-16988.

Tanré, D., Bréon, F. M., Deuzé, J. L., Herman, M., Goloub, P., Nadal, F., Marchand, A., 2001. Global observation of anthropogenic aerosols from satellite. Geophys. Res. Lett., 28(24), 4555-4558.

Tanré, D., Haywood, J. M., Pelon, J., Léon, J. F., Chatenet, B., Formenti, P., Francis, P., Goloub, P., Highwood, E. J., Myhre, G., 2003. Measurement and modeling of the Saharan dust radiative impact: Overview of the Saharan Dust Experiment (SHADE). J. Geophys. Res., 108, 8574, doi:10.1029/2002JD003273.

Tanré, D., Bréon, F. M., Deuzé, J. L., Dubovik, O., Ducos, F., François, P., Goloub, P., Herman, M., Lifermann, A., Waquet, F., 2011. Remote sensing of aerosols by using polarized, directional and spectral measurements within the A-Train: the PARASOL mission. Atmos. Meas. Tech., 4, 1383-1395, doi:10.5194/amt-4-1383-2011.

Tegen, I., Hollrig, P., Chin, M., Fung, I., Jacob, D., Penner, J., 1997. Contribution of different aerosol species to the global aerosol extinction optical thickness: Estimates from model results. J. Geophys. Res., 102(D20), 23,895–23,915, doi:10.1029/97JD01864.

Tegen, I., Werner, M., Harrison, S. P., Kohfeld, K. E., 2004. Relative importance of climate and land use in determining present and future global soil dust emission. Geophys. Res. Lett., 31, L05105, doi:10.1029/2003GL019216.

Tesche, M., Ansmann, A., Müller, D., Althausen, D., Engelmann, R., Freudenthaler, V., Groß, S., 2009. Vertically resolved separation of dust and smoke over Cape Verde using multiwavelength Raman and polarization lidars during Saharan Mineral Dust Experiment 2008, J. Geophys. Res., 114, D13202, doi:10.1029/2009JD011862.

Textor, C., Schulz, M., Guibert, S., Kinne, S., Balkanski, Y., Bauer, S., Berntsen, T., et al., 2006. Analysis and quantification of the diversities of aerosol life cycles within AeroCom, Atmos. Chem. Phys., 6, 1777-1813.

Textor, C., et al., 2007. The effect of harmonized emissions on aerosol properties in global models – an AeroCom experiment. Atmos. Chem. Phys., 7, 4489-4501, doi:10.5194/acp-7-4489-2007.

Thieuleux, F., Moulin, C., Breon, F. M., Maignan, F., Poitou, J., Tanre, D., 2005. Remote sensing of aerosols over the oceans using MSG/SEVIRI imagery, Annales Geophysicae, 23, 1-8.

Tian, B., Waliser, D. E., Kahn, R. A., Li, Q., Yung, Y. L., Tyranowski, T., Geogdzhayev, I. V., Mishchenko, M. I., Torres, O., Smirnov, A., 2008. Does the Madden-Julian Oscillation influence aerosol variability?. J. Geophys. Res., 113, D12215, doi:10.1029/2007JD009372.

Tian, B., Waliser, D. E., Kahn, R. A., Wong, S., 2011. Modulation of Atlantic aerosols by the Madden-Julian Oscillation. J. Geophys. Res., 116, D15108, doi:10.1029/2010JD015201.

Torres, O., Bhartia, P. K., Herman, J. R., Sinyuk, A., Ginoux, P., Holben, B. N., 2002. A long-term record of aerosol optical depth from TOMS observations and comparison to AERONET measurements. J. Atmos. Sci., 59(3), 398-413.

Torres, O., et al., 2007. Aerosols and surface UV products from Ozone Monitoring Instrument observations: An overview. J. Geophys. Res., 112, D24S47, doi:10.1029/2007JD008809.

Torres, O., Jethva, H., & Bhartia, P. K., 2012. Retrieval of aerosol optical depth over clouds from OMI observations: Sensitivity analysis and case studies. J. Atmos. Sci., 69, 1037-1053, doi:10.1175/JAS-D-11-0130.1

Twomey, S. 1977. The influence of pollution on the shortwave albedo of clouds, J. Atmos. Sci., 34, 1149-1152.

Uematsu, M., Duce, R. A., Prospero, J. M., 1985. Deposition of atmospheric mineral particles in the North Pacific Ocean. J. Atmos. Chem., 3, 123-138.

Uematsu, M., Wang, Z. F., Uno, I., 2003. Atmospheric input of mineral dust to the western North Pacific region based on direct measurements and a regional chemical transport model. Geophys. Res. Lett., 30(6), 1342, doi:10.1029/2002GL016645.

Uno, I., Yumimoto, K., Shimizu, A., Hara, Y., Sugimoto, N., Wang, Z., Liu, Z., Winker, D. M., 2008. 3D structure of Asian dust transport revealed by CALIPSO lidar and a 4DVAR dust model. Geophys. Res. Lett., 35, L06803, doi:10.1029/2007GL032329. .

Uno, I., Eguchi, K., Yumimoto, K., Takemura, T., Shimizu, A., Uematsu, M., Liu, Z., Wang, Z., Hara, Y., Sugimoto, N., 2009. Asian dust transported one full circuit around the globe. Nat. Geosci., 2, 557–560, doi:10.1038/ngeo583.

Uno, I., Eguchi, K., Yumimoto, K., Liu, Z., Hara, Y., Sugimoto, N., Shimizu, A., Takemura, T., 2011. Large Asian dust layers continuously reached North America in April 2010, Atmos. Chem. Phys., 11, 7333-7341, doi:10.5194/acp-11-7333-2011.

Val Martin, M., Logan, J. A., Kahn, R. A., Leung, F-Y., Nelson, D., Diner, D., 2010. Fire smoke injection heights over North America constrained from the Terra Multi-angle Imaging SpectroRadiometer. Atmos. Chem. Phys. 10, 1491-1510.

VanCuren, R.A., Cahill, T. A., 2002. Asian aerosols in North America: Frequency and concentration of fine dust. J. Geophys. Res., 107, D24, 4804, doi:10.1029/2002JD002204.

van der Werf, G. R., Randerson, J. T., Giglio, L., Collatz, G. J., Mu, M., Kasibhatla, P. S., Morton, D. C., DeFries, R. S., Jin, Y., van Leeuwen, T. T., 2010. Global fire emissions and

the contribution of deforestation, savanna, forest, agricultural, and peat fires (1997-2009), Atmos. Chem. Phys., 10, 11707-11735, doi:10.5194/acp-10-11707-2010.

Veefkind, J. P., Boersma, K. F., Wang, J., Kurosu, T. P., Krotkov, N., Chance, K., Levelt, P. F., 2011. Global satellite analysis of the relation between aerosols and short-lived trace gases. Atmos. Chem. Phys., 11, 1255-1267.

Veihelmann, B., Levelt, P. F., Stammes, P., Veefkind, J. P., 2007. Simulation study of the aerosol information content in OMI spectral reflectance measurements. Atmos. Chem. Phys., 7, 3115-3127.

Vermote, E., Ellicott, E., Dubovik, O., Lapyonok, T., Chin, M., Giglio, L., Roberts, G. J., 2009. An approach to estimate global biomass burning emissions of organic and black carbon from MODIS fire radiative power. J. Geophys. Res., 114, D18205, doi:10.1029/2008JD011188.

Wang, J., Xu, X., Henze, D. K., Zeng, J., Ji, Q., Tsay, S.-C., Huang, J., 2012. Top-down estimate of dust emissions through integration of MODIS and MISR aerosol retrievals with the GEOS-Chem adjoint model. Geophys. Res. Lett., 39, L08802, doi:10.1029/2012GL051136.

Waquet, F., Riedi, J., Labonnote, C., Goloub, P., Cairns, B., Deuze, J.-L., Tanre, D., 2009. Aerosol remote sensing over clouds using A-Train observations. J. Atmos. Sci., 66, 2468-2480.

Warner, J., Comer, M. M., Barnet, C. D., McMillan, W. W., Wolf, W., Maddy, E., Sachse, G., 2007. A comparison of satellite tropospheric carbon monoxide measurements from AIRS and MOPITT during INTEX-A. J. Geophys. Res., 112, D12S17, doi:10.1029/2006JD007925.

White, W. H., 1976. Reduction of visibility by sulfates in photochemical smog. Nature, 264, 735-736.

Wilcox, E. M., 2010. Stratocumulus cloud thickening beneath layers of absorbing smoke aerosol. Atmos. Chem. Phys., 10, 11769-11777.

Wilcox, E. M., Lau, K.-M., K.-M., Kim, 2010. A northward shift of the North Atlantic Ocean Intertropical Convergence Zone in response to summertime Saharan dust outbreaks. Geophys. Res. Lett., 37, L04804, doi:10.1029/2009GL041774.

Winker, D. M., Osborn, M. T., 1992. Preliminary analysis of observations of the Pinatubo volcanic plume with a polarization-sensitive lidar. Geophys. Res. Lett., 19(2), 171–174, doi:10.1029/91GL02866.

Winker, D. M., Couch, R., McCormick, M., 1996. An overview of LITE: NASA's Lidar In-Space Technology Experiment. Proc. IEEE **84(2):**164-180.

Winker, D. M., Vaughan, M. A., Omar, A., Hu, Y., Powell, K. A., Liu, Z., Hunt, W. H., Young, S. A., 2009. Overview of the CALIPSO mission and CALIOP data processing algorithms. J. Atmos. Oceanic Technol., 26, 2310-2323.

Winker, D. M., et al., 2010. The CALIPSO mission: A global 3D view of aerosols and clouds. Bull. Amer. Met. Soc., 91, 1211-1229.

Winker, D., Liu, Z., Omar, A., Tackett, J., Fairlie, D., 2012. CALIOP observations of the transport of ash from the Eyjafjallajokull volcano in April 2010. J. Geosphys. Res., **117**, D00U15, doi:10.1029/2011JD016499.

Yu, H., Liu, S. C., Dickinson, R. E., 2002. Radiative effects of aerosols on the evolution of the atmospheric boundary layer. J. Geophys. Res. **107**, 4142.

Yu, H., Dickinson, R. E., Chin, M., et al., 2003. Annual cycle of global distributions of aerosol optical depth from integration of MODIS retrievals and GOCART model simulations. J. Geophys. Res., 108, 4128, doi:10.1029/2002JD02717.

Yu, H., Kaufman, Y. J., Chin, M., et al., 2006. A review of measurement-based assessments of the aerosol direct radiative effect and forcing. Atmos. Chem. Phys., 6, 613-666, 2006.

Yu, H., Remer, L. A., Chin, M., Bian, H., Kleidman, R., Diehl, T., 2008. A satellite-based assessment of trans-Pacific transport of pollution aerosol, J. Geophys. Res., 113, D14S12, doi:10.1029/2007JD009349.

Yu, H., P. K. Quinn, G. Feingold, L. A. Remer, R. A. Kahn, M. Chin, and S. E. Schwartz, 2009a: Remote Sensing and In Situ Measurements of Aerosol Properties, Burdens, and Radiative Forcing, in Atmospheric Aerosol Properties and Climate Impacts, A Report by the U.S. Climate Change Science Program and the Subcommittee on Global Change Research. [Mian Chin, Ralph A. Kahn, and Stephen E. Schwartz (eds.)]. National Aeronautics and Space Administration, Washington, D.C., USA.

Yu, H., Chin, M., Remer, L. A., Kleidman, R. G., Bellouin, N., Bian, H., Diehl, T., 2009b. Variability of marine aerosol fine-mode fraction and estimates of anthropogenic aerosol component over cloud-free oceans from the Moderate resolution Imaging Spectroradiometer (MODIS). J. Geophys. Res., 114, D10206, doi:10.1029/2008JD010648.

Yu, H., Chin, M., Winker, D. M., Omar, A., Liu, Z., Kittaka, C., Diehl, T., 2010. Global view of aerosol vertical distributions from CALIPSO lidar measurements and GOCART simulations: Regional and seasonal variations. J. Geophys. Res., 115, D00H30, doi:10.1029/2009JD013364.

Yu, H., Chin, M., West, J., Atherton, C. S., Bellouin, N., Bey, I., Bergmann, D., Bian, H., Diehl, T., Forberth, G., Hess, P., Schulz, M., Shindell, D., Takemura, T., Tan, Q., 2012a. A HTAP multi-model assessment of the influence of regional anthropogenic emission reductions on aerosol direct radiative forcing and the role of intercontinental transport. J. Geophys. Res., submitted.

Yu, H., Zhang, Y., Chin, M., Liu, Z., Omar, A., Remer, L. A., Yang, Y., Yuan, T., Zhang, J., 2012b. An integrated analysis of aerosol above clouds from A-Train multi-sensor measurements. Remote Sens. Environ., 121, 125-131, doi:10.1016/j.rse.2012.01.011.

Yu, H., Remer, L. A., Chin, M., Bian, H., Tan, Q., Yuan, T., Zhang, Y., 2012c. Aerosols from Overseas Rival Domestic Emissions over North America, Science, in press.

Yumimoto, K., Eguchi, K., Uno, I., Takemura, T., Liu, Z., Shimizu, A., Sugimoto, N., 2009. An elevated large-scale dust veil from the Taklimakan Desert: Intercontinental transport and

three-dimensional structure as captured by CALIPSO and regional and global models. Atmos. Chem. Phys., 9, 8545–8558, doi:10.5194/acp-9-8545-2009.

Yumimoto, K., Eguchi, K., Uno, I., Takemura, T., Liu, Z., Shimizu, A., Sugimoto, N., Strawbridge, K., 2010. Summertime trans-Pacific transport of Asian dust. Geophys. Res. Lett., 37, L18815, doi:10.1029/2010GL043995.

Yumimoto, K., Takemura, T., 2011. Direct radiative effect of aerosols estimated using ensemble-based data assimilation in a global aerosol climate model. Geophys. Res. Lett., 38, L21802, doi:10.1029/2011GL049258.

Zender, C. S., Bian, H., Newman, D., 2003. Mineral Dust Entrainment and Deposition (DEAD) model: Description and 1990s dust climatology. J. Geophys. Res., 108(D14), 4416, doi:10.1029/2002JD002775.

Zhang, J., Reid, J. S., Holben, B. N., 2005. An analysis of potential cloud artifacts in MODIS over ocean aerosol optical thickness products. Geophys. Res. Lett., 32, L15803, doi:10.1029/2005GL023254.

Zhang, J., Reid, J. S., Westphal, D., Baker, N., Hyer, E., 2008. A System for Operational Aerosol Optical Depth Data Assimilation over Global Oceans. J. Geophys. Res., 113, D10208, doi:10.1029/2007JD009065.

Zhang, J., Reid, J. S., 2009. An analysis of clear sky and contextual biases using an operational over ocean MODIS aerosol product. Geophys Res Lett, 36, L15824, doi:10.1029/2009GL038723.

Zhang, J., Campbell, J. R., Reid, J. S., Westphal, D. L., Baker, N. L., Campbell, W. F., Hyer, E. J., 2011. Evaluating the impact of assimilating CALIOP-derived aerosol extinction profiles on a global mass transport model. Geophys Res Lett, 38, L14801, doi:10.1029/2011GL047737.

Zhang, J., Reid, J. S., 2010. A decadal regional and global trend analysis of the aerosol optical depth using a data-assimilation grade over-water MODIS and Level 2 MISR aerosol products. Atmos. Chem. Phys., 10, 10949-10963.

Zhang, R., Li, G., Fan, J., Wu, D. L., Molina, M. J., 2007. Intensification of Pacific storm track linked to Asian pollution. Proc. Natl. Acad. Sci., 104(13), 5295-5299, doi:10.1073/pnas.0700618104.

Zhang, X., Kondragunta, S., 2008. Temporal and spatial variability in biomass burned areas across the USA derived from the GOES fire product. Remote Sens. Environ., 112, 2886–2897, doi:10.1016/j.rse.2008.02.006.

Zhang, Y., Fu, R., Yu, H., Qian, Y., Dickinson, R. E., Silva Dias, M. A. F., da Silva Dias, P. L., Fernandes, K., 2009. Impact of biomass burning aerosol on the monsoon circulation transition over Amazonia, Geophys. Res. Lett., 36, L10814, doi:10.1029/2009GL037180.

Zhang, Y., Yu, H., Eck, T. F., Smirnov, A., Chin, M., Remer, L. A., Bian, H., Tan, Q., Levy, R., Holben, B. N., Piazzolla, S., 2012. Aerosol Daytime Variations over North and South

America Derived from Multiyear AERONET Measurements. J. Geophys. Res., s, 117, D05211, doi:10.1029/2011JD017242.

Zhao, X.-P., Laszlo, I., Guo, W., Heidinger, A., Cao, C., Jelenak, A., Tarpley, D., Sullivan, J., 2008. Study of long-term trend in aerosol optical thickness observed from operational AVHRR satellite instrument. J Geophys Res, 113, D07201.

Zwally, H. J., Schutz, B., Abdalati, W., Abshire, J., Bentley, C., Brenner, A., Bufton, J., Dezio, J., Hancock, D., Harding, D., Herring, T., Minster, B., Quinn, K., Palm, S., Spinhirne, J., Thomas, R., 2002. ICESat's laser measurements of polar ice, atmosphere, ocean, and land. J. Geodynamics, 34, 405-445.

Table 1: Summary of major operational and research products from satellite remote sensing that can be applied for characterizing aerosol intercontinental transport.

Sensor/platform	Swath	Measurement Period	Column load	Particle Properties (for aerosol type characterization)					Transport Heights		
			AOD	AE	FMF /size	SSA	AAI	NSF	LH	VP	ACA
TOMS/Nimbus, ADEOS, EP	~2700 km	1979 - 2001	√				√				√
AVHRR series	~2400 km	1981 - present	√ (O)	√ (O)							
A(A)TSR/Envisat	~500 km	1995 - present	√	√							
GOME/ERS-2 GOME-2/METOP	~2000 km	1995 – 2003 2007 - present	√				√				
POLDER/ADEOS 1, 2/PARASOL	~2400 km	1996, 2003 2004 - present	√	√	√	√		√			√
SeaWiFS/SeaStar	~2800 km	1997 - 2010	√	√							
MISR/Terra	~360 km	2000 - present	√	√	√	√		√	√		
MODIS/Terra MODIS/Aqua	~2300 km	2000 - present 2002 - present	√	√	√ (O)	√ (L)					
MERIS/Envisat	~1150 km	2003 - present	√	√							
SCIAMACHY/ Envisat	~960 km	2003 - present	√				√				
AIRS/Aqua	~1600 km (night)	2004 - present	√ (dust)						√ (dust)		
OMI/Aura	~2600 km	2004 - present	√			√	√				√
GLAS/ICESat	~70 m, day & night	2003 –present	√							√	
CALIOP/CALIPSO	~70 m, day & night	2006 - present	√	√				√		√	√
IASI/MetOp	~2050 km	2006 - present	√ (dust)						√ (dust)		
VIIRS/NPP Soumi	~3000 km	2012 - present	√	√ (O)	√ (O)						
VISSR/GOES series	~half-hourly, North and Central America	2003 - present	√								
SEVIRI/MSG	~hourly, West Europe, Africa, and the Atlantic	2004 - present	√								

Acronyms: L – Land only; **O** – Ocean only; **AOD** - aerosol optical depth; **AE** – Angstrom exponent; **FMF** – fine-mode fraction (with respect to AOD); **SSA** – single-scattering albedo; **AAI** – absorbing aerosol index; **NSF** – non-spherical fraction of AOD; **LH** – layer height; **VP** – vertical profile; **ACA** – above-cloud aerosol.

Table 2: Comparisons of trans-Pacific dust transport efficiency (a ratio of dust mass flux in North America inflow to that in East Asia outflow) and dust deposition to the North Pacific.

Transport efficiency	Dust deposition (Tg a^{-1})	Region	Notes	Source
Satellite-based estimate				
40%	84	30º-60ºN, 140ºE-130ºW	Deposition estimate should bias high because of the existence of northward transport to Arctic	Yu et al. (2012c)
Estimate based on in-situ measurements				
-	10	East China Sea only	Using 20g m^{-2} a^{-1} deposition rate over the $0.5x10^{12}$ m^2 area	Hsu et al. (2009)
-	67 (18 - 260)	*East China Sea only*	Estimated based on surface concentration measurements and model-based deposition rates	Gao et al. (1997)
-	96	North Pacific		Prospero et al. (1996)
-	480	North Pacific		Duce et al. (1991)
-	20	0º-50ºN, 150ºE-130ºW		Uematsu et al. (1985)
Model simulations				
34%	88	30º-60ºN, 140ºE-130ºW	GOCART model; including northward transport to Arctic	Yu et al. (2012c)
25%	92	30º-60ºN, 140ºE-130ºW	GMI model; including northward transport to Arctic	Yu et al. (2012c)
40%	-	25º-55ºN, 150ºE-130ºW	2007	Su and Toon (2011)
15%	-	120ºE-120ºW	For events in mid-August of 2009	Yumimoto et al. (2010)
30%	-	0º-70ºN, 140ºE-120ºW	For events during May 5-15, 2007	Eguchi et al. (2009)
43%	-	0º-90ºN, 120ºE-120ºW	Highly lofted (8-10km) dust event in May 2007	Uno et al. (2009)
35%	-	140ºE-130ºW	Taklimakan dust storm in May 2007	Yumimoto et al. (2009)
-	68	North Pacific	3-model composite; constrained by observations	Jickells et al. (2005)
-	56	North Pacific		Tegen et al. (2004)
-	35	North Pacific		Luo et al. (2003)
-	64	*western North Pacific (~25% of the basin)*	March 1994-May 1995	Uematsu et al. (2003)
-	31	North Pacific		Zender et al. (2003)
-	92	North Pacific		Ginoux et al. (2001)

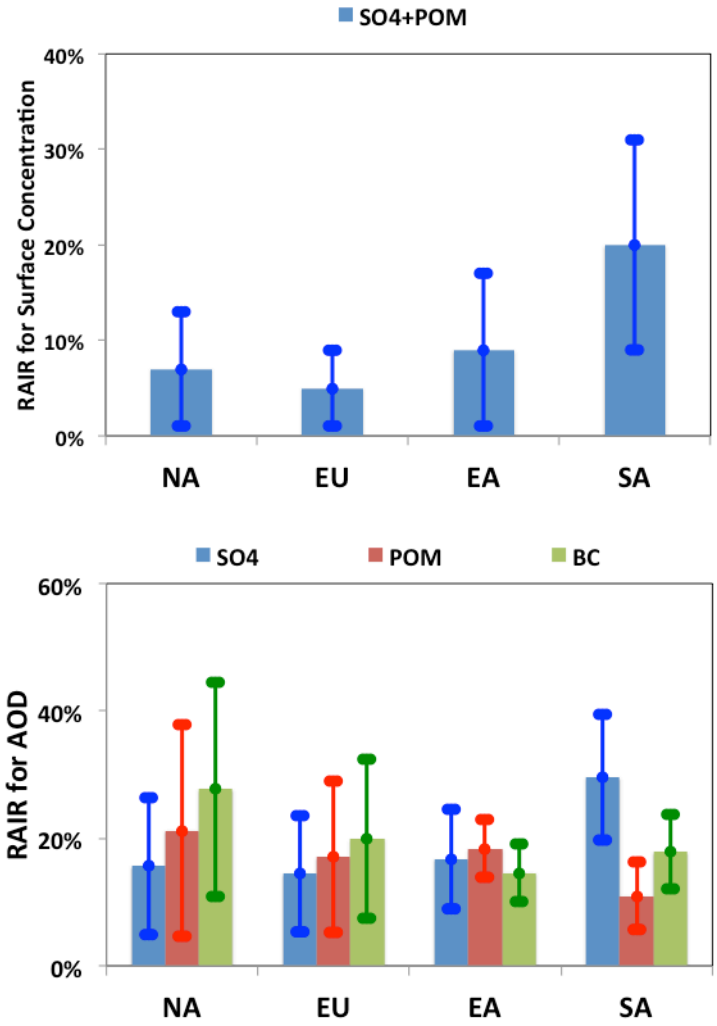

Figure 1: Multi-model derived average relative annual intercontinental response (RAIR) for surface concentration of SO4+POM and aerosol optical depth (AOD) by chemical component in four major pollution regions (NA – North America, EU – Europe, EA – East Asia, SA – South Asia), which is based on HTAP source/receptor relationship experiments by reducing anthropogenic emissions by 20% in each of the four regions. RAIR in a receptor region represents the percentage contribution of the intercontinental transport of foreign sources relative to the sum of foreign and domestic sources. Standard deviations, as indicated by error bars, reflect the variability of the 10 models in the ensemble. *Figures are adapted from HTAP (2010) for surface concentration and Yu et al. (2012a) for AOD.*

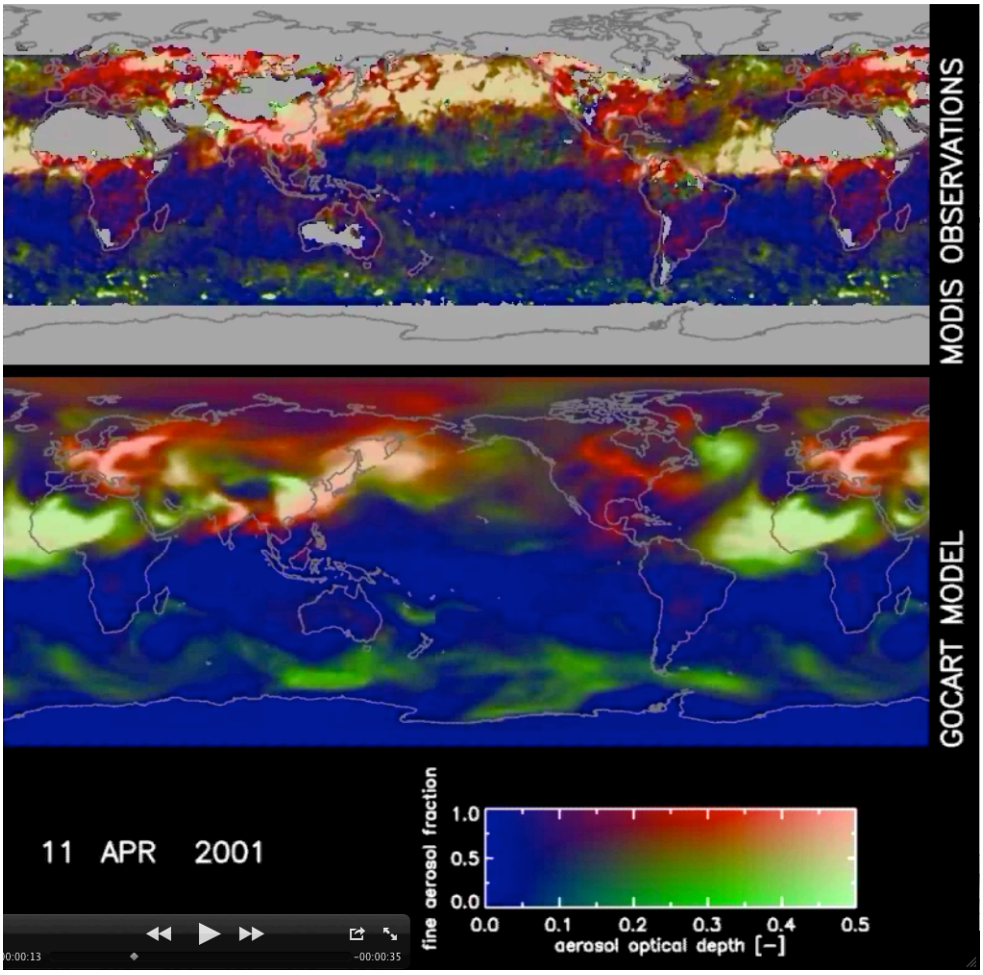

Figure 2: Spatial variations of aerosol type on April 11, 2001 as revealed by a composite of aerosol optical depth (at 550 nm) and fine-mode fraction observed by MODIS/Terra (top panel) and simulated by GOCART model (bottom panel) for April 11, 2001. Industrial pollution and biomass burning aerosols are predominated by small particles (shown as red), while mineral dust consists of a large fraction of large particles (shown as green). Bright red and bright green indicate heavy pollution and dust plumes, respectively *(image credit: Reto Stockli and Yoram Kaufman)*.

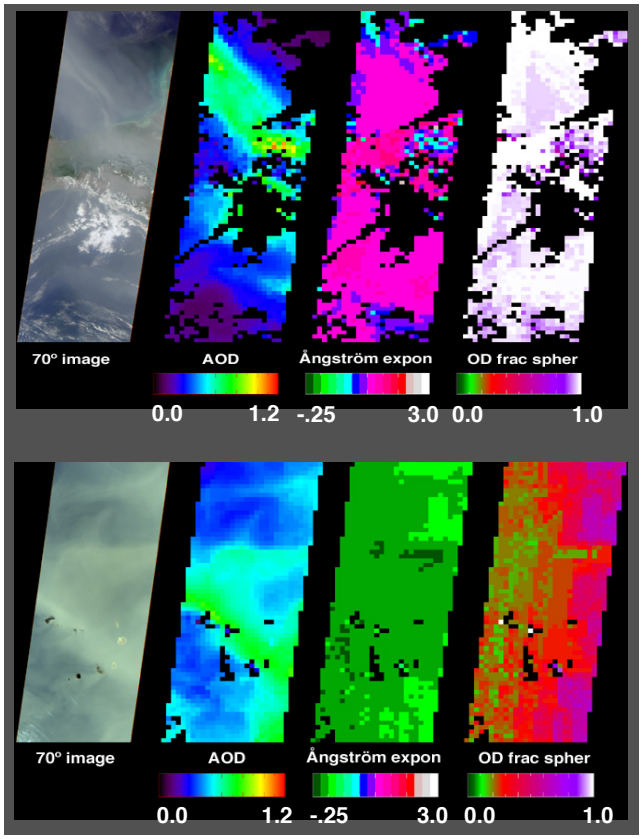

Figure 3. MISR oblique-camera images and retrievals of optical depth, Angstrom exponent, and non-spherical fraction of aerosol plumes. Top: southern Mexico smoke plumes drifting northward over the Gulf of Mexico on May 2, 2002 (Terra orbit 12616) Bottom: dust blowing off Sahara desert to Cape Verde islands on February 6, 2004 (Terra orbit 22006). The width of each image it the full MISR swath – about 400 km acorss; the vertical dimension is presented at the same spatial scale. (*Adapted from Diner et al., 2005. Image credit: MISR Team, Jet Propulsion Lab/Caltech and NASA Goddard Space Flight Center)*

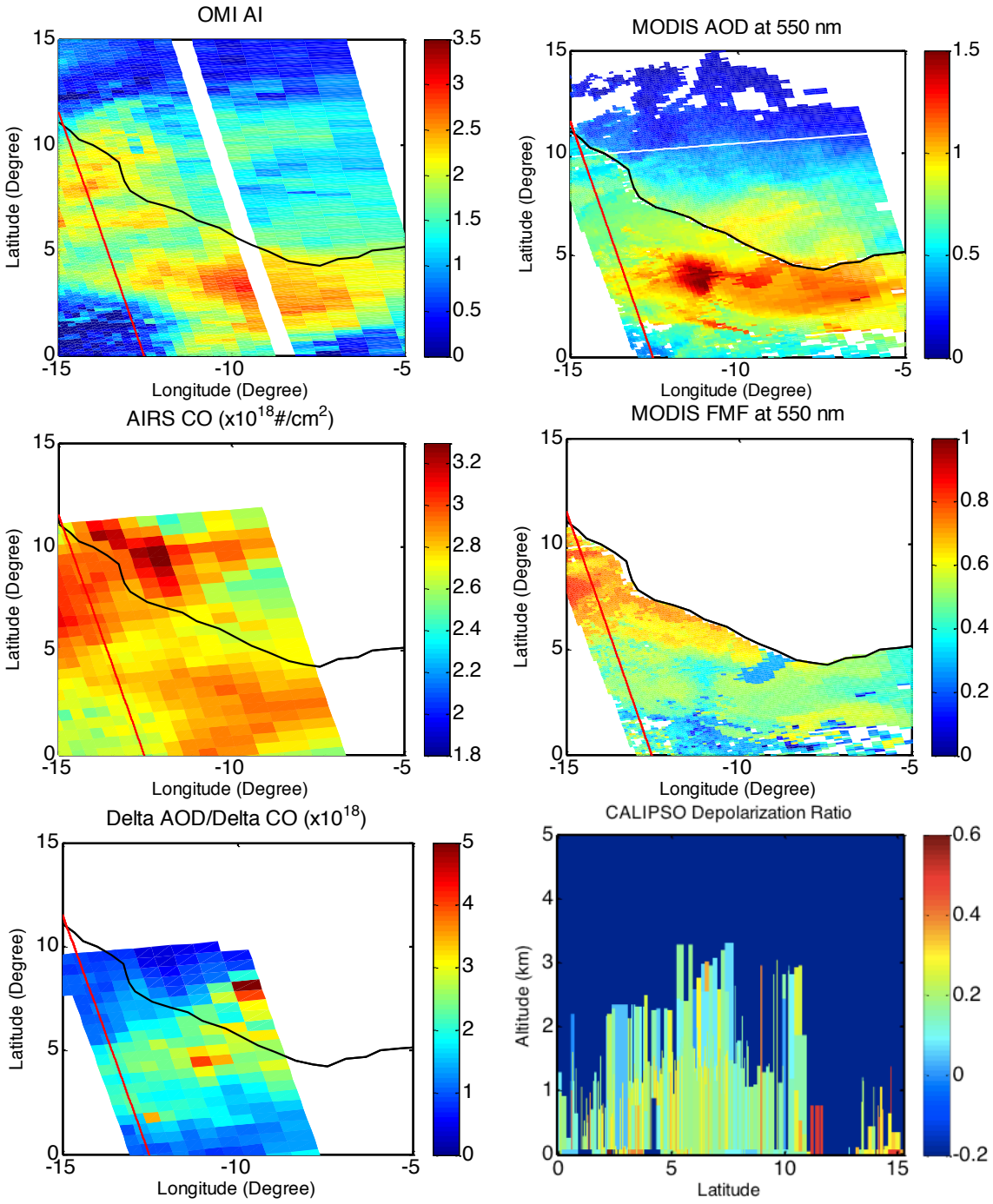

Figure 4a: An A-Train integrated characterization of dust and smoke aerosols transported over the Gulf of Guinea on January 31, 2008. Red line in maps of aerosol and CO horizontal distribution indicates the CALIPSO track.

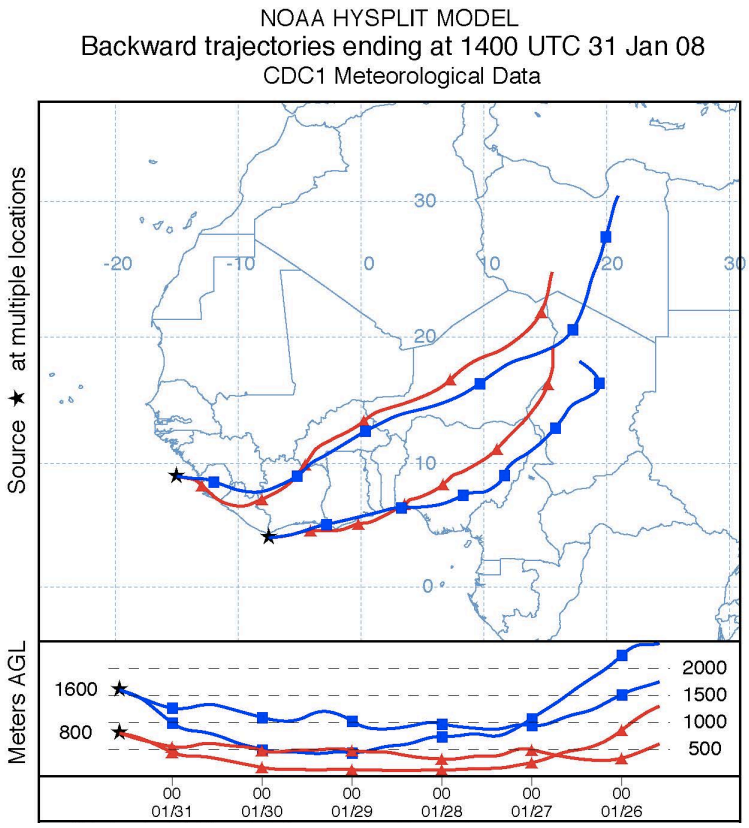

Figure 4b: 6-day HYSPLIT backward trajectories ending at [9ºN, 15ºW] in the smoke-dominated regime and at [4ºN, 7.5ºW] in the dust-smoke mixed regime on January 31, 2008 1400UTC. The air mass arrived at both locations passed over the smoke-active Sahel region during the January 28-30 period. During the January 26-27 period, the air mass arriving at [4ºN, 7.5ºW] originated from the Bodèlè Depression – the major source of Saharan dust in the winter, whereas that arriving at [9ºN, 15ºW] drifted off north to the Bodèlè Depression and were influenced less by dust.

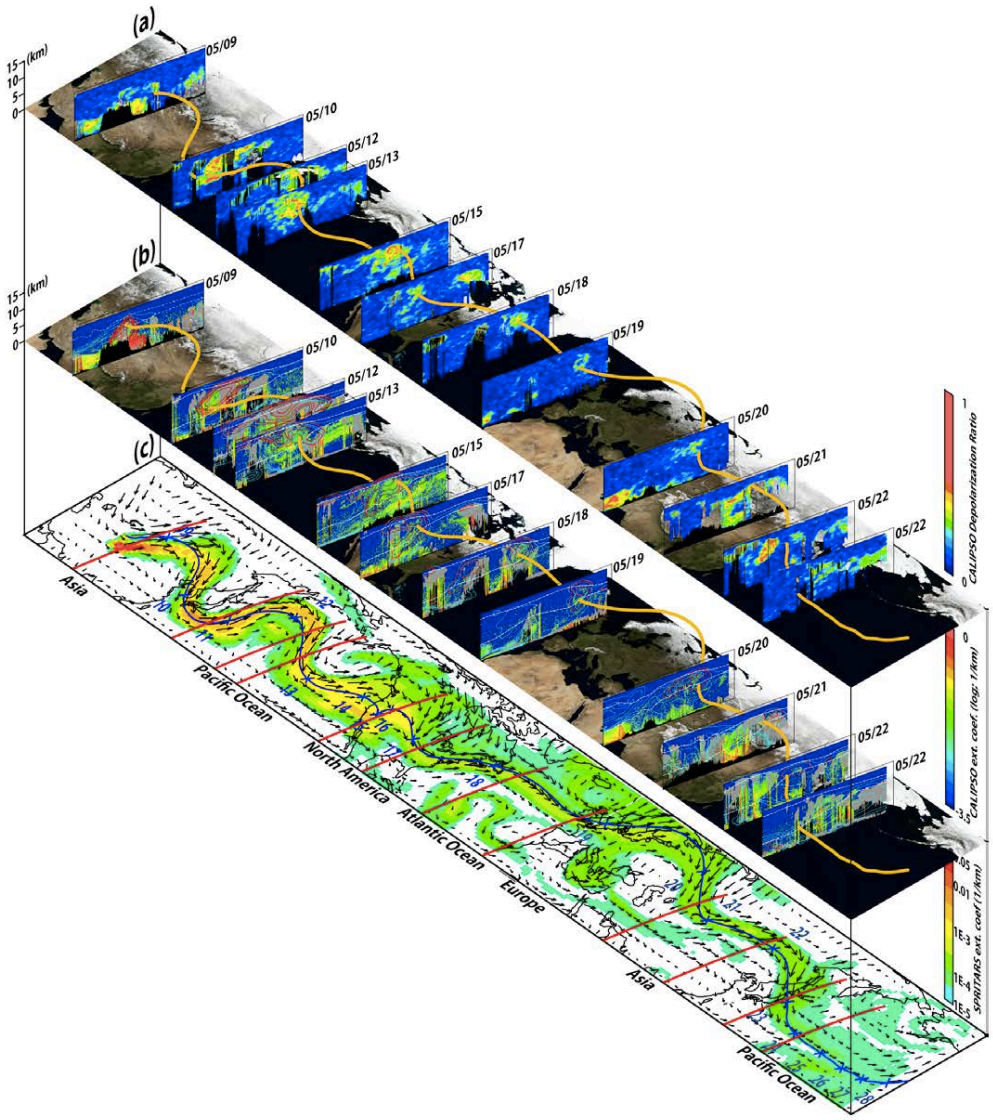

Figure 5. A three-dimensional view of the hemispherical transport of Asian dust during May 9-22, 2007 as provided by CALIOP measurements of vertical distributions of depolarization ratio (a, dust is distinguished from other types of aerosols by exhibiting high depolarization ratio) and extinction coefficient (b), and a global model simulation of extinction coefficient in the dust layer (c). The vertical and horizontal transport paths are further illustrated by HYSPLIT trajectories. *(Figure taken from Uno et al., 2009, with permission from Nature Geoscience)*

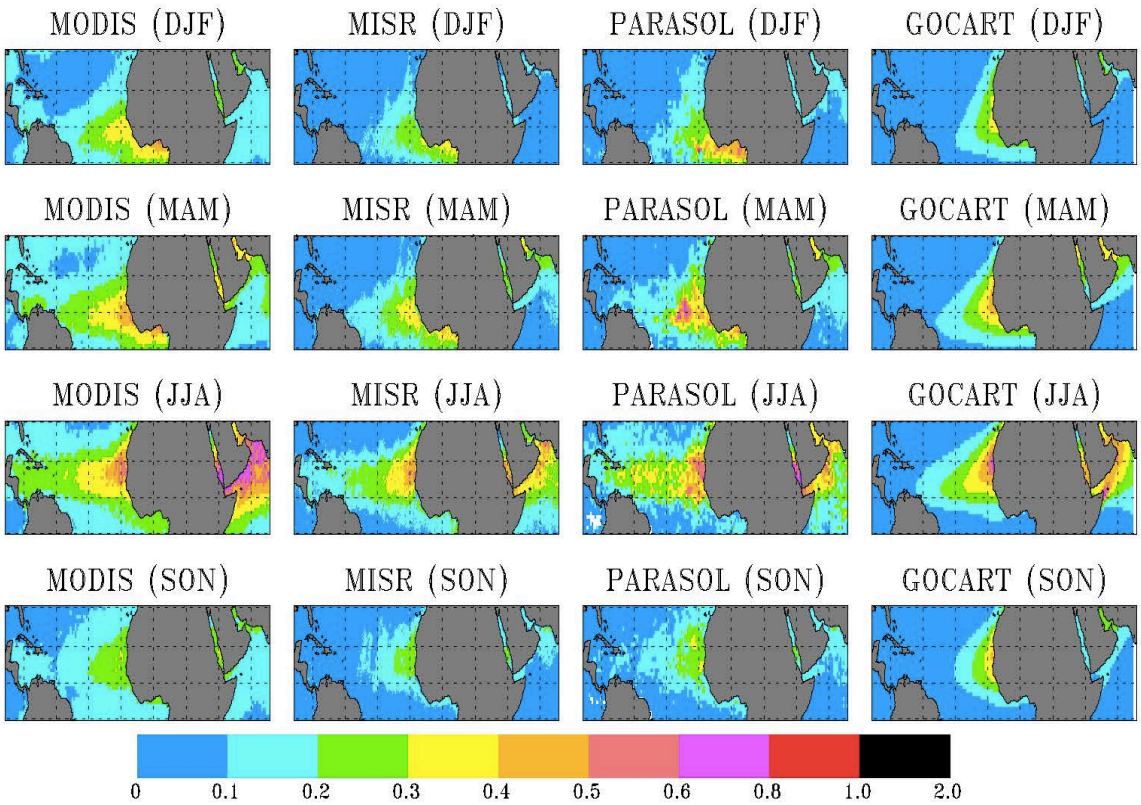

Figure 6: Seasonal variations of trans-Atlantic transport of dust AOD observed by MODIS, MISR, and PARASOL, and simulated by GOCART model.

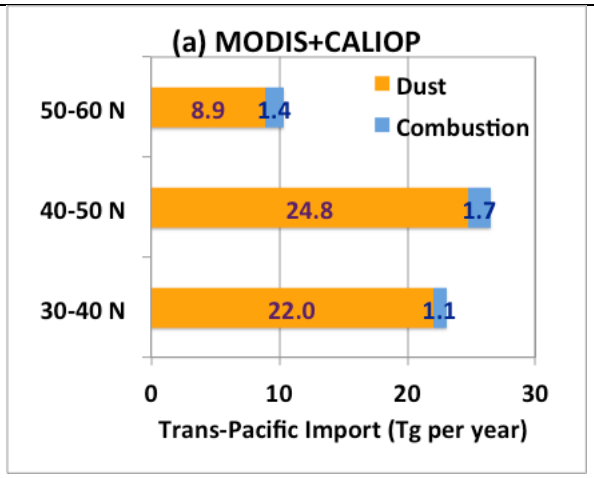

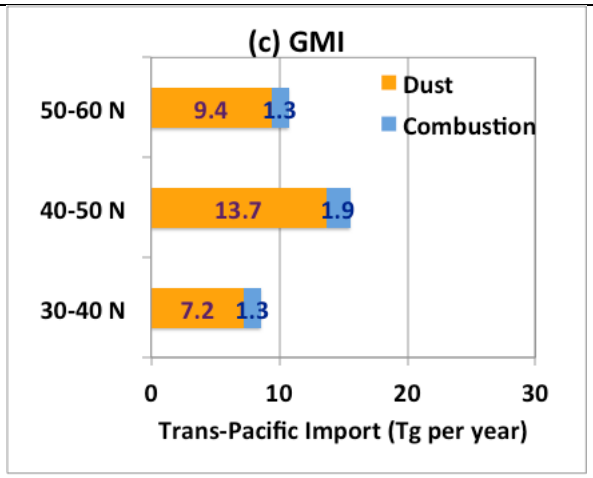

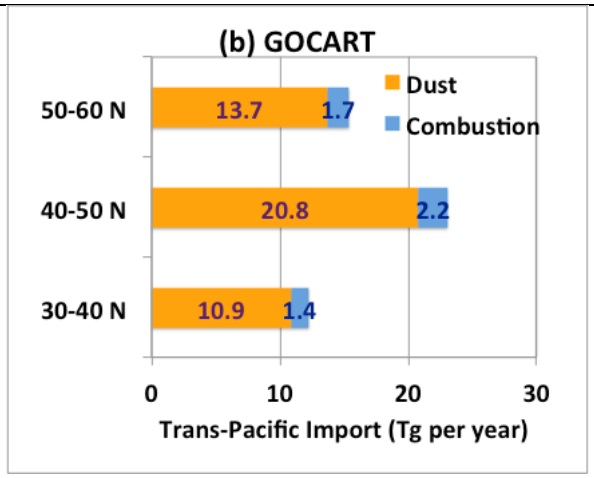

Figure 7: Meridional variations of annual trans-Pacific aerosol import to North America as estimated from MODIS and CALIOP measurements (a) and simulated by GOCART (b) and GMI (c) model, which is summarized from results documented in Yu et al. (2008) and Yu et al. (2012c).

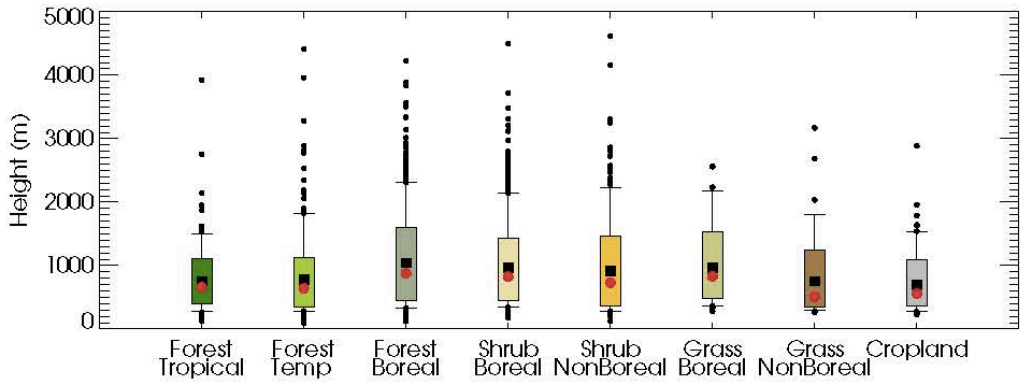

Figure 8. MISR observed smoke plume heights (above the ground level) in each biome over North America in 2002, and 2004-2007. Bar plots indicate the distribution of the data. The medians (red circles) and the means (black squares) are shown along with the central 67% (color coded box) and the central 95% (thin black lines). Data that fall outside the bar plots are plotted with black circles. *(Figure taken from Val Martin et al., 2010, with permission from Atmospheric Chemistry and Physics).*

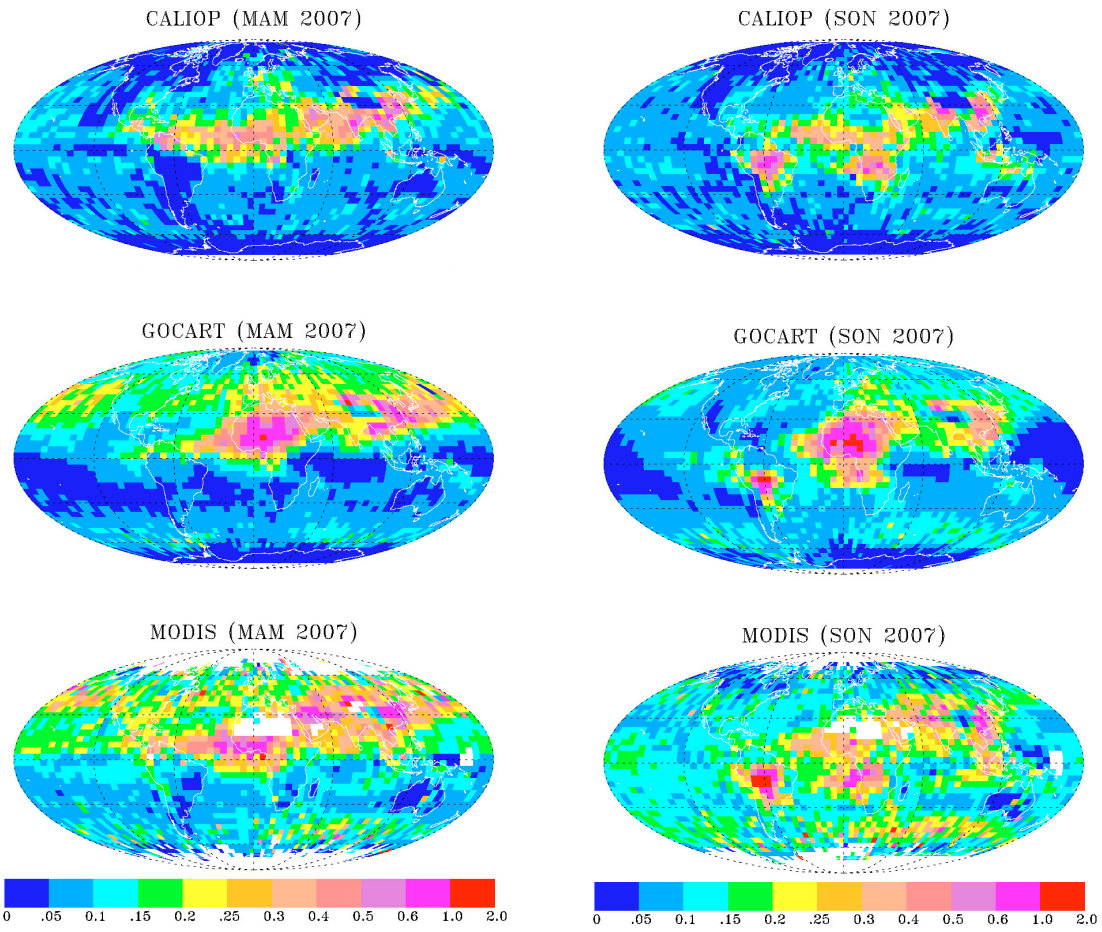

Figure 9. Comparisons of seasonal AOD between GOCART model, CALIOP and MODIS retrievals. *(adapted from Yu et al., 2010, with permission from American Geophysical Union)*

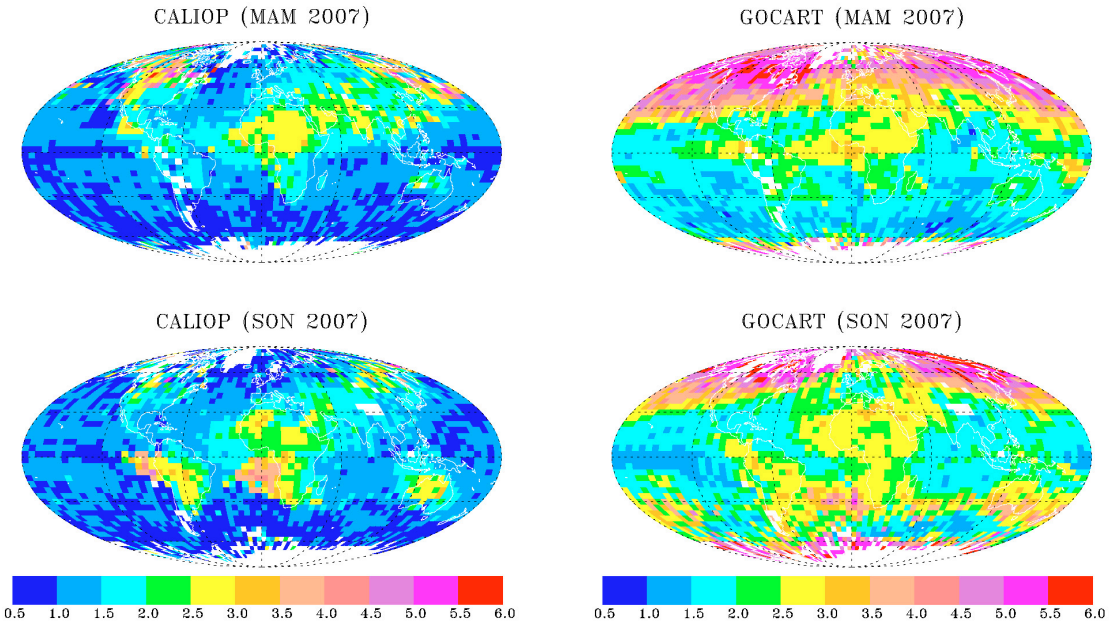

Figure 10: Comparison of aerosol scale height between GOCART model and CALIOP measurements *(adapted from Yu et al., 2010, with permission from American Geophysical Union).*

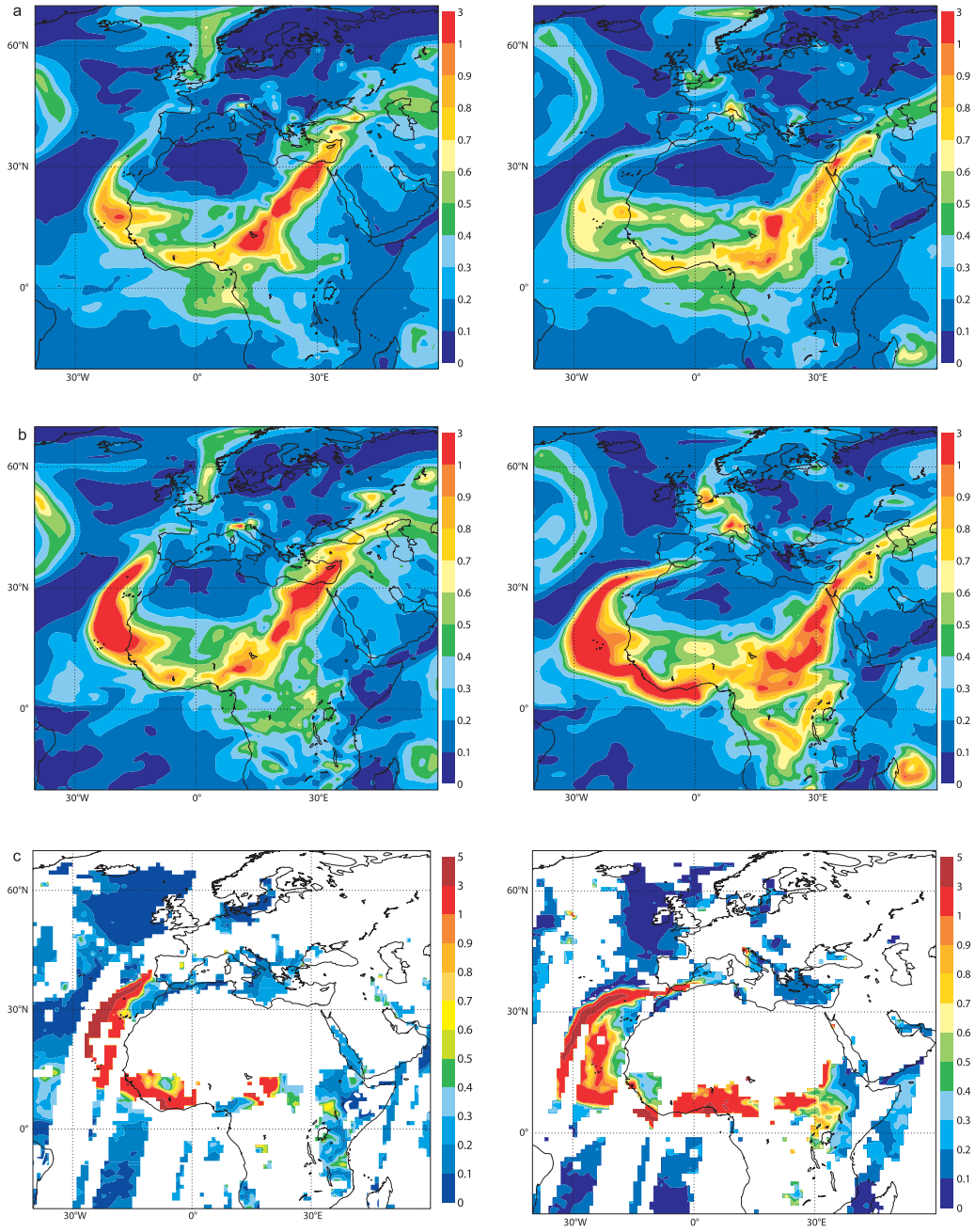

Figure 11. AOD (at 550 nm) distributions of March 2004 Saharan dust outbreak as simulated by the ECMWF model: (a) free-running model, (b) assimilation with MODIS observations, and (c) MODIS observations for (left) 5 March 2004 at 1200 UTC and (right) 6 March 2004 at 1200 UTC. *(Figure taken from Benedetti et al., 2009, with permission from American Geophysical Union).*

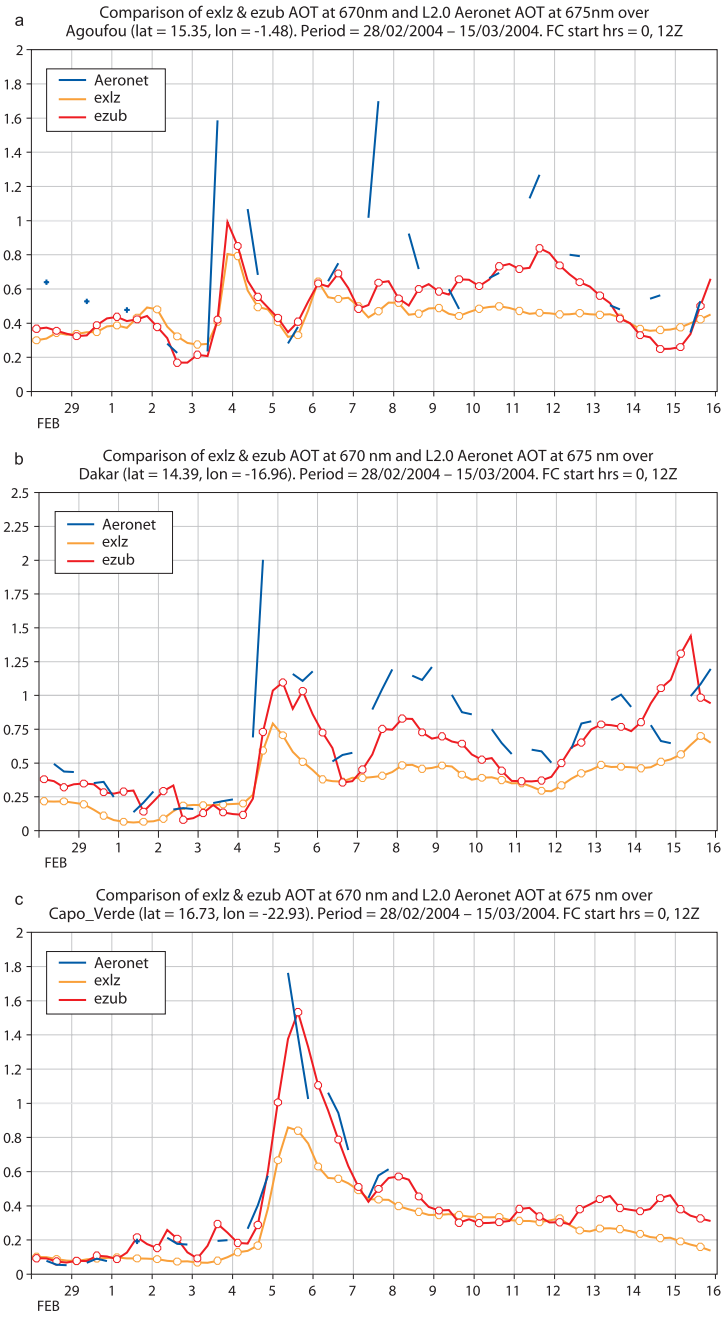

Figure 12. Comparisons of ECMWF analysis AOD at 675 nm with AERONET observations for the Saharan dust outbreak of March 2004 at: (a) Agoufou (Mali), (b) Dakar (Senegal), and (c) Cape Verde. AERONET data are shown in light blue, the analysis is in red, and the free-running forecast is in dark yellow. *(Figure taken from Benedetti et al., 2009, with permission from American Geophysical Union).*

Supplementary Online Materials
for
Satellite Perspective of Aerosol Intercontinental Transport
From Qualitative Tracking to Quantitative Characterization

Hongbin Yu, Lorraine A. Remer, Ralph A. Kahn, Mian Chin, Yan Zhang

A. Descriptions of Major EOS-era Aerosol Sensors

NASA's Earth Observing System (EOS) is an ambitious program designed in the 1980s, implemented in the 1990s and executed beginning with the launch of the Terra satellite at the end of 1999. The program has resulted in a constellation of polar orbiting satellites, equipped with sensors that provide observations in support of Earth system science. The main satellites and sensors providing aerosol information include: Terra-MODIS, Terra-MISR, Aqua-MODIS, Aura-OMI, PARASOL-POLDER and CALIPSO-CALIOP.

A.1. MODIS multi-wavelength measurements: Each MODIS sensor obtains near global, daily observations of atmospheric aerosols with a swath width of 2330 km and 36 channels ranging from 0.41 to 15 μm. Eight channels, nominally, 0.41, 0.47, 0.55, 0.66, 0.87, 1.24, 1.63 and 2.13 μm are used to retrieve aerosol properties in cloud-free scenes with appropriate surface features (Martins et al., 2002; Li et al., 2005; Remer et al., 2005; Hsu et al., 2006). Because of its wide spectral range, and the simplicity of the dark ocean surface, MODIS has the capability of retrieving aerosol optical depth with a relatively high accuracy of $\pm 0.03 \pm 0.05\tau$ (Remer et al., 2002; 2005; Levy et al., 2010). The ocean conditions also permit retrieval of information on particle size. This can take the form of Angstrom Exponent, effective radius or fine mode fraction (See Eq. 3 of Section 3.2). The three retrieved size parameters are all inter-related and represent the same basic information content available from the

spectral signature of the satellite-measured radiances against the dark ocean surfaces. Over vegetated land, the MODIS dark-target algorithm estimates surface reflectance in the blue and red channels based on an empirical relationship using the shortwave infrared radiance and retrieves AOD (Kaufman et al., 1997; Levy et al., 2007). AOD is retrieved at 0.55 μm with an accuracy of $\pm 0.05 \pm 0.15\tau$ and then extrapolated to 0.47 μm and 0.66 μm using the selected aerosol model (Chu et al., 2002; Remer et al., 2005; Levy et al., 2010). Because of the complex spectral structure of the land surface (note that vegetation is bright, not dark in the near-IR), retrieval of aerosol information beyond AOD is not possible.

Alternative aerosol algorithms have been developed and applied to MODIS radiances. The Deep Blue (Hsu et al., 2004) and the MultiAngle Implementation of Atmospheric Correction (MAIAC) algorithms (Lyapustin et al., 2011) offer complementary and alternative products to the original Dark Target algorithm described above. The Deep Blue algorithm takes advantage of the much darker surface reflectance in the blue than at red wavelengths (Hsu et al., 2004). This is especially useful for retrieving AOD over bright surfaces such as deserts, although Deep Blue is not limited to desert scenes. MAIAC retrieves aerosol information over land simultaneously with parameters of a surface bidirectional reflectance factor model using image-based processing applied to the time series of MODIS measurements (Lyapustin et al., 2011). The Deep Blue products are being produced operationally from Aqua-MODIS data (currently not Terra-MODIS). The MAIAC products are not operational at this time. There is a possibility that the time series of MODIS aerosol measurements may be continued from measurements of the Visible/Infrared Imager Radiometer Suite (VIIRS) onboard the most recently launched Suomi National Polar-orbiting Partnership (NPP). VIIRS has aerosol remote sensing capabilities similar to those of MODIS (Lee et al., 2006), with a broader swath

width than MODIS that fully covers the Earth every day. However, the spectral response of each channel is not identical to MODIS and other differences require analysis to determine to what accuracy can VIIRS continue the MODIS aerosol record.

A.2. MISR multi-angle measurements: MISR, aboard the sun-synchronous polar orbiting Terra satellite, measures upwelling solar radiance in four spectral bands (centered at 446, 558, 672, and 866 nm) at each of nine view angles spread out in the forward and aft directions along the flight path (at nadir, ±70.5°, ±60.0°, ±45.6°, and ±26.1° of nadir) (Diner et al., 2002). It acquires global coverage about once per week. Having observations taken through air-mass-factors ranging systematically from one to three gives the instrument greater sensitivity to optically thin aerosol. MISR's wide range of along-track view angles also makes it feasible to more accurately evaluate the surface contribution to the TOA radiances and hence retrieve aerosols over both ocean and land surfaces, including bright desert aerosol source regions and ocean regions that are contaminated by sun glint for mono-directional instruments (Diner et al., 1998; Martonchik et al., 1998; 2002; 2009; Kahn et al., 2005; 2010; Kalashnikova and Kahn, 2006; 2008). MISR constraints on aerosol type also enhance MISR AOD accuracy compared to single-angle instruments in many circumstances. MISR provides particle type classification, based on particle size, shape and SSA constraints. These amount to distinguishing three-to-five particle size bins, two-to-four bins in SSA, and spherical vs. non-spherical particles, provided the mid-visible AOD exceeds 0.15 or 0.2, and the scene meets other basic retrieval-quality criteria (Kahn et al., 2001; 2010). Cloud screening includes tests based on location-and-time specific camera-by-camera radiometric thresholds, reflecting-layer stereo-derived height above the surface; and angular smoothness and correlation (Martonchik et al., 2009). Stereo-derived reflecting-layer heights also provide maps of aerosol plume elevation near sources, where contrast features can be matched in

multi-angular views, at 1.1 km horizontal resolution and about 0.5 km vertical resolution. More details about the MISR aerosol products are given in the references cited above.

A.3. POLDER multi-directional and polarization measurements: There have been three POLDER instruments launched into space ADEOS-POLDER (1996-1997), ADEOS2-POLDER (2003) and PARASOL-POLDER (2005 – still operating at time of writing). PARASOL-POLDER flew in formation with the other A-Train sensors until 2010, when fuel considerations caused the satellite to drop to a lower orbit. Each POLDER sensor consists of a wide field-of-view imaging spectro-radiometer capable of measuring multi-spectral, multi-directional, and polarized radiances with a global coverage within two days (Tanré et al., 2011). POLDER measures in nine spectral channels from 0.443 μm to 1.020 μm, and in several polarization orientations at 0.49 μm, 0.67 μm and 0.87 μm. As the satellite passes over a surface target that target will be viewed at different spots in the image, at different angles. This provides multi-angle observations for each target, ± 51^{o} along track.

The observed multi-angle polarized radiances can be exploited to better separate atmospheric from surface contributions over both land and ocean (Deuzé et al., 2001). Over ocean, the total and polarized radiances at 670 and 865 nm are used to retrieve total AOD (Deuzé et al., 1999), with a typical accuracy of $\pm 0.05 \pm 0.05\tau$ (Goloub et al., 1999). When the geometrical conditions are optimal (scattering angle ranging between 90°-160°), POLDER can derive the shape of coarse-mode particles (Herman et al., 2005). Over land, the aerosol retrieval is based on measurements using only polarized light at the two wavelengths (Herman M. et al., 1997; Deuzé et al., 2001), to capitalize on the small and fairly spectrally neutral polarized reflectance typical of land surfaces. Because large aerosol particles polarize sunlight much less than sub-micron particles (except in very intense dust storm

events), the POLDER over-land AOD retrieval is largely sensitive to spherical, accumulation-mode particles (Tanré et al., 2011), providing the fine mode aerosol optical depth but not the total.

Recently, advanced algorithms are being developed that will further exploit the information content of the POLDER measurements (Dubovik et al., 2011; Kokhanovsky et al., 2010). The retrieval is designed as a statistically optimized multi-variable fitting of the complete PARASOL observation set: all wavelengths, all angles, and all states of polarization. The algorithm allows for a large number of unknown parameters and retrieves a set of parameters affecting measured radiation. The algorithm simultaneously retrieves aerosol and surface properties and should provide information about aerosol sizes, shape, absorption and refractive index.

A.4. OMI near-UV measurements: OMI flies on the Aura satellite with a swath width of 2600 km that covers the Earth in one day. OMI is a hyperspectral instrument that measures from 0.27 to 0.50 μm in bandwidths of 1 μm or less. The Aerosol Index (AI; sometimes referred to as the UV Aerosol Index, UVAI; or the Absorbing Aerosol Index, AAI) provides a measure of absorbing aerosol and a simple index to distinguish between absorbing and non-absorbing aerosols elevated above the ABL. AAI is calculated without assuming aerosol particle properties. It has been frequently used to characterize aerosol transport.

There are two operational aerosol retrievals making use of OMI measurements, the OMAERUV and OMAERO. The OMAERUV algorithm uses the measured radiances at 0.354 and 0.388 μm to derive AOD and absorbing AOD at 0.388 μm (Torres et al., 2007). Because the surface is obscured by atmospheric gas Rayleigh scattering at these wavelengths, and in addition, because most surfaces have

very low and homogeneous reflectance in the UV range, OMAERUV retrievals cover global ocean and land free of snow and ice. The algorithm is based on the deviation of observed radiances from expected values from Rayleigh scattering and is sensitive to AOD, aerosol absorption and height of the aerosol layer. With only two pieces of information from the two measured channels, OMAERUV cannot retrieve all three unknowns. The operational algorithm assumes aerosol layer height from climatology, specifically the climatology as observed from CALIOP lidar, and returns AOD in the UV and information on aerosol absorption. The AOD is extrapolated to the visible regions using the selected aerosol spectral model (Torres et al., 2002, 2007). The OMAERO algorithm uses up to 19 channels in the spectral range of 0.33 μm to 0.50 μm to derive quantitative aerosol information. The oxygen absorption band at 0.477 μm is used to enhance the sensitivity to the aerosol layer height (Veihelmann et al., 2007) in a way similar to its use in the retrieval of cloud height (Acarreta et al., 2004), and becomes one of the retrieved parameters. The primary retrieved parameters are AOD and the best fitting aerosol model. Both OMAERUV and OMAERO retrieve quantitative AOD. This is AOD of the entire column, including the surface layer.

Due to its low spatial resolution, i.e., 13 x 24 km^2 at nadir, OMI AOD retrievals are prone to sub-pixel cloud contamination. OMI AOD values are generally biased high with respect to MODIS measurements, likely as a result of a calibration offset and subpixel cloud contamination (Ahn et al., 2008). In comparison, OMI absorbing AOD is less sensitive to the cloud contamination because of a partial cancellation of cloud contamination effects on AOD and single-scattering albedo (Torres et al., 2007).

A.5. CALIOP vertical profiling: Following the Lidar In-space Technology Experiment (LITE) demonstration mission in 1994 (Winker et al., 1996), the Geoscience Laser Altimeter System (GLAS) was launched in early 2003, becoming the first polar-orbiting satellite lidar (Schulz, 2001; Zwally et al., 2002). It detects clouds and aerosols (Spinhirne et al., 2005) for one month out of every three-to-six, due to the unfortunate failure of a laser. Because of its inconsistency of making measurements, GLAS has not often been used for aerosol transport studies.

In 2006, the Cloud-Aerosol Lidar and Infrared Pathfinder Satellite Observations (CALIPSO) was launched, carrying a two-wavelength, polarization lidar, namely the Cloud-Aerosol Lidar with Orthogonal Polarization (CALIOP). Since then, CALIPSO has been collecting an almost continuous record of high-resolution (333 m in the horizontal and as fine as 30 m in the vertical) profiles of aerosols and clouds attenuated backscatter at 532 and 1064 nm wavelengths, along with polarized backscatter in the visible channel, day and night, covering 82°N and 82°S (Winker et al., 2009; 2010). The polarization measurement allows for the separation of non-spherical dust particles from other types of aerosol. CALIOP algorithms use all the information: backscatter, the color ratio (ratio of 532 to 1064 nm) and depolarization signal to first distinguish between clouds and aerosols in the column (Liu et al., 2009), and then to identify different aerosol types: namely smoke, polluted continental, polluted dust, dust, clean continental, and clean marine, with respective extinction-to-backscatter ratio or lidar ratio (S) of 70, 70, 65, 40, 35, and 20 sr at 532 nm (Omar et al., 2009). Once aerosol type is determined, aerosol extinction profiles are retrieved by applying the extinction-to-backscatter ratio for the particular aerosol type identified. Alternative algorithms have been explored that attempt to provide a direct route to retrieving aerosol extinction without first assuming an extinction-to-backscatter ratio. For example, using the reflected laser signal from cloud tops as a light source, the

extinction of absorbing aerosol overlaying a cloud can be retrieved directly (Hu et al., 2007; Chand et al., 2008).

The major limitation of CALIOP measurement is its near-zero swath. However, successive profiles observed over a period day and night have played important role in characterizing aerosol transport events. Aggregation of observations over seasonal and yearly time scales yields a climatology of aerosol vertical distribution, which has been used to determine aerosol transport height and provide vertically resolved mass fluxes.

B. A movie: Aerosol intercontinental transport in 2001 as captured by MODIS and GOCART

The movie illustrates the day-to-day evolution of aerosol optical depth and fractional contributions of fine and coarse particles for 2001. Top is derived from MODIS aerosol retrievals. Each frame represents a 5-day Gaussian weighted average centered on the indicated day. Bottom is derived from GOCART model simulations. Green indicates coarse mode dominated aerosol (dust), while red indicates fine mode dominated aerosol (smoke and pollution). Intensity of green and red increases as AOD increases. Individual images and movie were created by Reto Stöckli under the umbrella of NASA's Earth Observatory and with input from Yoram Kaufman.